New pyrazolyl functionalized *N*-heterocyclic carbene ligand precursors and their transition metal complexes for the catalytic oxidation of paraffins

by

Liziwe Ndamase

Dissertation submitted in fulfilment of the academic requirements of

Master of Science in Chemistry

School of Chemistry and Physics

College of Agriculture, Engineering and Science

University of KwaZulu-Natal

Westville

South Africa

Supervisors: Professor M. D. Bala & Professor B.O. Owaga

2021

PREFACE

The research contained in this dissertation was completed by the candidate while based in the Discipline of Chemistry, School of Chemistry and Physics of the College of Agriculture, Engineering and Science, University of KwaZulu-Natal, Westville Campus, South Africa. The research was financially supported by National Research Foundation (NRF) and C*Change South Africa.

The contents of this work have not been submitted in any form to another university and, except where the work of others is acknowledged in the text, the results reported are due to investigations by the candidate.

Supervisor signature:

Date: 23 August 2021

Co-supervisor signature:

Date: 23 August 2021

DECLARATION: PLAGIARISM

I, Liziwe Ndamase, declare that:

(i)   the research reported in this dissertation, except where otherwise indicated or acknowledged, is my original work;

(ii)   this dissertation has not been submitted in full or in part for any degree or examination to any other university;

(iii)   this dissertation does not contain other persons' data, pictures, graphs or other information, unless specifically acknowledged as being sourced from other persons;

(iv)   this dissertation does not contain other persons' writing, unless specifically acknowledged as being sourced from other researchers. Where other written sources have been quoted, then:

a)   their words have been re-written but the general information attributed to them has been referenced;

b)   where their exact words have been used, their writing has been placed inside quotation marks, and referenced;

(v)   where I have used material for which publications followed, I have indicated in detail my role in the work;

(vi)   this dissertation is primarily a collection of material, prepared by myself, published as journal articles or presented as a poster and oral presentations at conferences. In some cases, additional material has been included;

(vii)   this dissertation does not contain text, graphics or tables copied and pasted from the Internet, unless specifically acknowledged, and the source being detailed in the thesis and in the References sections.

_____
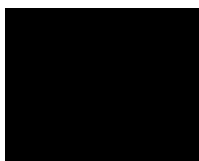
Signed by: Liziwe Ndamase

Date: 10/06/2021

ABSTRACT

New pyrazolyl functionalized *N*-heterocyclic carbene ligand precursors and their transition metal complexes for the catalytic oxidation of paraffins

The synthesis and characterization of four pyrazolyl functionalized *N*-heterocyclic carbene (NHC) ligand precursors namely: **2.1a)** 3-(2-(3,5-dimethyl-1H-pyrazol-1-yl)ethyl)-1-methyl-1H-imidazol-3-ium chloride), **2.2a)** 3-(2-(3,5-dimethyl-1H-pyrazol-1-yl)ethyl)-1-ethyl-1H-imidazol-3-ium chloride), **2.3a)** (1-benzyl-3-(2-(3,5-dimethyl-1H-pyrazol-1-yl)ethyl)-1H-imidazol-3-ium chloride) and **2.4a)** 3-(2-(3,5-dimethyl-1H-pyrazol-1-yl)ethyl)-1-(4-nitrophenyl)-1H-imidazol-3-ium chloride) was conducted. Thereafter the salts were subjected to anion metathesis with $NaBF_4$ resulting in yields ranging between 82.7 and 99 % (**2.1b** – **2.4b**). After salt metathesis with $NaBF_4$, the ^1H NMR (400 MHz, DMSO-d_6) data showed that the imidazolium acidic C_2 protons of the salts shifted slightly upfield from circa δ 9.0 to 8.9, suggesting that it was more shielded. **2.1b** and **2.4b** were the most stable, with **2.2b** being very unstable. The synthesis of Ni(II), Cu(I) and Co(II) complexes was completed for the most stable ligand precursors using direct deprotonation and were obtained in low yields (≤ 35 %). Characterization was carried out using NMR, FTIR, and MS. The broadness of the ^1H NMR for complex **3.1**, $[Co^{II}(3-(2-(3,5\text{-dimethyl-1H-pyrazol-1-yl})ethyl)-1-(4\text{-nitrophenyl})-1H\text{-imidazol-3-ium})_2]\bullet 2BF_4$ together with the complementary lack of the expected far downfield carbene signal in its ^{13}C NMR spectrum, suggest that the complex exhibits behaviour typical of paramagnetic high–spin Co(II) ions in a tetrahedral geometry. Complex **3.3,** $[Cu^I(3-(2-(3,5\text{-dimethyl-1H-pyrazol-1-yl})ethyl)-1\text{-methyl-1H-imidazolylidene}) (NCCH_3)_2]\bullet BF_4$ and complex **3.5**, $[Ni^{II}(3-(2-(3,5\text{-dimethyl-1H-pyrazol-1-yl}) ethyl)-1\text{-methyl-1H-imidazol-3-ium})\bullet 2BF_4,$ were the least stable of all the complexes. All the complexes showed significant downfield shift of aryl protons peaks in their ^1H NMR spectra. This indicated the effect of metal coordination to the NHC ligand. All the synthesized complexes were hygroscopic. Consequently, only two of the five successfully synthesized and characterized complexes were thermodynamically stable to be tested as catalysts in the oxidation of cyclohexane. The most stable complexes are **3.2,** $[Cu^I(CH_2CN)_2((3-(2-(3,5\text{-dimethyl-1H-pyrazol-1-yl})ethyl)-1-(4\text{-nitrophenyl})-1H\text{-imidazol-3-ium})]\bullet BF_4$ and **3.1,** $[Co^{II}((3-(2-(3,5\text{-dimethyl-1H-pyrazol-1-yl})ethyl)-1-(4\text{-nitrophenyl})-1H\text{-imidazol-3-ium})_2]\bullet 2BF_4$ both derived from the ligand precursor **2.4b**. Catalytic oxidation of cyclohexane was done to test the catalytic activity of these stable complexes. The catalytic oxidation of cyclohexane results in the production of the alcohol

(cyclohexanol, A) and the ketone (cyclohexanone, K) products, with the K resulting from the secondary oxidation of the A. As a result, one of the measures of oxidation catalytic efficiency is chemoselectivity of the catalyst expressed as the K/A ratio. Hence, the pyrazolyl-functionalized NHC-Co(II) **3.1** and NHC-Cu(I) **3.2** complexes with H_2O_2 as the oxidant in refluxing acetonitrile were the catalytic systems used to oxidise cyclohexane into cyclohexanone and cyclohexanol. Complex **3.1** had a higher TON of 104 and had a higher conversion of 38 % after a reaction time of 24 h, but exhibited poor selectivity with 53 % chemoselectivity towards cyclohexanone after 24 h. Complex **3.2** had a low TON of 18 at a correspondingly low conversion of 19%, showed a good selectivity towards cyclohexanol at 83 % after 24 h. The K/A ratio for **3.1** calculated using number of moles is 1.11, while for **3.2** is 0.2.

DEDICATION

I dedicate this dissertation to my parents, baby Simanye Hope Ndamase and myself.

ACKNOWLEDGMENTS

There are quite a few acknowledgments that deserve a special mention:

My family, mom, dad, and all my siblings for their support and encouragement from my undergraduate degree through to my MSc.

To Professor M. D. Bala of the University of KwaZulu-Natal, my supervisor, I'd like to extent my sincerest and heartfelt gratitude for his guidance, academic and emotional support throughout my MSc. The faith he had in me made me want to better myself.

Ms Thabisile Clementine Dlamini, Lungani Nhlenyama and Mpho Mkhwanazi of UKZN for their administrative support.

The technical stuff of the School of Chemistry at UKZN.

Kike Adewusi and Micaela Van Wyk of the UKZN for academic counselling when needed.

Dr Ibrahim Halliru, for his mentorship and guidance throughout my MSc.

My research group and colleagues for assistance, support and for respecting the work place.

Financial support for this research awarded by NRF and C*Change

And lastly, I would like to extend my gratitude to the University of KwaZulu-Natal, Westville Campus, for providing the infrastructure and resources necessary for me to obtain my MSc in Chemistry.

TABLE OF CONTENTS

LIST OF TABLES

LIST OF FIGURES

LIST OF REACTION SCHEMES

List of abbreviations

Bz-imid	1-benzyl-3-(2-(3,5-dimethyl-1H-pyrazol-1-yl)ethyl)-1H-imidazol-3-ium
Et-imid	3-(2-(3,5-dimethyl-1H-pyrazol-1-yl)ethyl)-1-ethyl-1H-imidazol-3-ium
EA	Elemental Analysis
GC	Gas Chromatography
h (s)	hour(s)
H_2O_2	Hydrogen peroxide
IR	Infrared spectroscopy
LRMS	Low Resolution Mass Spectroscopy
min (s)	minute(s)
Me-imid	3-(2-(3,5-dimethyl-1H-pyrazol-1-yl)ethyl)-1-methyl-1H-imidazol-3-ium
NHC	*N*-Heterocyclic Carbene
pyrazole-OH	2-(3,5-dimethyl-1*H*-pyrazol-1-yl)ethanol
pyrazole-Cl	1-(2-chloroethyl)-3,5-dimethyl-1*H*-pyrazole
p-NO₂Ph-imid	3-(2-(3,5-dimethyl-1H-pyrazol-1-yl)ethyl)-1-(4-nitrophenyl)-1H-imidazol-3-ium
substituted-imidazole	1-(2-(cyclopenta-2,4-dienyl)ethyl)-3,5-dimethyl-1H-pyrazole
TM (s)	Transition Metal(s)
TLC	Thin Layer Chromatography
TBHP	Tert-butylhydroperoxide

CHAPTER 1: INTRODUCTION

1.1. PARAFFINS

Many industrial processes such as Sasol's low-temperature Fischer-Tropsch process produce copious quantities of paraffins. Paraffins or alkanes are saturated, non-polar chemical compounds constituted of only hydrogen (H) and carbon (C) atoms. The general chemical formula for paraffins is C_nH_{n+2}, where n is equal to the number of carbon atoms in the compound. Paraffins can structurally be grouped according to whether they are linear / straight chain alkanes (*n*-alkanes), branched alkanes or cyclic alkanes. While straight-chain alkanes have larger surface areas thus higher boiling points. Branched alkanes on the other hand are more compacted and therefore have a smaller surface area. Paraffins (*n*-alkanes) that are composed of fewer than five carbon atoms per molecule are usually gaseous at room temperature. Those with 5-15 carbon atoms are generally liquids, and the *n*-alkanes that have more than 15 carbon atoms, solids, traditionally referred to as waxes.

Paraffins are so vastly abundant in nature that they are also considered to be the most hydrocarbons in pollutants.[1] Paraffins constitute most of natural gas and crude oil, and to-date, direct conversion of low cost and highly abundant paraffins such as methane (natural gas) to value added compounds economically under mild conditions still remains a challenge to researchers.[2] Because of their abundance, paraffins are consequently used as the primary feedstock in the chemistry industry.[3] One of the most common commercially and/or industrially used processes in the transformation of paraffins is hydrocracking, where long-chain paraffins such as heavy fuel oils are converted into products such as high-quality diesel and kerosene. However, such a process requires very high temperatures (400-600 °C) when using heterogeneous catalysts[1] making it expensive.

1.1.1. Catalytic oxidation of alkanes

The field of alkane oxidation remains challenging to synthetic chemists because of the difficulty in selective oxidation of the C-H bond in hydrocarbons. The conversion of these saturated compounds into valuable products such as alcohols, carboxylic acids and alkenes under controlled catalytic conditions has the potential to offer large economic benefits.[2, 4] Paraffins derived from natural gas, such as methane, are present in large quantities at remote locations,

however, transportation is quite expensive. Consequently, converting natural gas into liquids such as methanol would make natural gas a very reliable source of energy and transportation would be much cheaper.[4] Currently, paraffins derived from both petroleum and natural gas can be converted (Scheme 1.1) into energy, fuel and chemicals at high temperatures.
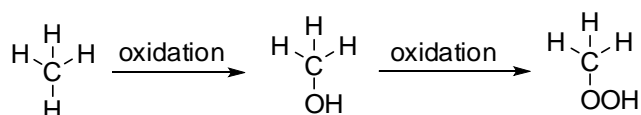
Scheme 1.1: Catalytic activation of methane to methanol and methanoic acid

There are hardly any functioning catalytic processes for converting paraffins directly to more valuable products. The major hurdle that chemists are battling with when functionalizing paraffins on an industrial scale is regioselectivity and while operating under mild conditions and consuming as little energy as possible.[3,5] With paraffins, since all the bonds in the molecule between C-H and C-C are sp^3 hybridized single bonds, no one position is preferred in the molecule for functionalization to occur , hence, the product stream is a mixture of all possible products.

1.2. CATALYSIS

Catalysis in chemistry can be defined as a process of employing a catalyst to accelerate the rate of a reaction. A catalyst can be defined as a compound or substance that accelerates the rate of a reaction, this process involves the kinetics of the reaction. The catalyst can accelerate the reaction in both the forward and reverse directions by lowering the activation energy of the reactants without it being changed in the process, this allows for the position of equilibrium of the reaction to be left unchanged. Any process that makes use of a catalyst is referred to as catalysis. The catalyst does not affect the state of equilibrium of the reaction, hence catalysis is a kinetic phenomenon. Figure 1.1 shows a graphical representation of the effect of using a catalyst on the activation energy of the reaction.
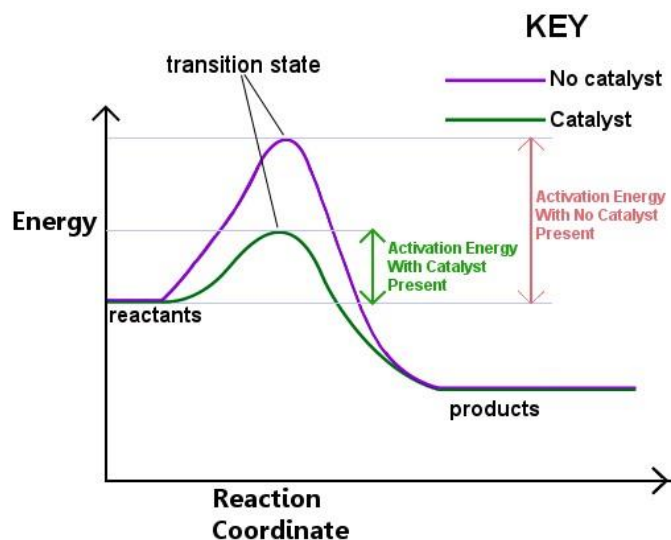
Figure 1.1: Effect of using a catalyst on the activation energy of a reaction

The term catalysis is a very broad term for different processes which can be classified into three main groups as shown in Figure 1.2.
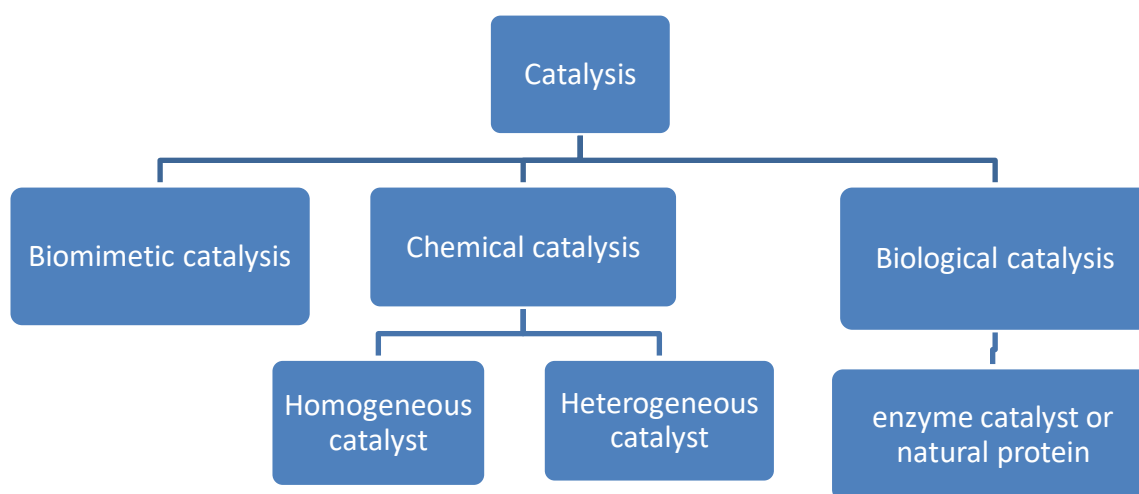
Figure 1.2: Flow diagram showing different sub-sections under the umbrella of catalysis

1.2.1. *Biological catalysts / Biocatalysts*

Biological catalysts or biocatalysts are natural proteins or nucleic acids which catalyse a specific biochemical reaction inside a living cell. The most common example of a biological

catalyst is an enzyme. Enzymes are natural proteins that possess catalytic activity. Enzymes can speed up a reaction without altering the equilibrium and they do not get consumed in the chemical reaction they are speeding up. These proteins are responsible for catalysing some of the fastest reactions known to humanity. Enzymes are very complex proteins that have a well-defined structure. They can also be classified as chiral organic molecules which contain metal ions and H_2O molecules to aid in preserving their structure and activity.[6]

The selective oxidation of the inert C-H bond in hydrocarbon compounds is still a long-standing problem for synthetic chemists. This is because activating the inert bonds require harsh conditions and very strong oxidants to force the substrate to react. Metalloenzymes are to date regarded as the perfect model to obtain the desired end results. Scheme 1.2 illustrates an example that shows how a perfectly controlled reductive activation of an oxidant *e.g.* O_2 on the active site of P450 cytochrome can produce powerful oxidising species.[7]
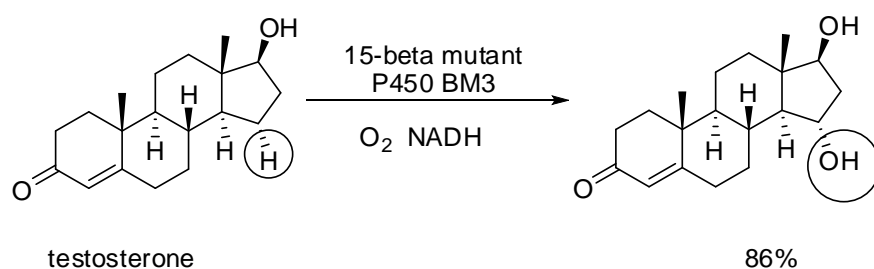
Scheme 1.2: Example of selective oxidation of a saturated C-H bond by a biological agent (mutant cytochrome)[7]

1.2.2. *Biomimetic catalysts*

Biomimetic chemistry is a term that is used to describe chemical processes that mimics certain important principles of enzymatic systems or biological catalytic systems.[8] Ronald Breslow first introduced this field of chemistry in 1972.[9] Biomimetic chemistry consists of areas such as bioorganic, bioinorganic and biophysical chemistries. Biomimetic chemistry can be thought of as an umbrella covering a wide range of topics including the synthesis of artificial enzymes.[10] Biocatalysts generally bind to their substrate through metal ions, ion-pairing or Lewis acid-base coordination and use the functional groups' chemistry in its structure to achieve catalysis.[10] This reaction scheme results in a catalytic process that is selective to the substrate reaction, and

that is high in stereo selectivity.   The mechanism of acid-base catalysis modelled the mechanism of catalysis depicted by the active cites of biocatalysts.[8, 11]

Synthetic metalloporphyrins have been studied extensively as biomimetic mock-ups of cytochromes P450 (biological catalysts). The first group of biomimetic catalysts for the oxidation of compounds such as adamantane and cyclohexane were introduced by Groves *et al.*[12] Since then, this field has taken on a life of its own. Researchers have introduced electron withdrawing groups as substituents and introduced additives such as imidazole and pyridine and choosing the relevant oxidant to achieve biomimetic catalysts that are as efficient as a biological catalyst such as cytochrome P450.

1.2.3. *Chemical catalyst*

Chemical catalysts can be split into homogeneous catalysts and heterogeneous catalysts. Homogeneous catalysts are in the same phase as the reactants and the products, usually in the liquid phase. Homogeneous catalysts are characterised by high selectivity and operating at milder conditions. However, it is quite difficult to separate the product from the catalyst, making it expensive to recycle the catalyst. On the other hand, heterogeneous catalysts are in a different phase from the reactant and the product, they are usually in the solid phase. These catalysts have lower selectivity, but can be easily separated from the products, making them recyclable and reusable, resulting in a high turnover number. To date, the mechanism of the heterogeneous catalytic process is poorly understood. But because the catalyst is recovered at the end of the reaction, heterogeneous catalysts are largely used on an industrial scale.[13-14]

Heterogeneous organometallic catalysis has evolved tremendously over the past five decades hence aided in the development of organic synthesis.[15] The Heck reaction is considered a prototypical reaction example of organometallic catalysis. The evolution of organic chemistry had aided greatly in the functionalization of C-H bonds. The direct transformation of C-H bonds to C-C or C-X (where X is N, O or S) bonds was reported as far back as 1885 in the Hofmann-Löffler-Freytag reaction[16], and more recently in reactions such as the Suzuki cross-coupling reaction. Hemilabile complexes such as pyrazolyl-functionalized *N*-heterocyclic carbene palladium catalyst reported by Wang *et al.* are excellent catalysis for C-C coupling reactions such as the Heck and Suzuki reactions.[17]

1.2.3.1. Fenton and Shul'pin chemistry

Selective oxidation of the inert C-H bond in hydrocarbons under mild conditions still remains a huge impediment for synthetic chemists. Fenton reported the first generation of successful oxidation of alkanes over a century ago. Fenton used iron (Fe) based catalysts for the oxidation of alkanes, however very low selectivity and yields were reported towards alcohols and tended towards carboxylic acids. This was because alkane oxidation occurs via radical chain reactions that consists of hydroperoxyl intermediate species as shown in reaction Scheme 1.3. This intermediate species is far more reactive than the substrate and thus can undergo excessive oxidation leading to products such as ketones, aldehydes and carboxylic acids depending on the nature and stability of the radical.[18]

$$Fe^{2+} + H_2O_2 \longrightarrow Fe^{3+} + HO\cdot + OH^-$$

ferrous   hydrogen   ferric   hydroxyl   hydroxyl

peroxide   radical

$$Fe^{3+} + H_2O_2 \longrightarrow Fe^{2+} + HO\dot{O} + H^+$$

$$2H_2O_2 \longrightarrow H\dot{O} + HO\dot{O} + H_2O$$
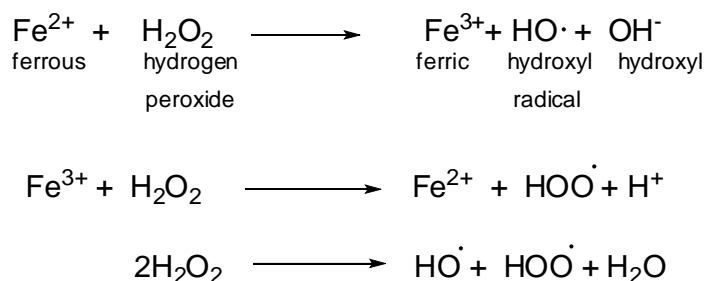
Scheme 1.3: Fenton reaction for the oxidation of organic compounds[18]

1.3. CARBENES

Carbenes are defined as neutral compounds containing a divalent carbon surrounded by a six-electron valence outer shell. Four of the six electrons are involved in σ-bonding, while the other two remain on the central carbon known as the carbene carbon. Free carbenes are unstable, highly reactive molecules due to their incomplete electron octet and coordination unsaturation. The first stable carbene was successfully isolated in the late 1980s.[19] Subsequently, experiments were conducted with the aim to explore and optimise the properties of stable carbenes. To date, three types of carbenes are recognized in carbene chemistry, namely Fischer carbenes or singlet carbenes, Schrock carbenes or triplet carbenes, and *N*-Heterocyclic carbenes (NHCs).

1.3.1. Singlet and triplet carbenes

Fischer carbenes also referred to as singlet carbenes, were the first reported carbenes in 1964 as ligands in transition metal complexes.[20] They were referred to as singlet carbenes due to the multiplicity of their ground state. Fischer carbenes form strong σ bonds with the metal centre. However, they contain a vacant p-orbital which allows for the π-back donation of electrons from the metal to the carbene. As a result, these carbenes contain both electrophilic and nucleophilic properties.[21] These ligands bind well with transition metals of low oxidation state. Thermodynamic stabilisation of singlet carbenes can be obtained when σ electron-withdrawing and π electron-withdrawing substituents are introduced to the σ and pπ orbitals, thus forcing the carbene orbitals to interact. The σ orbital is stabilized by mesomeric and inductive effects, while π electron donating groups such as $-OR$, $-SR$, $-NR_2$ and halides raise the energy of the vacant pπ orbital.

Schrock or triplet carbenes were reported ten years after the Fischer carbenes. They bind well with transition metals of high oxidation state and have a nucleophilic carbonic carbon. They are called triplet carbenes because of their electron spin. Triplet carbenes are generally more stable in a gaseous state. These carbenes behave as biradicaloid species[20] because they participate in a stepwise radical addition reaction, consequently, they go through an intermediate step with the two unpaired electrons, making these ligands stereoselective. Triplet carbenes are paramagnetic and the two unpaired electrons are either in a linear or bent (*i.e. sp* or *sp^2* hybrid, respectively) shape. [20-21] Figures 1.3 (a) and (b) show the ground states of the singlet and triplet carbene, resp.
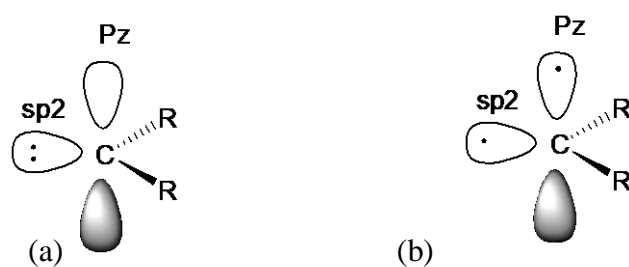
Figure 1.3: (a) Singlet carbene and (b) Triplet carbene

1.3.2. *N*-Heterocyclic carbenes

N-heterocyclic carbenes (NHCs) have attracted the most attention amongst other carbenes. NHCs were first introduced in the early 1960s when Wanzlick investigated their reactivity and stability.[19] In the late 1960s Wanzlick and Öfele independently reported on the application of NHCs as ligands for transition metal complexes.[22] In 1988 the first stable carbene was isolated; however, unfortunately, the isolated carbene, which was called the (phosphino)(silyl)carbene did not show any ability to bind to any metals. The coordination chemistry of NHCs was similar to that of phosphines in metal complexation; however, NHCs afforded more stable complexes, which are also more reactive. Thus, they have been used as phosphine substituents in most recent studies. The field of carbenes lay dormant for over twenty years because it was believed that carbenes were too reactive and too unstable to isolate. Figure 1.4 show the first *N*-heterocyclic carbene isolated was 1,3-di(adamantly)imidazole-2-ylidene in 1991 as reported by Arduengo and co-workers.[23] The carbene could be isolated because it was stable due to the bulky nature of the wing-tip substituent; this is due to the kinetic and electronic stabilization through orbital overlap.[24] NHCs are highly molecular ligands, and this accounts for their large structural and stereochemical diversity.
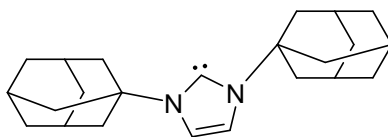
Figure 1.4: Structure of 1,3-di(adamantly)imidazole-2-ylidene, the first isolated NHC

NHCs or "Hot Carbenes" have become one of the most prominent class of ligands in organometallic and inorganic chemistry, thus, overshadowing the singlet and triplet carbenes.[17] NHCs can form complexes of higher thermal and hydrolytic stability with most transition metals (irrespective of whether they are in high or low oxidation state), and some main group elements *i.e.* Be, S, and I.[25-26] NHCs are strong two-electron sigma donor ligands that form very stable metal-ligand bonds, with negligible π-back bonding from the metal centre. Their coordination chemistry is similar to that of phosphines, however, the metal-ligand bond between phosphines and metals is weaker than that of NHC-metal bonds. The reaction Scheme 1.4 below shows the relative equilibrium probability of an NHC-metal bond to break compared to a phosphine-metal bond. The specific coordination chemistry allows NHCs to stabilize and activate metal centres.[27]
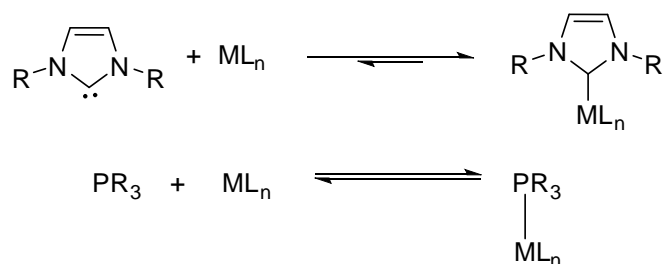
Scheme 1.4: Relative equilibrium probability of an NHC-metal bond to break compared to a phosphine-metal bond[27]

NHC are composed of two nitrogen (N) atoms adjacent to the carbene carbon atom. Figure 1.5 shows the structure of imidazol-2-ylidene which is the most stable NHC both in solution and in the solid state. This stability rises if the lone pair on the nitrogen is considered to be largely p-orbital based, and hence the strong π-donation from the N atoms can stabilize the carbene. This is known as the push-push mesomeric effect. Scheme 1.5 illustrates the mesomeric structures of NHC and the stabilization of the singlet state presented in Fig 1.3a. The sigma electron withdrawing and π-donating abilities of the nitrogen atoms relative to carbon also add to the NHC's stability. Additional stability is also due to the double bond in the ring.
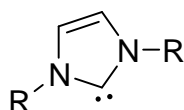
Figure 1.5: General structure of an N-heterocyclic carbene, R represents wingtip substituents
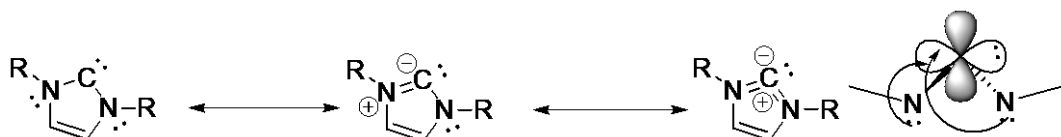
Scheme 1.5: Mesomeric structures of NHC depicting its stabilization of the singlet state

NHCs, like other ligands, can be characterised by two important parameters which influence the reactivity and stability of their respective complexes. These parameters are electronic parameters and steric bulk parameters. Electronic parameters are the σ- and π- donating and π-accepting abilities of a ligand. These properties depend on the frontier orbitals of the ligand. Figure 1.6 shows the frontier orbitals of imidazole and also depicts which orbitals are responsible for the electron-withdrawing and electron-donating groups. The electron-donating ability of a ligand is associated with the highest occupied molecular orbital (HOMO). The

higher the HOMO energy level, the stronger the electron-donating ability of the ligand. The electron-accepting ability is associated with the lowest unoccupied molecular orbital (LUMO). The lower the LUMO energy level, the stronger the electron-accepting ability.[28-29] The stability of a free *N*-heterocyclic carbene is said to be largely from the σ charge transfer from the carbonic carbon to the neighbouring heteroatom (nitrogen). However, the dominant factor in the stability of carbenes is the donation of the lone pair of electrons from nitrogen into the empty p(π) orbital of the carbonic carbon.

π- electron donating
σ- electron withdrawing
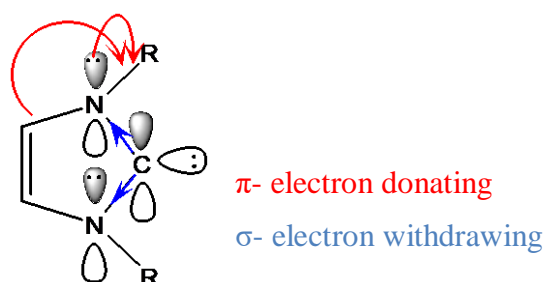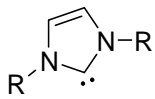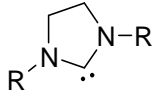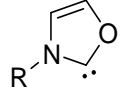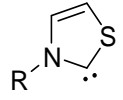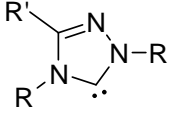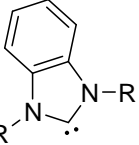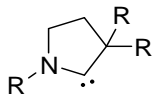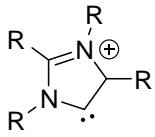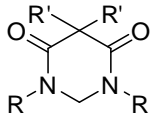
Figure 1.6: Frontier orbitals of imidazole

Steric bulk prevents optimum orbital overlap due to ligand repulsion, resulting in weak labile bonds. Steric bulk can be easily estimated in comparison to electronic factors by considering ligand coordination. In some cases, even the positive electronic factors can be overshadowed by the steric hindrance imposed by the ligand on the metal centre. However, these electronic and steric interactions can be manipulated to achieve reactivity, regio- or stereo-selectivity.

These two parameters combined are referred to as stereo-electronic properties. For NHCs, stereo-electronic properties can be fine-tuned to increase activity and selectivity of NHC-metal complexes by variations in the ring substituents (wing-tip substitutes,) and heterocyclic backbone (which influences electronic factors).[24] Altering the nature of the azole ring affects its electronic properties; for example, benzimidazole has the least amount of donating power followed by imidazole, and imidazoline has the highest electron-donating power. The type and number of heteroatoms in the azole ring affect the electronic properties of the carbene. Thus, altering the azole ring gives rise to the different types of NHCs with different stereo-electronic properties. Table 1.1 contains some of the most used NHCs reported to-date.

Table 1.1: Some of the most used *N*-heterocyclic carbenes

Name	Structure	Common examples
Imidazolylidene		R= Ad= IAd , R= Me= IMe, R= Mes= IMes, R= 2,6-(iPr)$_2$C$_6$H$_3$ = IPr, R = tBu= I*t*Bu
Imidazolinylidene		R = Mes= SIMes R = 2,6-(iPr)$_2$C$_6$H= SIPr
Oxazolylidene[30]		
Thiazolylidene[31]		
Triazolylidene[32]		R = R' = Ph TPT
Benzimidazolylidene[33]		
Pyrrolidinylidene[34]		
"Abnormal" imidazolylidene[35-36]		
N,N-diamidocarbene[36]		

1.4. DONOR FUNCTIONALIZED NHC

Many experiments have been conducted with the aim to optimise the reactivity and stability of NHC complexes; these include changes or modifications on the wingtips (the nitrogen atoms

in the ring) and on the ring backbone.[37] Steric protection from the wingtip substitution provides extra stability. Recent studies show that the use of a chelating ligand motif, particularly where N-donor ligands such as pyrazole, pyrrole, pyridine, *etc*., are tethered to NHCs to form bidentate or polydentate ligands has the potential to moderate the lability of each of the individual ligands and increase stability and reactivity.[38]

The reactivity of NHCs can be investigated by measuring their nucleophilicity and Bronsted basicity. The pKa of the NHCs can be determined both experimentally in water and THF, or computationally by determining the pKa of their corresponding conjugated acids and by measuring their proton affinity.[19] The pKa of NHCs was found to increase with an increase in the electron-donating character of the wing tip substituents.[19] The nucleophilicity or Lewis basicity of NHCs was studied extensively by Mayr *et al*. who studied the kinetics between NHCs towards reference electrophiles. It was determined that the IMes and SIMes were 10^3 times more nucleophilic than triazol-ylidene.[23] The Lewis basicity of the NHCs was determined computationally using the methyl cation affinity. It was established that imidazole and imidazoline type NHCs are stronger Lewis bases than triazole ones.[23]

Owing to their strong Lewis basicity, NHCs can bind to almost any substrate, from transition metals,[39] main group elements,[40] to organic molecules forming very stable adducts.[24] Hence, NHCs are able to form very strong metal-ligand bonds. N-donor ligands such as pyrazole on the other hand form weak labile metal ligand bonds. Often it is beneficial to incorporate these weaker N-donors into the metal catalyst because they can easily dissociate to give room for the reaction to occur (active site). However, due to the weak metal-ligand bond, N-donor ligands can be lost through self-reductive elimination, where the labile ligand dissociates from the metal centre resulting in undesired products, and ultimately complex or catalyst deactivation.[38, 41] When tethered to a stable NHC donor, a relatively labile sp^2 N-donor will become anchored to the metal centre thereby allowing only partial ligand dissociation, this phenomenon is referred to as hemilability.[42] When a hemilabile complex is applied as a catalyst, the hemilabile arm allows temporary coordination of the substrate and improve the stability of the metal centre within the catalytic cycle. Scheme 1.6 depicts the hemilabile coordination of a bidentate ligand motif. The electronic and steric properties (including the number and type of connecting atoms) of the hemilabile ligand restrict the size and shape of the reactants entering the active site and the products leaving the active site, hence, resulting in high product selectivity, which is essential in catalysis.
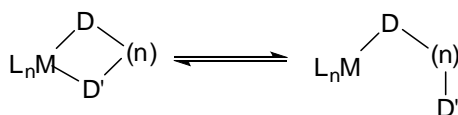
Scheme 1.6: Hemilabile coordination of a bidentate ligand motif.[43]

Complexes that have the hemilability property have showed excellent results in various types of catalytic reactions *e.g.* exceptional results have been obtained by Burgess and co-workers with the Ir(I) hydrogenation catalyst which contains a chiral NHC-oxazolyl chelate.[44] These compounds showed high activity and enantioselectivity (>98% ee) for the reduction of highly substituted prochiral olefins. Nonetheless, the hydrogenation activity of the catalyst was dependant on the stereo-electronic properties of the NHC-oxazolyl ligand. Satisfactory results under mild conditions have also been reported for the Rh(I) mixed donor pyrazolyl functionalised NHC chelate complexes as hydrogenation catalysts.[26] However, to the best of our knowledge, complexes similar to the ones reported here containing hemilabile ligands have not yet been applied in oxidation catalysis, or paraffin activation catalysis, which is the main aim of this study.

NHCs have a high σ-basicity (donating ability) and a low π-acidity (accepting ability), properties like these increase the catalytic activity of metal-NHC complexes for numerous organic transformations. Steric and electronic properties can be fine-tuned to increase activity and selectivity of the metal-NHC complexes by varying wingtip substituents or N-substituents on the NHC while increasing or decreasing the number of connecting atoms (n) between NHC-N donor ligands to respectively increase flexibility by decreasing rigidity or vice versa.

Tethering a donor ligand to the NHC forming a polydentate ligand can potentially increase the stability of the resulting complex. Donor ligands are ligands that contain at least one anionic or neutral 2e$^-$ donor atom (*e.g.* S, N, O, C, or P). N-donor ligands such as pyrazole form very weak labile metal-ligands bonds which, break easily, unlike the stable and strong bonds formed between metal-NHC. Hence, when the two are chelated together, they form a stable hemilabile ligand which allows partial dissociation creating a vacant coordination site, stabilizing the intermediate species and activating the substrate. This also allows the ligand to open room for reactions like oxidative addition to occur on the active site in the catalyst, resulting in very stable and yet active catalysts.

1.5. PYRAZOLYL FUNCTIONALISED NHC TRANSITION METAL COMPLEXES

Most published articles on mixed donor NHC-X ligands (X= N, O or S) or hemilabile ligands reported using platinum group metals (PGM) as the metal centres.[45-46, 26] This is because they are more effective in providing more active, selective and stable catalysts. However, one major disadvantage is that they are costly and toxic. The synthesized catalysts can perform different organic transformations depending on the metal centre, the ligands used and the type of coordination chemistry. Most reported catalysts containing hemilabile ligands and PGM as metal sources are hydrogenation catalysts.[26, 41, 44]

Researchers are now considering first-row transition metals such as nickel (Ni), copper (Cu), and cobalt (Co) because they are cheaper and less toxic in comparison to the PGM, and consequently more favourable.[47,48] Furthermore, they are easier to separate from products, resulting in catalysts with high turnover numbers (TON) and high turnover frequencies (TOF). Copper complexes have been reported to have high activity in oxidation catalysis, as they often mimic nature.[18]

Research shows that a symmetrical NCN (Fig. 1.7) ligand is quite challenging to coordinate to any metal, using either direct deprotonation or the Ag_2O route. This is because the α- carbon on the imidazole is highly acidic, leading to bond cleavage at the α-position. However, a few articles have reported on the successful use of trans metalation as a method for complexation. Thus, for the symmetric ligands, the Ag_2O route will be used, because many researchers have had outstanding results using the route, and the mechanism is easy to understand.
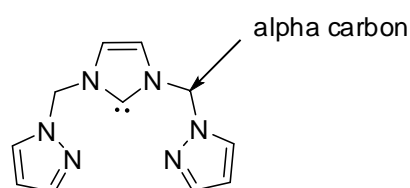
Figure 1.7: Proposed symmetrical ligand

1.6. SYNTHESIS OF NHC-TRANSITION METAL COMPLEXES

N-heterocyclic carbene-transition metal complexes can be successfully synthesized using two well-established methods, namely *i.* free carbene and *ii.* transmetalation.

1.6.1. *Free carbene method*

The generation of a free carbene can be done by deprotonating the salt or ligand precursor using a strong base in a suitable solvent under inert (air and moisture-free) conditions.[49] The resulting free carbene can then be reacted with an appropriate metal source to obtain the desired corresponding complex. Scheme 1.7 shows an example of the generation of free carbene using the direct deprotonation of a salt. This route was commonly used for the synthesis of NHC-transition metal complexes of non-noble transition metals such as cobalt and iron.[50]
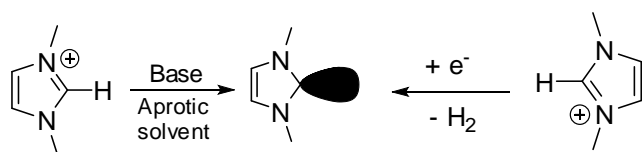
Scheme 1.7: Generation of free carbene using direct deprotonation of a salt

Complications that have been reported include decomposition when attempting to isolate the free carbene. This is because the free carbene is very unstable and highly reactive. However, these complications can be bypassed by using alternative methods such as *in-situ* reactions to generate free carbenes as intermediate species and reacted them with the metal centres to produce the desired complex. These reactions involve reacting the salt with a basic ligand of a suitable metal source generating the free carbene following the subsequent binding of the metal source to the free carbene *in-situ* resulting in the desired complex.[51]

1.6.2. *Transmetalation method*

This method involves the transfer of ligands from one metal to another. The metal that the ligands are transferred from is usually silver (Ag), this is because the bonds between ligands such as NHCs and the Ag (I) ion are very weak and highly active and break easily once the intermediate silver complex is reacted with a required metal precursor that will yield the desired complex.[52] There are reports on other metals such as copper being used in transmetalation.

The first transmetalation reaction was reported in 1998 by Wang after the isolation of the first Ag complex by Arduengo *et al.*[53-54] This method is the most commonly used method in the synthesis of noble metal-NHC complexes.[13, 49] However, this method has its faults, for example, this reaction has to be carried out in the absence of UV light since some intermediate silver complexes are very sensitive to sunlight and may decompose if exposed.

1.7. CATALYSED ALKANE OXIDATION USING COPPER, NICKEL AND COBALT COMPLEXES

First-row transition metal complexes such as that of copper[18, 55] , nickel[56], cobalt[56], iron[7, 57], vanadium[58] *etc.*, have been reported to display fairly good catalytic activity under mild conditions towards the oxidative functionalization of alkanes. Itoh *et al.* reported that the Ni(II) complex [Ni(TPA)CH$_3$COO)(H$_2$O)(BPh$_4$)] was a very robust and effective catalyst that showed high alcohol-product selectivity towards alkane hydroxylation using *m*-chloroperbenzoic acid as the oxidant. The TON for the Ni(II) complex was much higher than that of Co(II), Fe(II) or Mn(II) complexes of the same ligand. Co(II) followed by Ni(II) complexes showed excellent alcohol-product selectivity, while Fe(II) and Mn(II) showed the least selectivity.[56, 59] This indicated that although the Ni(II) complex had the highest catalytic activity, followed by Fe(II)> Co(II)> Mn(II), the Co(II) complex had the highest alcohol product selectivity. Copper based intermediates such as [CuO$^•$] with a Cu(II) oxyl radical character have been reported to exhibit excellent reactivity and selectivity towards hydrogen abstracting from saturated hydrocarbons.[60]

1.8. AIMS AND OBJECTIVES

This study aimed to successfully synthesize and fully characterise four pyrazolyl-functionalized imidazolium salts varying in bulkiness and electronic properties and consequently examine the stability of the salts in various conditions. Thereafter to use the most stable salts to synthesize and characterize their Cu(II), Ni(II) and Co(II) complexes for the catalytic activation of paraffins. Due to their hygroscopic nature, only the complexes showing the most stability were chosen as the catalysts. The substrates chosen for this study were cyclohexane and *n*-octane. Cyclohexane was chosen as a substrate because of the value of its oxidised products which are cyclohexanol and cyclohexanone, both of which are industrially and commercially important for the manufacturing of Nylon-6,6, adipic acid and polyamide-6.[5, 61]

The first goal was to synthesize and characterise the starting materials required using NMR and mass spectrometry (MS) *i.e.* functionalised pyrazole, benzyl bromide, 1-(4-nitrophenyl)-1H-imidazole, ethyl imidazole, *etc*. Secondly, synthesize the pyrazolyl functionalised imidazolium salts and characterize them using NMR, MS, FTIR and elemental analysis (EA) and thereafter synthesize their corresponding transition metal complexes and characterize them using NMR,

MS, EA. Lastly to test the catalytic activity of the least hygroscopic complexes in the peroxidation of the saturated substrates.

1.9. OUTLINE OF DISSERTATION

Each chapter is typically independent, containing a general introduction with a brief literature review, experimental section, results and discussion (- as one section), and conclusions.

Chapter 2: Synthesis and characterization of novel pyrazolyl functionalized *n*-heterocyclic carbene ligands

Chapter 3: Synthesis and characterization of pyrazolyl functionalized NHC transition metal complexes

Chapter 4: Preliminary studies of cyclohexane oxidation

The last chapter, Chapter 5, amalgamates all the chapters and provides conclusions and documentation of the contributions of this research and future learning and research possibilities.

CHAPTER 2: SYNTHESIS AND CHARACTERIZATION OF NOVEL PYRAZOLYL FUNCTIONALIZED *N*-HETEROCYLIC CARBENE LIGAND PRECURSORS

2.1. SUMMARY

N- heterocyclic carbenes (NHC(s)) are among the most versatile and active donor ligands in transition-metal catalysis, organic and organometallic chemistries. Donor functionalized NHCs have attracted a lot of attention after the isolation of stable NHCs. This is because donor ligands such as pyridine and pyrazole form very weak labile bonds when coordinated to metal centres that break very easily and may lead to catalyst deactivation. NHCs, on the other hand form very strong σ bonds with metal centres; this is owed to the strong σ donating ability of the NHCs. When the two monodentate ligands (N-donor and NHC) are tethered together the strongly bonded NHCs anchors the labile ligand to the metal centre allowing for stronger binding to the metal centres. The ligand precursors (salts) introduced in this chapter vary in bulkiness and electronic properties of varying the substituents on the imidazole ring. All the ligand precursors proved to be unstable in air and moisture and decompose rapidly. They showed stability in solution in deuterated DMSO and dry solvents. The salts were synthesized under inert conditions and stored in a desiccator while further characterization was conducted. The salts were analysed using NMR (^{1}H, ^{13}C, ^{19}F), mass spectrometry, elemental analysis and FTIR. In addition, because all the salts had similar functional groups, the IR spectra were similar, varying only in peak intensities. Most of the salts were obtained as amorphous solids at best, and thus, no crystallographic data could be obtained. They are highly air-sensitive and quickly imbibed varying quantities of moisture upon exposure to air. Salt **2.2a,** (3-(2-(3,5-dimethyl-1H-pyrazol-1-yl)ethyl)-1-ethyl-1H-imidazol-3-ium chloride), was a highly viscous golden-brown oil that rapidly decomposed into a blackish paste when exposed to air for as little as a few seconds. The salts reported in this chapter are new with the exception of salts **2.1a,** (3-(2-(3,5-dimethyl-1H-pyrazol-1-yl)ethyl)-1-methyl-1H-imidazol-3-ium chloride) and **2.1b** (3-(2-(3,5-dimethyl-1H-pyrazol-1-yl)ethyl)-1-methyl-1H-imidazol-3-ium tetrafluoroborate).

2.2. INTRODUCTION

N- heterocyclic carbenes (NHCs) have become one of the most versatile and active donor ligands in homogeneous transition-metal (TM) catalysis.[26] They can stabilize and activate metal centres and due to their high trans effect and they can bind very tightly to metal centres.[62]

Since the pioneering work of Ölefe and Wanzlick which highlighted the transition metal coordination of azolium-based NHCs, the field of NHCs has exploded.[13, 27] The isolation of bench stable NHCs meant they could now be treated in the same way as the electron-rich phosphine ligands. Hermann and co-workers were some of the first to note the similarities between the electron-rich phosphine ligands and NHCs in their coordination chemistry.[27] NHCs have a strong σ donating ability with a negligible amount of π-back donation resulting in complexes of higher thermal and hydrolytic stability.[51] To take advantage of these properties the NHCs were applied as phosphine substitutes in homogeneous catalytic systems. It was most successful with catalytic systems such as the Pd(0) Heck reaction (C-C coupling) catalyst and the Ru(II) Grubbs metathesis catalyst where the substitution resulted in a considerable increase in catalytic activity.[41, 51] However, a null result was observed when an NHC was substituted into the Wilkinson's ([RhCl(PPh$_3$)$_3$]) hydrogenation catalyst and the Crabtree's ([Ir(PCy$_3$)(pyridine)(COD)]) catalyst, where very little to no improvement were observed. Nolan *et al.* reported that when NHC has substituted into the [Rh(IMes)PPh$_3$)$_2$ Cl] a decrease in the catalytic activity was observed.[63] Nevertheless, Crudden *et al.* discovered that the use of a phosphine scavenger such as CuCl resulted in a significant increase in the hydrogenation catalyst activity.[26]

Donor functionalized NHCs have attracted a lot of attention after the isolation of NHCs and their use as electron-rich phosphine substitutes. Donor functionalized NHCs are NHCs that contain at least one other anionic or neutral 2 electron donor atom such as C, N, O, S or P, resulting in a polydentate ligand on coordination to a metal centre. The interest in these ligands for applications in catalysis grew immensely due to the strong bonds formed between the NHC and the metal centre. However, despite the strong-bonding interactions, major complications existed.[51] Some electronic and structural (steric bulk) factors related to NHC ligands generated conditions where the ligands became susceptible to reductive elimination, leading to catalyst decomposition. The most stable and thermodynamically favoured conformation is the square planar arrangement for NHC ligated complexes.[51] A micro review on donor functionalized NHCs showed that these problems were related to the pπ orbitals of the ligand and d orbitals from the metal centre. One way to overcome this was to reduce the dihedral angle between the carbene ligand plane and the coordination plane.[51] This would require the use of an inflexible chelating NHC based ligand, hence the wing tip substitution on NHCs (resulting in polydentate

ligands) producing more rigid complexes. It is for this reason that donor functionalized NHCs in catalysis has gained so much attention.

Messerle *et al.* reported on the pyrazolyl functionalized NHC complexes of rhodium and iridium as excellent hydrogenation catalysts (the ligands used by Messerle are similar to salt **2.1a** reported herein), while Wang *et al.* have reported C-C coupling reactions using pyrazolyl functionalized NHCs as ionic liquids.[17, 26, 41] The strong σ donating ability of NHCs (resulting in very strong metal-ligand bonds), when coupled with an N-donor ligand such as pyrazole that bind loosely to a metal centre, where the NHCs anchor the labile ligand to the metal centre allowing for only partial dissociation gives rise to more active and selective catalysts. Donor functionalised NHC ligands were created as means to alleviate or reduce catalyst deactivation, which results from the dissociation of donor ligands. Pyrazole was selected as the *N*-donor ligand because of the properties it possesses. Pyrazole and its derivatives are excellent dinucleating ligands since they allow the formation of short and robust metal-metal bonds, hence resulting in bimetallic complexes.[64]

With the intent to exploit these properties, this study was aimed to synthesize and fully characterize four ligand precursors using spectroscopic and analytical techniques that include melting point, NMR, MS, EA and IR. The ligand precursors were chosen because of (*i.*) the novelty in terms of their synthesis and characterisation (except for ligand precursor **2.1a**), and (*ii.*) the effect of steric and electronic properties was evaluated by comparing subsequent reactivity of the ligand precursors. For the ligand synthesis, two routes were developed from 2-(3,5-dimethyl-1H-pyrazol-1-yl)ethanol. Both of the routes were used to synthesize ligand precursor **2.1**. However, Route 1 (the 1-(2-chloroethyl)-3,5-dimethyl-1H-pyrazole route) resulted in a product with a higher percentage yield and a higher percentage purity, hence it was chosen as the synthesis route for all four ligand precursors **2.1 – 2.4** (Scheme 2.1).
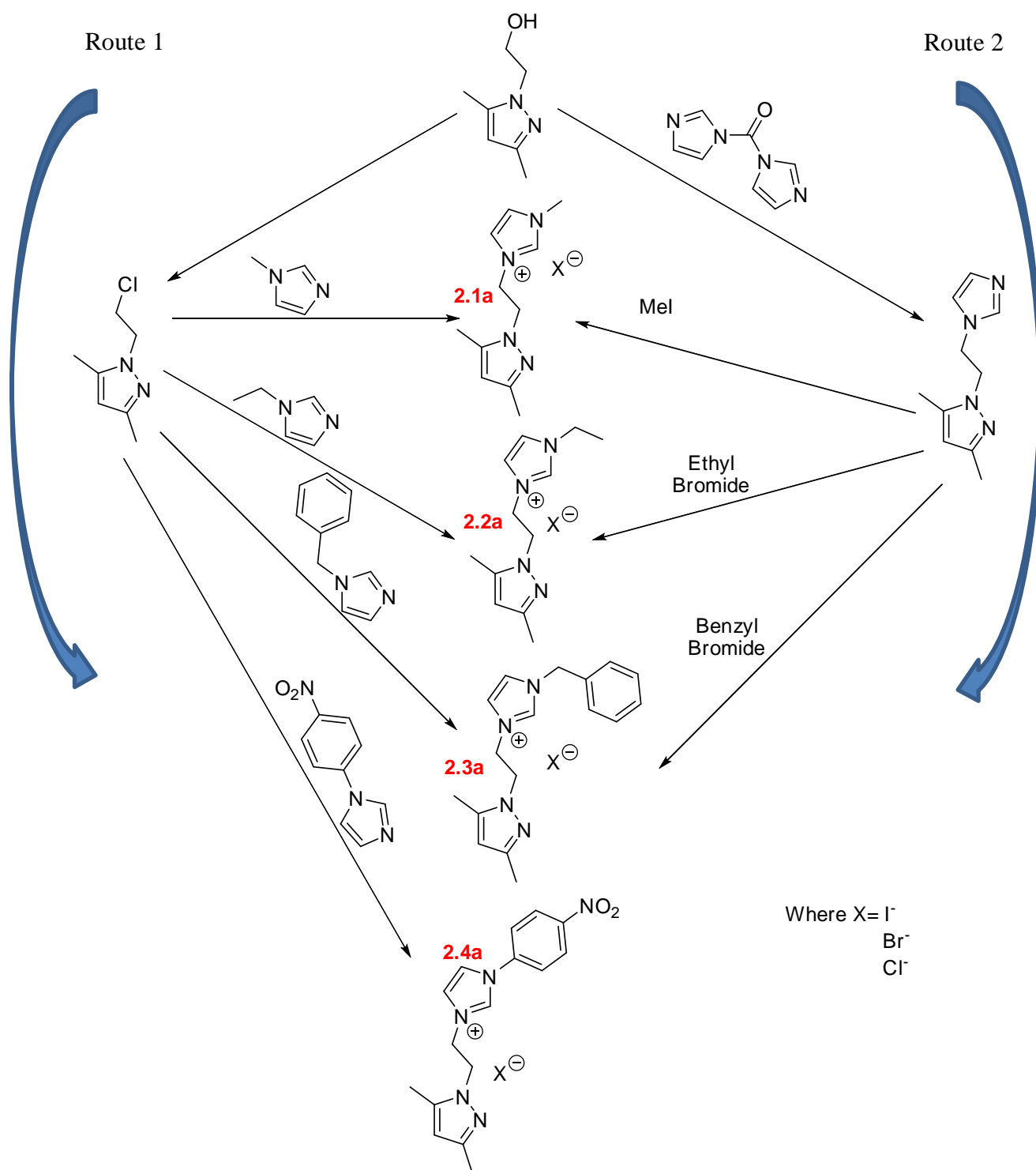
Scheme 2.1a: Routes for the synthesis of the ligand precursors. Route 1 is generally more productive

A study to improve the stability of the ligand precursors was done by changing the counter ion (anion metathesis) on the ligand precursors from chloride to tetrafluoroborate (BF_4^-). The method for the anion metathesis was the same for all the ligand precursors with percentage yields ranging between 80-90 %. Scheme 2.1b indicates the method for anion metathesis. Tetrafluoroborate was chosen over hexafluorophosphate (PF_6) because the tetrafluoroborate ligand precursors were more stable. This was determined using NMR, where the proton on the carbene (C_2) carbon was monitored. The C_2-H proton NMR as observed to slight shift upfield after changing the counter ion from chloride to PF_6 to BF_4. The observation suggest that the C_2-H proton was more shielded and hence more stable with BF_4 as the counter ion.
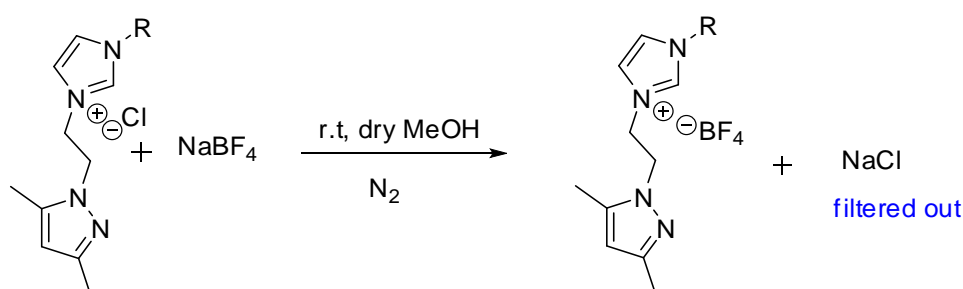
Scheme 2.1b: Method for anion metathesis

All raw data and supporting information such as tables, NMR spectra, FTIR spectra, MS spectra and EA graphs can be found in the appendix (appendix A, B, C and D, respectively) section of the dissertation.

Table 2.1: Characterization methods conducted for the ligand precursors

Salt ID	Ligand Precursor	NMR	MS	IR	Melting point	EA
2.1a	Me-Imid Cl⁻	√	√	√	√	√
2.1b	Me-Imid BF_4^-	√	√	√	√	√
2.2a	Et-Imid Cl⁻	√	√	√	- (oil)	√
2.2b	Et-Imid BF_4^-	√	√	√	- (paste)	√
2.3a	Bz-Imid Cl⁻	√	√	√	√	√
2.3b	Bz-Imid BF_4^-	√	√	√	- (paste)	√
2.4a	p-NO₂Ph-Imid Cl⁻	√	√	√	- (oil)	√
2.4b	p-NO₂Ph-Imid BF_4^-	√	√	√	- √	√

2.3. METHODS AND MATERIALS

2.3.1. *General information*

All solvents and reagents used in this study are HPLC grade, obtained from Sigma Aldrich or Merck with a minimum of 98% purity. The salts were tored in airtight clear glass vials, wrapped with parafilm for extra protection and placed in a desiccator. Some of the starting material that are already known *i.e.* 2-(3,5-dimethyl-1H-pyrazol-1-yl) ethanol, 1-(2-chloroethyl)-3,5-dimethyl-1H-pyrazole, *N*-benzyl imidazole, and *N*-ethyl imidazole were synthesized in the laboratory and characterized before use. Methods for their synthesis are included in this section.

2.3.2. *Synthesis of starting materials*

1. 2-(3,5-dimethyl-1H-pyrazol-1-yl) ethanol (Pyrazole-OH)
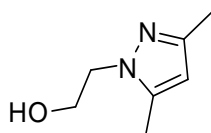
Pyrazole hydroxide was synthesized using a solvent free method adapted from van Wyk *et al*.[65] A mass of 10.31 g (10.2 mL, 0.1 mol) of 2,4-pentanedione (acetyl acetone or acac) was added dropwise to 2-hydroxyethyl hydrazine (7.61 g, 6.98 mL, 0.1 mol) in a Schlenk tube immersed in an ice bath with consistent stirring. The acac was added to the 2-hydroxyethylhydrazine dropwise to firstly prevent self-aldol condensation of acetyl acetone and to control the exothermic nature of the reaction. Thus, addition had to be done in such a way to prevent overheating while stirring vigorously to evenly distribute the droplets in the reaction chamber and forcing it to react by causing collision of particles in solution. Addition was completed within 20 min. The resultant liquid was stirred in an ice bath for 24 h and the solid product was recrystallised using diethyl ether at -20 °C. Actual yield = 9.94g, 70.9 %. Melting point 70-72 °C, LRMS =141.1 m/z (TOF MS ES+), ^{1}H NMR (400 MHz, CDCl$_3$): δ 5.79 (CH, s, 1H), 4.08 (OH, s, 1H), 4.03 (CH, m, 2H), 3.94 (CH, t, 2H), 2.22 (CH$_3$, s, 3H), 2.19 (CH, s, 3H). ^{13}C NMR (400 MHz, CDCl$_3$): δ 10.946, 13.348, 49.758, 61.598, 104.89, 139.53, 147.75

2. Synthesis of 1-(2-chloroethyl)-3,5-dimethyl-1H-pyrazole (pyrazole-Cl)
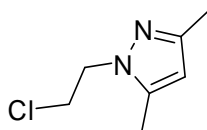
Pyrazole-OH (5 g, 0.035 mol) was dissolved in chloroform (20 mL) on an ice bath. After that thionyl chloride (SOCl$_2$) (18.8 g, 0.158 mol) was added dropwise to the solution while stirring, SO$_2$ gas escaped as vapour. The addition was completed after 5 min and the reaction was stirred in an ice bath for one hour and then completed at ambient temperature overnight. The reaction was monitored using TLC plates. Thereafter, the crude product was treated with 2×20 mL of 10% ammonia solution to neutralize the HCl while monitoring using blue litmus paper. The organics were extracted using chloroform (3 x 20 mL). The pH of the solution was monitored using litmus blue paper. The combined chloroform extract was then concentrated at reduced pressure. The target molecule was then isolated via column chromatography as eluent of DCM Both starting materials have divergent behaviour when spotted on TLC, as SOCl$_2$ was not visible in the iodine tank but visible under short wavelength UV light, while the (2-(3,5-dimethyl-1H-pyrazol-1-yl) ethanol) was visible only in an iodine tank. However, the desired product was visible both under UV light and in an iodine tank. All fractions containing the target molecule were pooled together and concentrated using rotavapour to afford the product as a golden-brown, viscous oil at room temperature. Actual yield= 3.33 g, 60%. LRMS =159.1 m/z (TOF MS ES+), ^{1}H NMR (400 MHz, CDCl$_3$): δ 5.67 (CH, s, 1H), 4.12 (CH, m, 2H), 3.73 (CH, t, 2H), 2.15 (CH$_3$, s, 3H), 2.010 (CH, s, 3H).

3. Synthesis of *N*-benzylimidazole
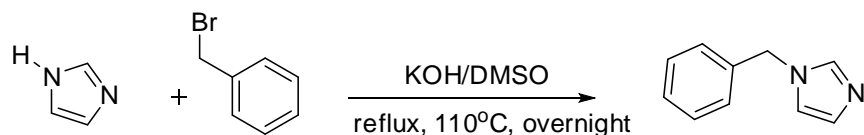
1*H*-imidazole (0.01 mol, 0.68 g) and KOH were crushed and dissolved in DMSO (40 mL) and stirred at room temperature for 1 h and then refluxed at 110 °C for an additional 1 h. To this solution was then added benzylbromide (0.01 mol, 1.71 g) dropwise and resulting mixture refluxed at 110 °C overnight while progress of the reaction monitored with TLC. Thereafter, chilled water was used to neutralize the unreacted base and all organics extract with DCM. The

combined organic extracted where then dried with anhydrous MgSO4 and filtered. Removal of all volatiles and subsequent column chromatography of the crude substance afforded the target product as eluent of ethyl acetate. The concentration of the eluent led to isolation of benzyl imidazole as an off-white solid. Yield: 1.30 g, 82%. Mp: 69 – 71 °C. LRMS = 158.08 m/z (TOF MS ES+), ^{1}H NMR (400 MHz, DMSO): δ 7.701 (CH, s, 1H), 7.442 (CH, s, 1H), 7.009 (CH, s, 1H), 7.335 (CH, s, 2H), 7.221 (CH, s, 3H), 5.532 (CH$_2$, s, 2H).

Solvent: 20% ethyl acetate: 80% DCM

Unreacted benzyl bromide

N-benzyl imidazole
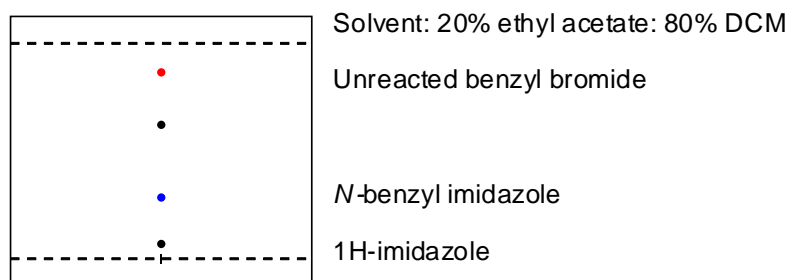
1H-imidazole

4. Synthesis of *N*-ethyl imidazole
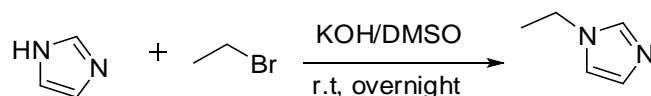
Imidazole (2.04 g; 0.03 mol) and excess KOH (2.52 g; 0.045 mol) were crushed together and dissolved in DMSO (40 mL). The solution was then stirred at room temperature for 5 h. Ethyl bromide (0.03 mol, 3.27 g) was then introduced dropwise at ice point, using a pasture pipette with continuous stirring. After the addition was completed, the ice bath was removed, and the mixture stirred overnight. The reaction content was then diluted with water and the crude product extracted using the liquid-liquid extraction method with chloroform (6×10 mL) as the extraction solvent. The organic layer containing the product was washed with water until the pH was approximately 7 and dried with CaCl$_2$. The product is a beige oil at room temperature. Yield: 1.96g, 68%. LRMS = 96.06 m/z (TOF MS ES+), ^{1}H NMR (400 MHz, DMSO): δ 7.403 (CH, s, 1H), 6.922 (CH, s, 1H), 6.659 (CH, s, 1H), 3.735 (CH$_2$, q, 2H), 1.077 (CH$_3$, t, 3H).

2.3.3. Synthesis of pyrazolyl functionalized imidazolium salts

1. Solvent free synthesis of 3-(2-(3,5-dimethyl-1H-pyrazol-1-yl) ethyl)-1-methyl-1H-imidazol-3-ium chloride (Salt **2.1a**)
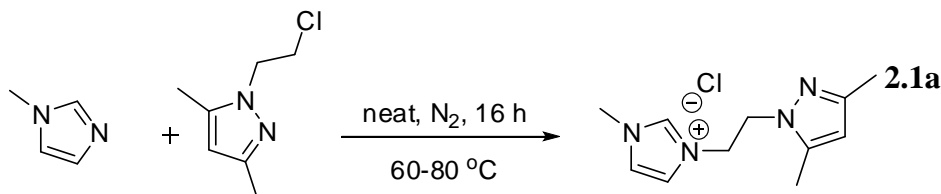
1-(2-chloroethyl)-1H-pyrazole (1.2 mmol, 0.2 g) was reacted with methylimidazole (1 mmol, 0.1 g) in a using Schlenk conditions neat, at 60-80 °C for 16h. The resultant brown oil (3-(2-(3,5-dimethyl-1H-pyrazol-1-yl) ethyl)-1-methyl-1H-imidazol-3-ium chloride) was cooled, and a TLC was done to determine the purity of the salt (it showed 100 % conversion). The oil formed light brown microcrystals when left to stand overnight. The crystals were washed first with dry ethyl acetate (2 x 10 mL) and then with diethyl ether (until the wash became clear). The crystals were then vacuum dried. Alternatively, the oil was washed with 10 mL aliquots of ethyl acetate until the wash became clear and the oil solidified, this is called crash cooling and results in smaller particles than when slow cooled. Yield: 0.239 g, 99 %. Molecular Formula: $C_{11}H_{17}ClN_4$. Mp: 170 – 175 °C. LRMS = 205.16 m/z (TOF MS ES+), ^{1}H NMR (400 MHz, DMSO-d_6): δ 9.14 (CH, s, 1H), 7.71 (CH, s, 1H), 7.58 (CH, s, 1H), 5.77 (CH, s, 1H), 4.58 (CH$_2$, t, ^2J=11 Hz, 2H), 4.38 (CH$_2$, t, ^3J= 5.89 Hz, 2H), 3.84 (CH$_3$, s, 3H), 2.06 (CH$_3$, s, 6H). ^{13}C NMR (400 MHz, DMSO-d_6): δ 146.79, 139.42, 137.05, 123.42, 122.54, 104.96, 48.391, 47.171, 35.663, 13.217, 10.212

Figures 2.1a and 2.1b show salt **2.1a** before anion metathesis.
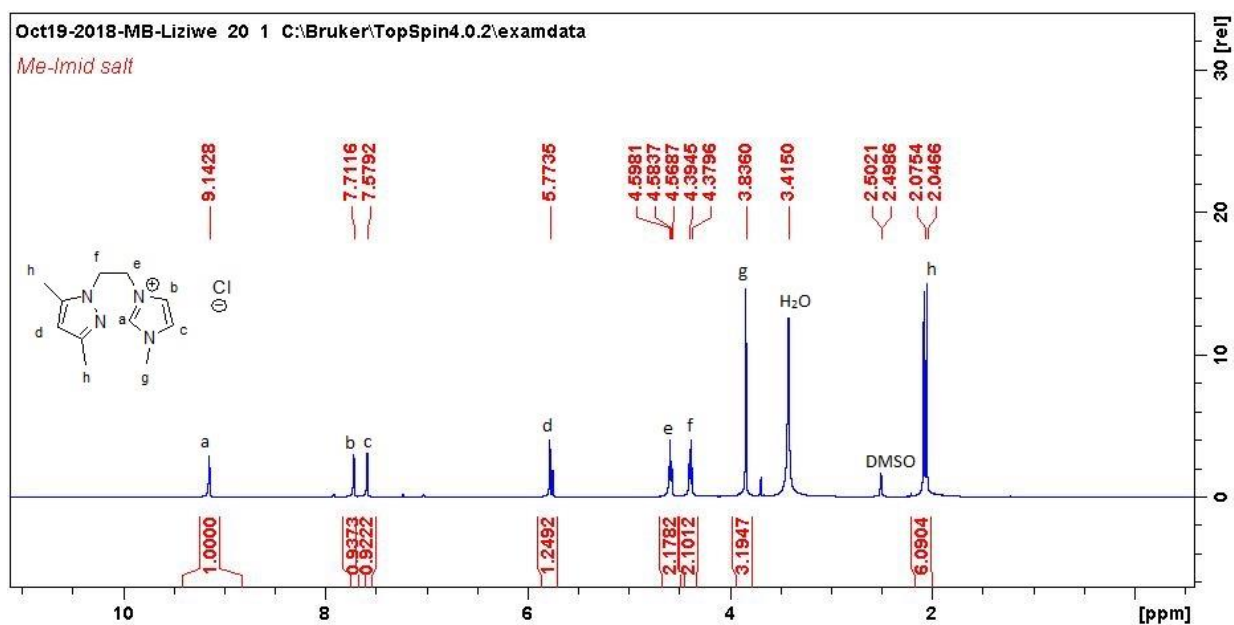
Figure 2.1a: ^{1}H NMR spectrum of salt **2.1a** (3-(2-(3,5-dimethyl-1H-pyrazol-1-yl) ethyl)-1-methyl-1H-imidazol-3-ium chloride)
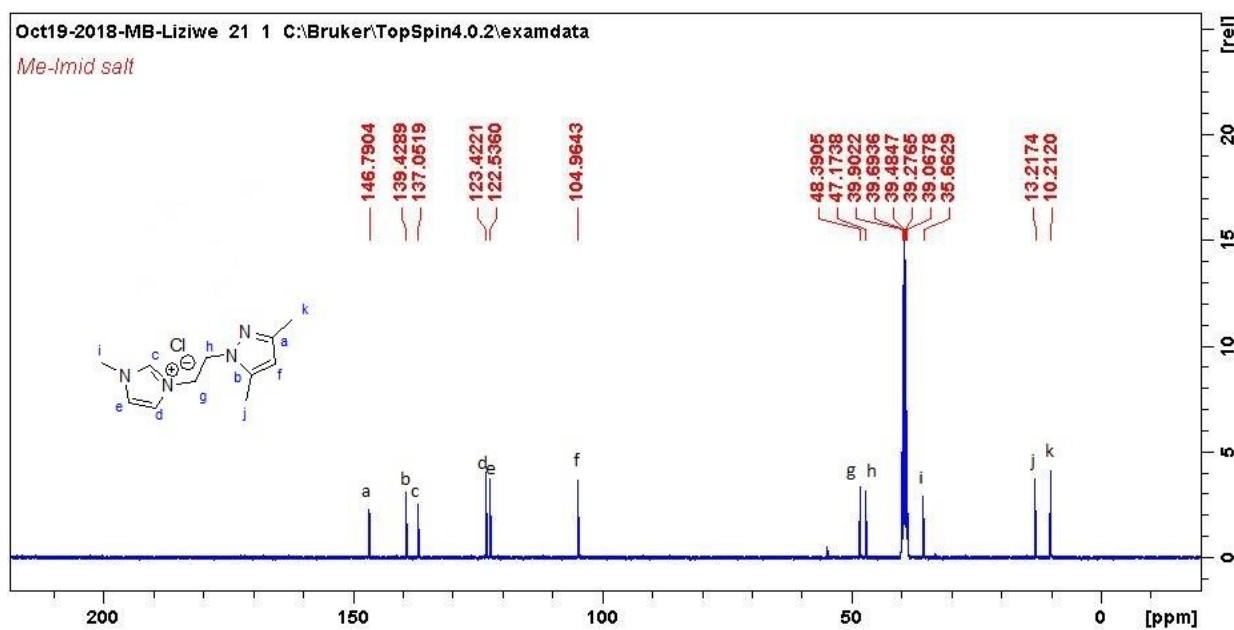
Figure 2.1 b: A representative ^{13}C NMR spectrum of salt **2.1a** (3-(2-(3,5-dimethyl-1H-pyrazol-1-yl) ethyl)-1-methyl-1H-imidazol-3-ium chloride)

Synthesis of Salt **2.1b**: 3-(2-(3,5-dimethyl-1H-pyrazol-1-yl) ethyl)-1-methyl-1H-imidazol-3-ium tetrafluoroborate
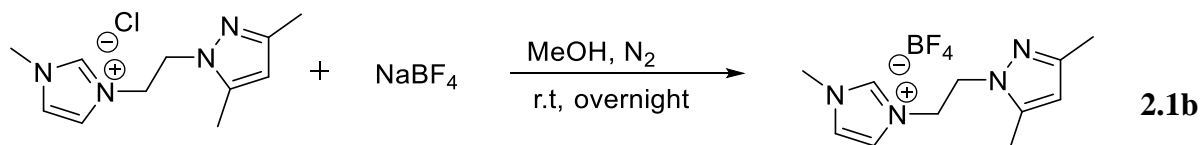
The chloride salt **2.1b** (0.50 g, 2.077 mmol) was dissolved in dry MeOH (15 mL) and stirred at room temperature under N_2 gas. $NaBF_4$ (0.228 g, 2.077 mmol) was added and a precipitate formed immediately and the reaction mixture allowed to stir overnight. Thereafter the reaction content was filtered and concentrated to 2 mL. The BF_4^- salt was then precipitated by addition of diethyl ether (2x10mL), decanted and residual solvent evacuated to dryness to yield the pure compound as brown powder. Yield: 0.422 g, 99 %. Molecular Formula: $C_{11}H_{17}BF_4N_4$. Mp: 84 – 87 °C, LRMS is similar for both salts **2.1a** and **2.1b** since only the cation is picked up by the detector. ^{1}H NMR (400 MHz, DMSO): Significant up field shift of the imidazolium proton resonance peak is the only noticeable different between the NMR spectra of both **2.1a** and **2.1b**. δ 8.82 (CH, s, 1H), 7.63 (CH, s, 1H), 7.49 (CH, s, 1H), 5.79 (CH, s, 1H), 4.54 (CH$_2$, t, ^{2}J=11 Hz, 2H), 4.34 (CH$_2$, t, ^{3}J= 5.89 Hz, 2H), 3.38 (CH$_3$, s, 3H), 2.05 (CH$_3$, s, 6H). ^{13}C NMR (400 MHz, DMSO-d$_6$): δ 146.84, 139.37, 136.87, 123.48, 122.51, 105.02, 48.457, 47.091, 35.644, 13.210, 10.097

Figure 2.2 shows salt **2.1b**
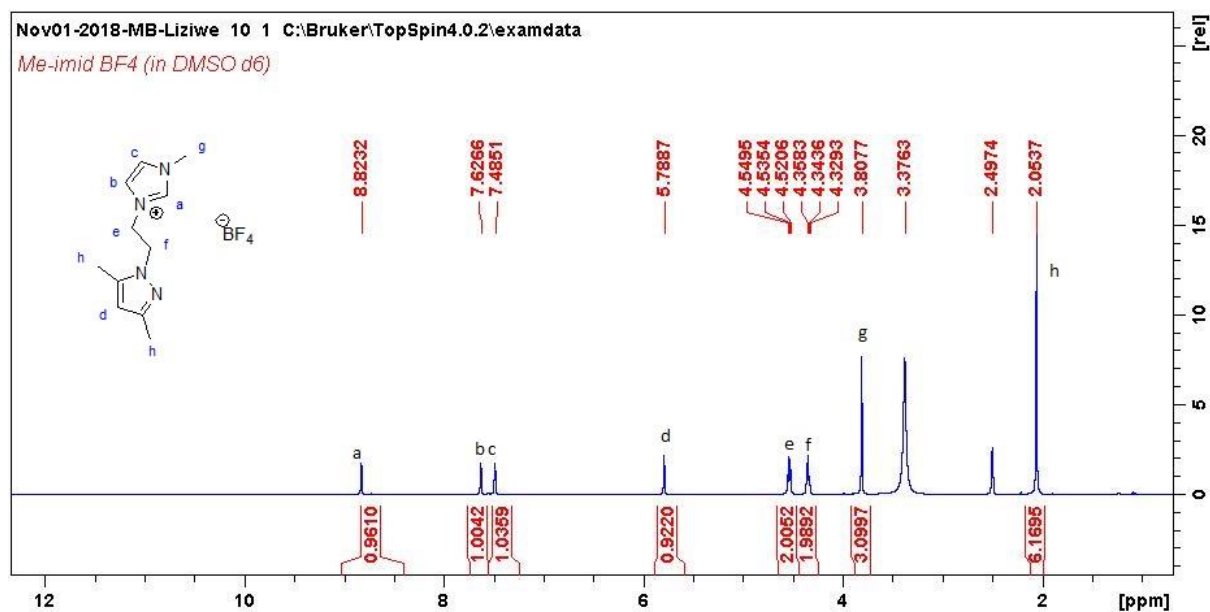
Figure 2.2: ^{1}H NMR spectrum of salt **2.1b** (3-(2-(3,5-dimethyl-1H-pyrazol-1-yl) ethyl)-1-methyl-1H-imidazol-3-ium tetrafluoroborate)

2. Solvent free synthesis of Salt **2.2a**: 3-(2-(3,5-dimethyl-1H-pyrazol-1-yl)ethyl)-1-ethyl-1H-imidazol-3-ium chloride
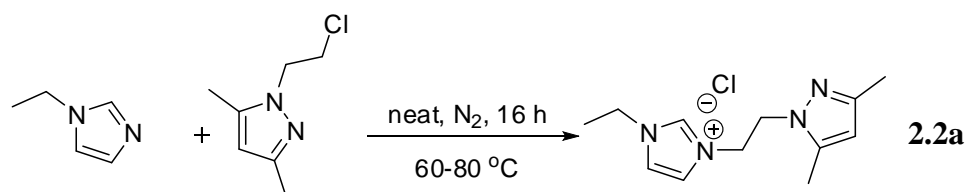
1-(2-chloroethyl)-1H-pyrazole (1.26 mmol, 0.2 g) was reacted with ethylimidazole (1.05 mmol, 0.1 g) in a similarly as salt **2.1a**. TLC was used to monitor the reaction. After 16 h (overnight) the reaction vessel still contained some unreacted starting material. The salt **2.2a** was sparingly soluble in ethyl acetate and completely soluble in methanol, while all starting material and other impurities were completely soluble in ethyl acetate; hence column chromatography was used to purify the crude product which afforded the salt as an eluent of methanol.[66] Removal of all volatiles and drying in vacuum yielded the pure **2.2a** as a highly viscous brown oil. Yield: 0.190 g, 71 %. Molecular Formula: $C_{12}H_{19}ClN_4$. LRMS = 219.17 m/z (TOF MS ES+), CHNS elemental analysis (experimental: theoretical): C= (40.733 %: 40.57 %), H= (7.800 %: 7.52 %), N= (14.361 %:14.99 %). ^{1}H NMR (400 MHz, DMSO-d_6): δ 9.096 (CH, s, 1H), 7.805 (CH, s, 1H), 7.611(CH, s, 1H), 5.770 (CH, s, 1H), 4.558 (CH$_2$, t, ^2J=11 Hz, 2H), 4.381 (CH$_2$, t, ^3J= 5.89 Hz, 2H), 4.169 (CH$_2$, q, ^2J=11.63 Hz, 2H), 2.043 (2CH$_3$ d, 6H), 1.349 (CH$_3$, t, 3H). ^{13}C NMR

(400 MHz, DMSO-d$_6$): δ 146.79, 139.39, 136.20, 122.64, 122.03, 104.93, 54.903, 48.515, 48.493, 15.286, 13.213, 10.150

Synthesis of Salt **2.2b**: 3-(2-(3,5-dimethyl-1H-pyrazol-1-yl) ethyl)-1-ethyl-1H-imidazol-3-ium tetrafluoroborate
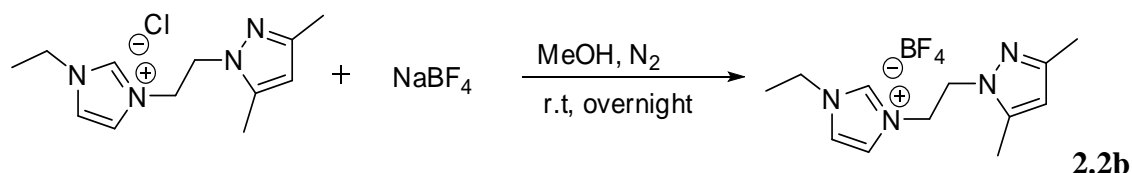
This salt was synthesized using the same method used to synthesize salt **2.1b**. The salt, **2.2b** was obtained as a highly hygroscopic pale brown paste. Yield: 0.595 g, 90 %. Molecular Formula: C$_{12}$H$_{19}$BF$_4$N$_4$. ^{1}H NMR (400 MHz, DMSO): δ 8.858 (CH, s, 1H), 7.729 (CH, s, 1H), 7.533 (CH, s, 1H), 5.783 (CH, s, 1H), 4.532 (CH$_2$, t, ^{2}J=11 Hz, 2H), 4.361 (CH$_2$, t, ^{3}J= 5.89 Hz, 2H), 4.1502 (CH$_2$, q, ^{2}J=11.63 Hz, 2H), 2.043 (2CH$_3$ s, 6H), 1.347 (CH$_3$, t, 3H). ^{13}C NMR (400 MHz, DMSO-d$_6$): δ 147.39, 139.93, 136.54, 123.08, 122.52, 105.49, 49.062, 47.609, 44.643, 15.702, 13.668, 10.521

3. Solvent free synthesis of salt **2.3a**: 1-benzyl-3-(2-(3,5-dimethyl-1H-pyrazol-1-yl) ethyl)-1H-imidazol-3-ium chloride
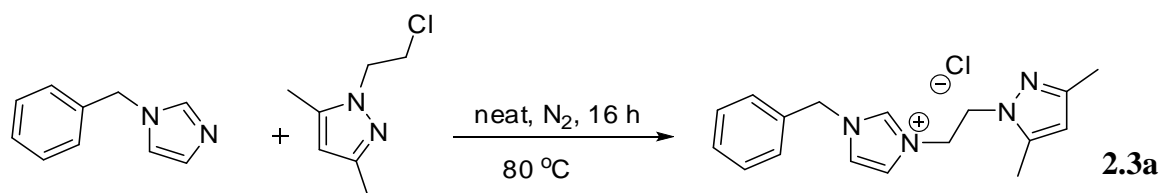
N-benzyl imidazole (0.23g, 1.45 mmol) and 1-(2-chloroethyl)-1H-pyrazole (0.277g, 1.74 mmol) were reacted neat in a Schlenk tube at 80 °C under inert N$_2$ for 16 h. Unlike other salts synthesized by solvent-free technique, this reaction tends to yield better when ran at higher temperature than the 60 °C in the analogues salts. The unreacted starting material may be removed by either (*i.*) running a column or, (*ii.*) washing the salt with diethyl ether (both starting materials are soluble in the ether). The salt precipitated out of solution, and was washed until the wash became clear, and was vacuum dried to give creamy white powder. Yield: 0.234 g, 51%. Molecular Formula: C$_{17}$H$_{21}$ClN$_4$ Mp.: 145 – 150 °C. LRMS = 281.18 m/z (TOF MS

ES+), ^{1}H NMR (400 MHz, DMSO): δ 9.008 (CH, s, 1H), 7.7714 (CH, s, 1H), 7.6295 (CH, s, 1H), 7.4120 (CH, m, 1H), 7.3179 (CH$_2$, m, ^{2}J= 2.0 Hz, 2H), 5.7328 (CH, s, 1H), 5.3925(CH$_2$, s, 2H), 4.5669 (CH$_2$, t, ^{2}J= 11.2462 Hz, 2H), 4.3676 (CH$_2$, t, ^{2}J=11.2462 Hz, 2H), 2.0066 (CH$_3$ s, 3H), 1.9601 (CH$_3$, t, 3H). ^{13}C NMR (400 MHz, DMSO-d$_6$): δ 146.87, 139.28, 136.55, 134.74, 128.91, 128.67, 128.00, 123.08 122.49, 104.94, 54.863, 51.773, 48.768, 44.643, 13.227, 10.059

Synthesis of salt **2.3b**: 1-benzyl-3-(2-(3,5-dimethyl-1H-pyrazol-1-yl) ethyl)-1H-imidazol-3-ium tetrafluoroborate

2.3b
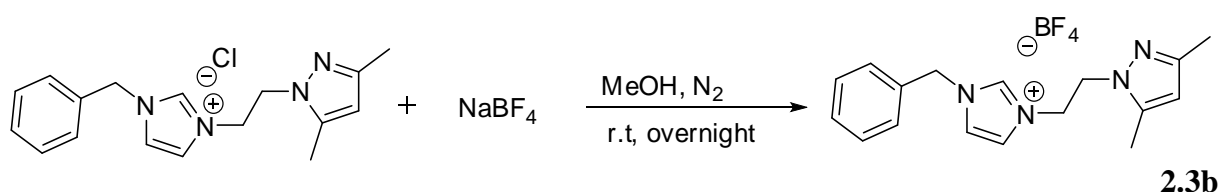
This salt was synthesized using the same method used to synthesize salt **2.1b**. The product was obtained as a highly hygroscopic creamy white paste, which decomposes when exposed to air. Yield: 0.081 g, 99%, Molecular Formula: C$_{17}$H$_{21}$BF$_4$N$_4$ (TOF MS ES+), ^{1}H NMR (400 MHz, DMSO): δ 8.9359 (CH, s, 1H), 7.7415 (CH, s, 1H), 7.5979 (CH, s, 1H), 7.4120 (CH, m, 1H), 7.3179 (CH$_2$, m, ^{2}J= 2.0 Hz, 2H), 5.729 (CH, s, 1H), 5.3793 (CH$_2$, s, 2H), 4.5626 (CH$_2$, t, ^{2}J= 11.2462 Hz, 2H), 4.3613 (CH$_2$, t, ^{2}J=11.2462 Hz, 2H), 2.0072 (CH$_3$ s, 3H), 1.9520 (CH$_3$, t, 3H). ^{13}C NMR (400 MHz, DMSO-d$_6$): δ 147.42, 139.82, 136.99, 135.18, 129.41, 129.19, 128.52, 123.53, 122.59, 105.46, 52.290, 49.168, 47.509, 13.693, 10.479

4.   Synthesis of salt **2.4a**: 3-(2-(3,5-dimethyl-1H-pyrazol-1-yl) ethyl)-1-(4-nitrophenyl)-1H-imidazol-3-ium chloride
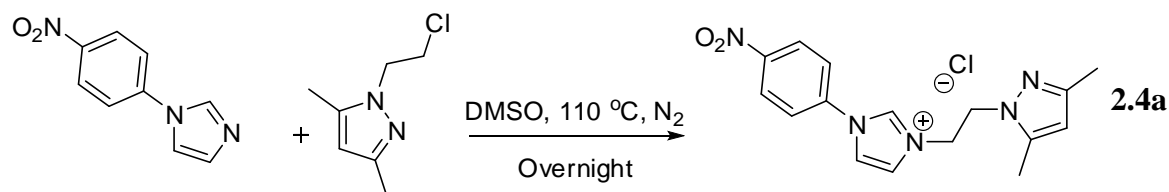
1-(4-nitrophenyl)-1H-imidazole (0.39g, 2.06 mmol) was dissolved in 1 mL of DMSO and then 1-(2-chloroethyl)-1H-pyrazole (0.39g, 2.47 mmol) was added dropwise and the two were reacted at 110 °C under inert conditions for 16 h. At the end of the reaction time, the content was washed with ether (4 x 30 mL) or till the washing becomes clear to displaced the DMSO.

Residual starting materials are thereafter washed out with ethyl acetate by trapping the salt on silica in a column. This made it possible to obtain the salt as eluent of ethyl acetate: MeOH (1:1). Removal of all volatiles in vacuo afforded the pure salt as highly viscous brown oil. Yield: 0.322 g, 50%. Molecular formula: $C_{16}H_{18}ClN_5O_2$, LRMS = 312.15 m/z (TOF MS ES+), viable CHNS elemental analysis data could not be obtained as the salt quickly imbibed varying quantities of moisture (FTIR broad peaks at 3349–3355 cm^{-1}). ^{1}H NMR (400 MHz, DMSO): δ 10.1084 (CH, s, 1H), 8.4944 (CH, m, 3H, ^{2}J= 8.701 Hz), 8.0746 (CH, m, 2H, ^{2}J= 8.730 Hz), 7.8853 (CH, s, 1H), 5.8601 (CH, s, 1H), 4.6892 (CH$_2$, t, 2H, ^{2}J= 10.825 Hz), 4.5323 (CH$_2$, t, 2H, ^{3}J= 5.473 Hz), 2.1787 (CH$_3$ s, 3H), 2.0212 (CH$_3$, s, 3H). ^{13}C NMR (400 MHz, DMSO-d$_6$): δ 147.61, 146.76, 140.05, 139.06, 136.87, 125.63, 124.01, 122.81, 120.90, 105.32, 48.766, 46.915, 12.975, 10.327

Synthesis of salt **2.4b**: 3-(2-(3,5-dimethyl-1H-pyrazol-1-yl)ethyl)-1-(4-nitrophenyl)-1H-imidazol-3-ium tetrafluoroborate
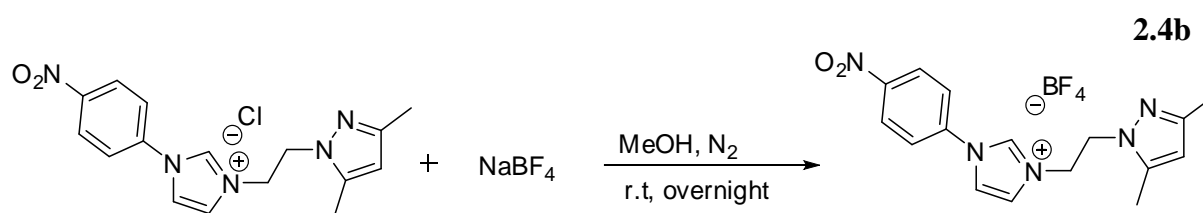
Salt **2.4b** was synthesized similarly to salt **2.1b**. The pure salt was obtained as a relatively, air stable yellowish-brown powder. Yield: 0.232 g, 83 %, Mp.: 127 – 130 °C. Molecular Formula: $C_{16}H_{18}BF_4N_5O_2$, LRMS = 312.15 m/z (TOF MS ES+), ^{1}H NMR (400 MHz, DMSO): δ 10.1084 (CH, s, 1H), 8.4944 (CH, m, 3H, ^{2}J= 8.701 Hz), 8.0746 (CH, m, 2H, ^{2}J= 8.730 Hz), 7.8853 (CH, s, 1H), 5.8601 (CH, s, 1H), 4.6892 (CH$_2$, t, 2H, ^{2}J= 10.825 Hz), 4.5323 (CH$_2$, t, 2H, ^{3}J= 5.473 Hz), 2.1787 (CH$_3$ s, 3H), 2.0212 (CH$_3$, s, 3H). ^{13}C NMR (400 MHz, DMSO-d$_6$): δ 147.59, 146.81, 139.71, 139.05, 136.82, 125.66, 123.99, 122.77, 120.89, 105.19, 49.058, 46.862, 13.110, 10.289

2.4. RESULTS AND DISCUSSION

This chapter reports on the synthesis and full characterization of ligand precursors with properties that are beneficial in organic transformations and catalysis. Salt **2.1a** has been previously reported and has shown remarkable activity as a ligand precursor for metal-NHC complexes applied as a catalyst in the hydrogenation reaction.[26, 41]

2.4.1. Synthesis and characterization of starting material

The adaptation of established experimental procedures was used to synthesize the starting material.[26, 65] First, 2-(1H-pyrazol-1-yl) ethanol was prepared by adding acetyl acetone (acac) dropwise to 2-hydroxyethyl hydrazine. The OH group was substituted with a Cl group by reacting 2-(1H-pyrazol-1-yl) ethanol with thionyl chloride at ambient temperature. The immediate and spontaneous effervescence of gas with a strong odour similar to that of a burnt match stick suggested the liberation of SO_2 as a by-product of the addition of $SOCl_2$ to the reaction vessel, the progress of the reaction was monitored using TLC. The nucleophilic substitution becomes necessary as alcohols are strong bases with a pKa 16-18, thus making the OH group a poor leaving group. However, halides are good leaving groups and a very poor base with a pKa value of -8, making the Cl a viable substitute for the OH group on the pyrazole moiety.[67] Other acid by-product, i.e. HCl, was removed from the resulting crude mixture with the addition of 10% aqueous ammonia solution, while the pH of the solution was monitored using litmus blue paper. Incomplete removal of the acidic by-product was observed to result in unsuccessful alkylation of *N*-substituted imidazole with pyrazolylalkyl chloride to yield corresponding imidazolium salt. The product, 1-(2-chloroethyl)-1H-pyrazole was purified by column chromatography. Both 1-(2-chloroethyl)-1H-pyrazole and 2-(1H-pyrazol-1-yl) ethanol were characterized using NMR, mass spectroscopy and IR.

Figure 2.3 shows a comparison between the proton NMR spectra of 1-(2-chloroethyl)-1H-pyrazole and 2-(1H-pyrazol-1-yl) ethanol. The absence of the OH proton (labelled e) in the NMR spectrum of 1-(2-chloroethyl)-1H-pyrazole suggests that the nucleophilic substitution was successful. Chloride has two isotopes that are NMR active, ^{35}Cl and ^{37}Cl, with ^{35}Cl being three times more abundant and more sensitive than ^{37}Cl, however, ^{35}Cl has a $^3/_2$ magnetic spin with a quadrupolar nucleus resulting in broad, short peaks. The chemical shift of ^{35}Cl is approximately 1100 ppm. This means that the CH_2 closest to chloride was split by the adjacent hydrogens on the CH_2 and the Cl group, resulting in a multiplet (d in Figure 2.3). The impurity

showed by the NMR of 1-(2-chloroethyl)-1H-pyrazole in the aromatic region corresponds to the solvent peak of ethyl acetate,[68] which was a side product of the synthesis reaction.
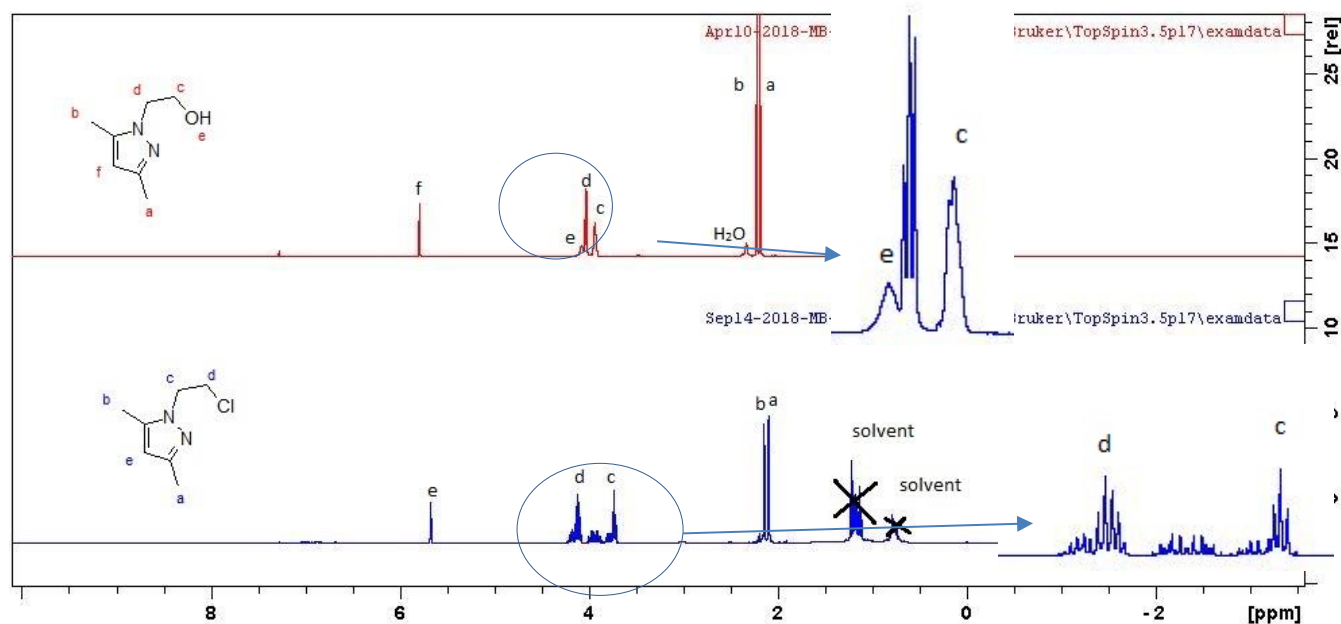
Figure 2.3: Comparison between the NMR spectra of 1-(2-chloroethyl)-1H-pyrazole and 2-(1H-pyrazol-1-yl) ethanol1-(2-chloroethyl)-1H-pyrazole and 2-(1H-pyrazol-1-yl) ethanol.

Analysis by FTIR spectroscopy shows the disappearance of the strong absorption peak at 3238 cm^{-1} corresponding to the vibrational stretch of an intermolecular OH in the spectrum of 1-(2-chloroethyl)-3,5-dimethyl-1H-pyrazole, as opposed to that observed in the spectrum of 2-(3,5-dimethyl-1H-pyrazol-1-yl) ethanol. This was positive evidence that the nucleophilic substitution was successful, which also supports the results obtained from the NMR data (Appendix A). The FT-IR data is included as Appendix B.

The mass to charge ratio (m/z) of the molecular ion peaks corresponding to each of the compounds reported herein is equivalent to the molar mass of the compounds because no fragmentation has occurred and only one electron has been removed or a proton added to make the species charged. The base peak which is usually the most intense peak is due to the most stable fragment of each compound. For example, the mass to charge ratio of 2-(3,5-dimethyl-1H-pyrazol-1-yl) ethanol is 141 m/z for TOF MS ES^{+}, while the mass to charge ratio of 1-(2-chloroethyl)-3,5-dimethyl-1H-pyrazole was 159 m/z TOF MS ES^{+}, corresponding to the molecular mass of each compound.

2.4.2. Synthesis and characterization of pyrazolyl functionalized imidazolium salts

Three of the four of the salts reported in this chapter are new *i.e.* salts **2.2**, **2.3** and **2.4**. Two routes for ligand precursor synthesis were developed successfully for the synthesis of **2.2a**, **2.3a**, **2.4a**. The first route involved a bimolecular nucleophilic substitution reaction (Scheme 2.2), where the halide was displaced from 1-(2-chloroethyl)-3,5-dimethyl-1H-pyrazole resulting in the formation of a primary carbocation intermediate molecule which is then substituted by *N*-methyl imidazole forming salt **2.1a** with chloride as the counter ion. Route two involved 1-(2-(1H-imidazol-1-yl) ethyl)-3,5-dimethyl-1H-pyrazole nucleophilic attack by the lone pair of electrons on the nitrogen on the polar covalent Me-I bond thereby displacing iodide (Scheme 2.3), and forming salt **2.1a** with iodide as the counter-ion.
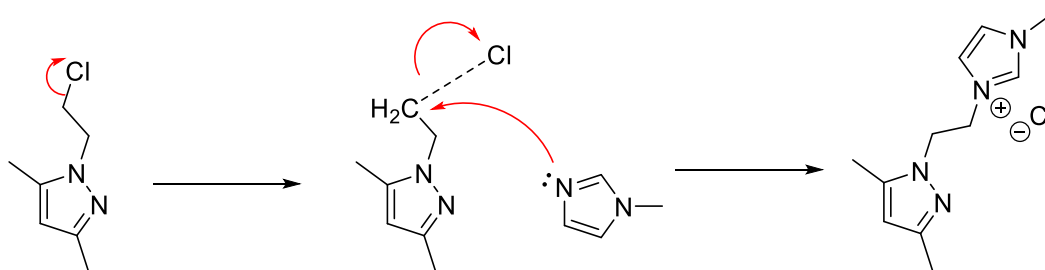
Scheme 2.2: Illustration of route one for ligand precursor synthesis
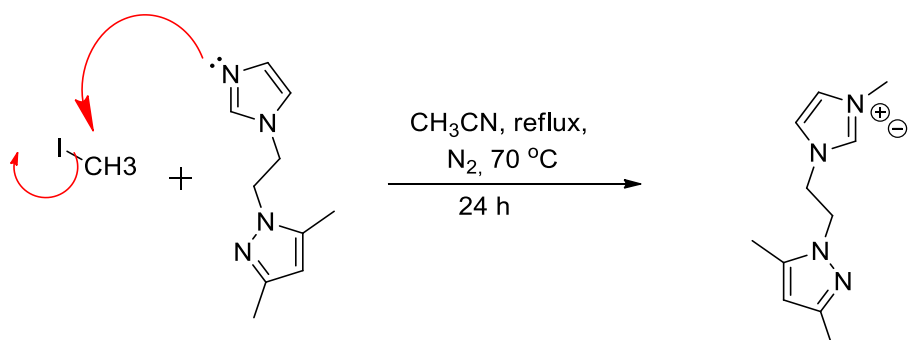
Scheme 2.3: Illustration of route two for ligand precursor synthesis

All the salts were characterized using NMR, mass spectrometry and FTIR. Obtaining viable elemental analysis data for the salts was difficult as most are hygroscopic solids or oils. This is common for imidazolium salts.[69] However, the clean/ well-resolved NMR data and exact HRMS results established their purity. Table 2.2 shows some of the physical properties of the salts such as colour, melting point and phase and chemical composition.

Table 2.2: Characterization data for the synthesis of the ligand precursors.

Salt ID	Ligand Precursor	M.p. / °C	Yield /%	Colour & Phase	Chemical composition
2.1a	Me-Imid Cl⁻	170-175	99	Beige Solid	$[C_{11}H_{17}N_4]^+ Cl^-$
2.1b	Me-Imid BF₄⁻	84-87	99	Beige Solid	$[C_{11}H_{17}N_4]^+ BF_4^-$
2.2a	Et-Imid Cl⁻	- (oil)	71	Brown Liquid	$[C_{12}H_{19}N_4]^+ Cl^-$
2.2b	Et-Imid BF₄⁻	- (paste)	90	Beige Paste	$[C_{12}H_{19}N_4]^+ BF_4^-$
2.3a	Bz-Imid Cl⁻	145-150	51	Beige Solid	$[C_{17}H_{21}N_4]^+ Cl^-$
2.3b	Bz-Imid BF₄⁻	- (paste)	99	Beige Paste	$[C_{17}H_{21}N_4]^+ BF_4^-$
2.4a	pNO₂Ph-Imid Cl⁻	- (oil)	50	Yellowish brown Liquid	$[C_{16}H_{18}N_5O_2]^+ Cl^-$
2.4b	pNO₂Ph-Imid BF₄⁻	127-130	83	Yellow Solid	$[C_{16}H_{18}N_5O_2]^+ BF_4^-$

Salt **2.1a** was synthesized using both routes to determine which one was better in terms of higher conversion, yield and selectivity. The salt synthesized using route one was a brown oily substance with a lot of impurities observed in the NMR spectrum, hence it required washing with diethyl ether since all the starting material was soluble in diethyl ether and the desired product was not. However, the yield was low (48%), which suggested that the selectivity to the desired product using route one was very low. When ethyl acetate was added to the reaction vessel containing the product it separated into an oily or gel-like substance that sank to the bottom of the reaction vessel. This indicated that the product was sparingly soluble in ethyl acetate while the starting material was completely soluble in the solvent. The LRMS obtained for this compound showed a lot of fractions in the molecule, which could not be accounted for; this was a clear indication of possible impurities which corroborated the NMR data obtained for this salt (Figure 2.4).

The product was purified using column chromatography to separate it from the unreacted starting material, and was obtained as an eluent of a mixture of ethyl acetate and methanol (50/50). Subsequent concentration in vacuo led to the isolation of the pure salt as an orange-brown oil. The salt synthesized using route two was a brown grainy solid. TLC was used to confirm if any reaction had occurred and its progress. 100% conversion was observed on the

TLC plate with only the spot for the salt unmoved from the origin in MeOH 100% solvent system. Both synthesized salts were highly hygroscopic and decomposed in minutes when exposed to air. The salt synthesized using route two was more stable due to higher purity. Hence, when the salt synthesized using route two was left overnight in a vacuum-sealed airtight reaction vessel to cool, it solidified forming pale brown rough granules. This is also the case as when the crude salt is washed with diethyl ether at least three times after it has cooled to room temperature. The granules observed when the salt is washed with diethyl ether are smaller and more defined. Therefore, route two was determined to produce a higher yield and higher selectivity to the desired product.
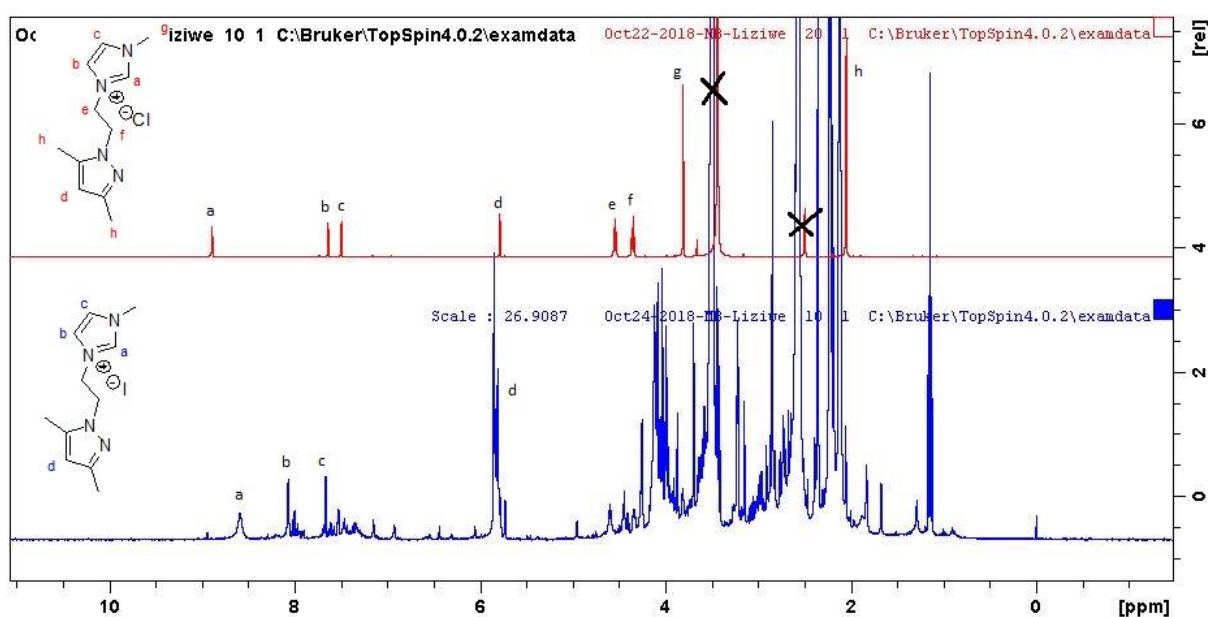
Figure 2.4: Comparison of H^1 NMR signals of Salt **2.1** synthesized using route 1 (bottom) and route 2 (top)

The salt synthesis of Salts **2.1 – 2.3** were first attempted using acetonitrile as the solvent; however, no reaction was observed. Messerle *et al.* reported that nucleophiles or polar solvents such as acetonitrile and DMF competed with the *N*-alkyl substituted imidazole in displacing chloride from the 1-(2-chloroethyl)-3,5-dimethyl-1H-pyrazole.[41] This would lead to either the formation of unwanted side products or no reaction. Messerle *et al.* used non-polar solvents such as toluene to synthesize salt **2.1** successfully. Salts **2.1 – 2.3** were therefore synthesized by a solvent free method by reacting 1-(2-chloroethyl)-3,5-dimethyl-1H-pyrazole and the imidazole source at mild temperatures. The reaction proceeds via the S$_N$2 reaction route where the halide on the 1-(2-chloroethyl)-3,5-dimethyl-1H-pyrazole was displaced by the lone pair of

electrons on the sp^2 nitrogen in the substituted imidazole (wingtip substituents are methyl, ethyl, benzyl and nitrobenzyl). However, the salt required recrystallization to purify it, unlike the method introduced in this study. No recrystallization was necessary since complete conversion was observed on a TLC plate. All starting material was soluble in diethyl ether, and all of the salts (**2.1 – 2.3**) were not. Hence, washing the salts with diethyl ether was sufficient for salts **2.1a** (1-(2-(3,5-dimethyl-1H-pyrazol-1-yl) ethyl)-3-methyl-1H-imidazol-3-ium chloride) and **2.3a** (1-benzyl-3-(2-(3,5-dimethyl-1H-pyrazol-1-yl) ethyl)-1H-imidazol-3-ium chloride), as they both precipitated out of solution immediately when the diethyl ether was added.

Salt **2.2a** (3-(2-(3,5-dimethyl-1H-pyrazol-1-yl) ethyl)-1-ethyl-1H-imidazol-3-ium chloride) was synthesized by the same method as salts **2.1a** and **2.3a**, and after several washes with diethyl ether, the salt remained as an oil. Despite all the washing, preliminary ^{1}H NMR spectrum of the washed salt indicated some level of impurities. Hence, purification was achieved using the improved technique of column chromatography reported by Ibrahim and Bala.[66] Salt **2.2a** was partially soluble in ethyl acetate and completely soluble in methanol. This required extreme caution to reduce the amount of salt **2.2a** discarded with the impurities since all the impurities were soluble in the ethyl acetate. The impurities were eluted out of the column using ethyl acetate, gradually the polarity of the elution solvent was increased by adding methanol. The salt was collected as an eluent of 50 % ethyl acetate: 50 % methanol after all the impurities had been eluted out. The column was flushed out with 100 % methanol and all remaining salt was collected.

The reactions were monitored using TLC and at 16 h, the limiting reagent (substituted imidazole) was fully consumed, and the reaction completed. Ligand precursor **2.1** could also be synthesized using toluene as the solvent. Unfortunately, the reaction route takes longer and requires recrystallization with diethyl ether and acetone to purify the salt. Whereas the solventless method introduced in this report shows a quantitative conversion and selectivity to the desired product only, hence there was no need for recrystallization. Page *et al.* reported on a method where a pyrazole moiety was reacted with formaldehyde under basic conditions producing a hydroxymethylpyrazole species, which was then reacted with thionyl chloride to give a chloromethylpyrazole intermediate that could be isolated as a hydrochloric acid salt. Subsequent reaction of the isolated hydrochloric acid intermediate with two equivalents of *N*-substituted imidazole yielded the desired pyrazolyl functionalized imidazole products.[26]

The observed similarity and excellent solubility of synthons for the preparation of salts **2.1a** and **2.3a** in diethyl ether was taken to advantage. It allows for the purification of the salts without much hassle. Thus, simple washing of the crude product with enough diethyl ether precipitated out the salts as air-sensitive hygroscopic, light beige amorphous solids differing in texture. **2.1a** is isolated as rough, large granules, while **2.3a** is very fine powder. The sensitivity of the salts to air was tested by taking small amounts of each and exposing them to air. Salt **2.1a** absorbed moisture and dissolved quicker than salt **2.1b**. However, after dissolution, **2.1a** retained its beige colour and **2.1b** changed from beige to a dark greenish-black colour suggesting decomposition. No further analysis was conducted on the salts exposed to air/ moisture.

After the synthesis, the salts were subjected to anion metathesis with the aim to improve their stability. This objective led to the formation of **2.1b** and **2.3b**, respectfully from salt **2.1a** and **2.3a**. Ligand anion metathesis was achieved by stirring methanolic solution of the chloride salts with sodium tetrafluoroborate. The chloride anion which initially forms the counter ion on the imidazolium moiety is then substituted by the tetrafluoroborate anion. Consequently, the precipitated sodium salt is trapped on bed of Celite during filtration. Both salts **2.1a** and **2.1b** were characterized by NMR, MS and CHN elemental analysis.

An up field shift in the ^{1}H NMR resonance peak for the C2-H imidazolium proton (Figure 2.5), from 9.14 ppm in the spectrum of salt **2.1a** to 8.82 ppm in the spectrum of salt **2.1b** suggested that the imidazolium proton was more shielded after the anion metathesis and thus more stable. Figure 2.6 shows an ^{1}H NMR spectra comparison of salt **2.1** (3-(2-(3,5-dimethyl-1H-pyrazol-1-yl) ethyl)-1-methyl-1H-imidazol-3-ium) before and after anion metathesis.
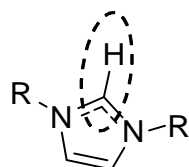
Figure 2.5: An illustration C$_2$-H that is affected by anion metathesis
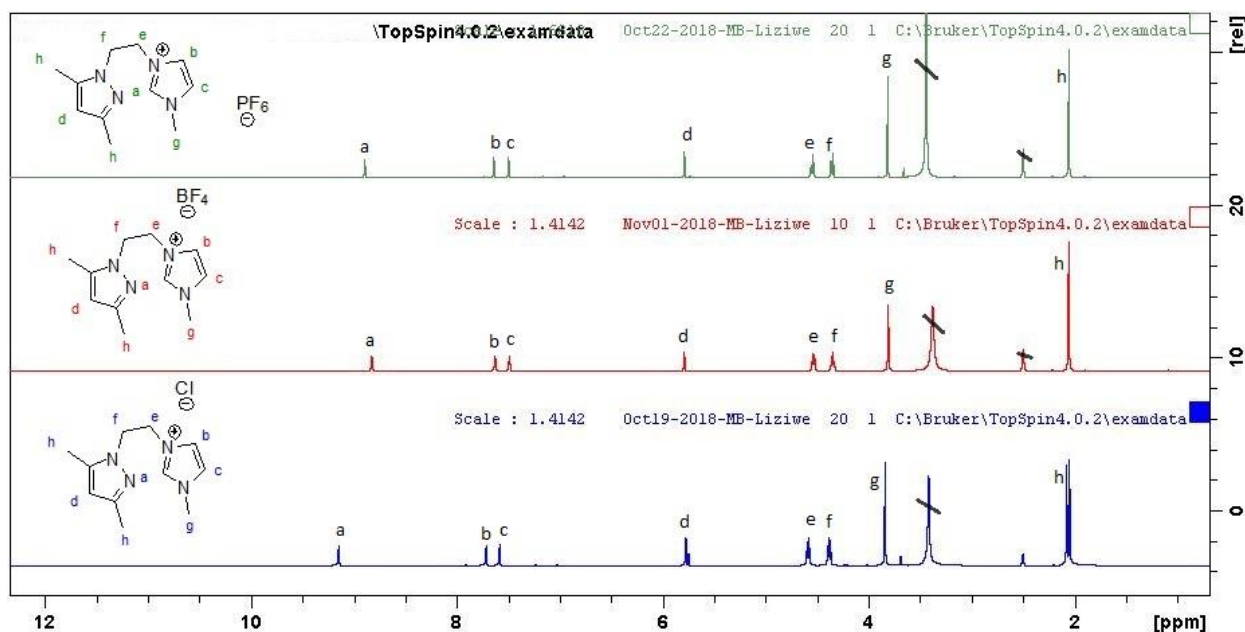
Figure 2.6: Comparison of the spectra of salt **2.1** (3-(2-(3,5-dimethyl-1H-pyrazol-1-yl) ethyl)-1-methyl-1H-imidazol-3-ium) before and after anion metathesis

Similarly, at the end of the synthesis reaction, salt **2.2a** was obtained as eluent of methanol, and removal of volatiles afforded the pure imidazolium salt as a golden-brown oil. The ligand precursor, **2.4a** was synthesized by dissolving both 1-(2-chloroethyl)-3,5-dimethyl-1H-pyrazole and the 1-(4-nitrophenyl)-1H-imidazole in a very minimal amount of DMSO (2.0 mL) and heating the solution to 110 °C under inert conditions for 20 hours. This was the only reaction that required somewhat harsh conditions for the formation of desired products to occur. It is assumed that the failure of the initial solventless technique as applied in the synthesis of the preceding salts was due to (*i.*) the steric hindrance from the bulky nitrophenyl wingtip on the imidazole, making it difficult for the SN_2 attack of imidazole on the haloalkyl arm of the 1-(2-chloroethyl)-3,5-dimethyl-1H-pyrazole; (*ii.*) high melting point of 1-(4-nitrophenyl)-1H-imidazole (309 – 311°C),[70-71] when compared with that of 1-(2-chloroethyl)-3,5-dimethyl-1H-pyrazole. Dissolving the two reactants in a polar solvent such as DMSO, coupled by heating and stirring at a high speed forced the two reactants to interact in solution and react. The harsh conditions used to obtain the salt resulted in low yields and poor selectivity. At the end of the reaction time, DMSO is removed by series of washing with diethyl ether, while the pure salt was obtained as an eluent of methanol from the column chromatography of the crude salt. The yield of the salt formed from this reaction was modest (54%). This reaction was also attempted using acetonitrile as the solvent, wherein 1-(4-nitrophenyl)-1H-imidazole was first dissolved in the solvent and then added dropwise to the reaction vessel containing 1-(2-chloroethyl)-3,5-

dimethyl-1H-pyrazole. Immediately upon addition, a precipitate formed, indicating that the 1-(2-chloroethyl)-3,5-dimethyl-1H-pyrazole is insoluble in acetonitrile.

Salt **2.4a** was a highly viscous oil that also contained many impurities and side products all of which were completely soluble in ethyl acetate. At the same time, the salt was only sparingly soluble in the ethyl acetate and completely soluble in methanol. Hence, purification of the salt was achieved via column chromatography, and was collected as an eluent of methanol that was evacuated to dryness before further analysis. The NMR spectrum showed that the salt was successfully synthesized, and all the expected signals were accounted for.

All the salts contained certain common features such as the ethylene linker (CH_2-CH_2) between the pyrazole and the imidazole which is observed at δ 4.5 ppm and 4.3 ppm, the 3,5-dimethyl group on the pyrazole (CH_3 and CH_3) were both observed at δ 2.05 ppm, pyrazolyl proton (CH) observed at δ 5.7 ppm and lastly the two CH protons on the backbone of the imidazole which is observed at δ 7.6 ppm and 7.4 ppm. All these signals were observed in the spectra of all of the salts and were used as evidence that confirms the successful synthesis of each salt.

2.4.3. *Mass spectroscopy analysis*

Mass spectrometry analysis was done before anion metathesis; this was because the anion is not detectable in the positive mode of the MS experiment. Instead, the ligand precursor is a charged species, and its mass to charge ratio (m/z) is picked up as the positive molecular ion peak (Table 2.3). The calculated mass to charge ratio gave comparable values to the experimental, indicating the purity of the compound and confirming its successful synthesis. The most intense fragments belonged to the molecular ion peaks, representing the molecular weight of each salt.

Table 2.3: MS experimental data vs calculated data (TOF MS ES$^+$)

Salt ID	Ligand Precursor	Experimental (Calculated)/(m/z)
2.1	Me-Imid	205.16 (205.15)
2.2	pNO$_2$Ph-Imid	312.15 (312.15)
2.3	Et-Imid	219.17 (219.16)
2.4	Bz-Imid	281.18 (281.17)

2.4.4. FT-IR spectroscopy analysis

Fourier-transform infrared spectroscopy, FTIR was used to characterize the functional groups in the synthesized salts by obtaining the spectrum of the vibrational absorption modes. Salts that were oily and paste *i.e.*, salts **2.3b** and **2.4a** were too hygroscopic and decomposed during analysis resulting in inconclusive absorption spectra. Hence, their IR data were not reported or included in the supporting documents. The vibrational frequencies, along with the corresponding functional groups for the analysed compounds, are presented in Table 2.4.

All the salts contain an ethylene linker between the imidazolyl and the dimethyl pyrazolyl moieties. This alkyl C-H (sp3) stretching vibration was observed at *circa* 2950 cm^{-1}. The C-C bending vibration was observed at about 1550 cm^{-1}, and corresponds to the aromatic heterocyclic imidazole and pyrazole rings. A C=N medium and broad bending vibration belonging to the heterocyclic rings was observed at about 1100 cm^{-1}. An equally medium/broad absorption stretch was observed at about 3384 cm^{-1} in the spectra of salts **2.1a**, **2.1b** and **2.3a**; this vibration is due to an N-H single bond stretch that occurs due to electron delocalization in the aromatic heterocyclic ring. Salt **2.4b** (1-(2-(3,5-dimethyl-1H-pyrazol-1-yl)ethyl)-3-(4-nitrophenyl)-1H-imidazol-3-ium tetrafluoroborate) or [*p*-NO$_2$Ph-imid]$^+$[BF$_4$]$^-$ has a vibration at 1555 cm^{-1}, this is corresponding to the bending vibration of NO$_2$.

Table 2.4: Main vibrational frequencies and their corresponding functional groups of the synthesized ligand precursors

Salt ID	Ligand Precursor	Aromatic C-H (cm^{-1})	Alkyl C-H stretch (cm^{-1})	Alkyl C-H bend (cm^{-1})	Aromatic C-C bend (cm^{-1})	C-N bend (cm^{-1})	Aromatic N-N (cm^{-1})
2.1a	[Me-Imid]$^+$ [Cl]$^-$	3119, 3057, 3010	2977, 2952, 2858	1456, 1421	1640, 1567, 1554	1169	1090
2.1b	[Me-Imid]$^+$ [BF$_4$]$^-$	3161, 3102	2969	1458, 1427	1557, 1578	1186	1029
2.3a	[Bz-Imid]$^+$ [Cl]$^-$	3133	3033	1496, 1443	1675, 1566, 1547	1166	1120
2.3b	[Bz-Imid]$^+$ [BF$_4$]$^-$	-	-	-	-	-	-
2.4a	[*p*-NO$_2$Ph-Imid]$^+$ [Cl]$^-$	-	-	-	-	-	-
2.4b	[*p*-NO$_2$Ph-Imid]$^+$ [BF$_4$]$^-$	3161, 3112	2935	1380	1615, 1525	1217	1045

2.4.5. Elemental analysis

Obtaining accurate theoretical values for CHN elemental composition proved very difficult. This was due to high moisture sensitivity of the ligand precursors leading to bulk impurity. Many reports are available in the literature to ascertain this characteristic behaviour of imidazolium salts and ionic liquids.[66] Data showing the experimental values is available in Appendix D

2.5.CONCLUSION

A series of new pyrazolyl-functionalized imidazolium precursors were synthesized and their structures characterized by NMR, mass spectrometry, infrared spectroscopy, and elemental analysis. This chapter aimed to synthesize and characterize the four ligand precursors which would be later coordinated on to transition metals.

All four ligand precursors were successfully synthesized and fully characterized. Both the chloride and tetrafluoroborate forms of salt **2.2** are highly unstable in air and hence, susceptible to decomposition. Specifically, **2.1a**, **2.1b**, **2.3a**, **2.4b** were amorphous solids; **2.2a**, **2.4a** exists as viscous oils while both **2.2b** and **2.3b** were pastes. This was observed to be due to electronic and steric factors impacting the structural properties of the salts. Salt **2.4b** was found to be the most stable been most sterically bulky ligand precursor. Its stability could also be related to the electronic nature of the phenyl wingtip and its substituent electron-withdrawing nitro group.

CHAPTER 3

SYNTHESIS AND CHARACTERIZATION OF PYRAZOLYL FUNCTIONALIZED *N*-HETEROCYCLIC CARBENE TRANSITION METAL COMPLEXES

3.1. SUMMARY

Pyrazolyl functionalized *N*-heterocyclic carbene transition metal complexes have attracted a lot of attention recently, due to their profound catalytic activities in various organic transformations.[72] To the best of our knowledge, some of the synthesized pyrazolyl-functionalized NHC-metal complexes herein are reported for the first time. Three out of the four synthesized ligand precursors that were reported in chapter two were stable enough to be coordinated to the chosen transition metals (Ni, Co, and Cu). The complexes reported in this chapter were synthesized using the free carbene route and were obtained in low yields ($\leq$ 35 %). Complex **3.2** was obtained in a meagre yield of 13 %. In total, five complexes were synthesized; $[Co^{II}(p\text{-}NO_2Ph\text{-}imid)_2][BF_4]_2$, **3.1**; $[Cu^{I}(CH_3CN)_2(p\text{-}NO_2Ph\text{-}imid)][BF_4]$, **3.2**; $[Cu^{I}(Me\text{-}imid)(NCCH_3)_2][BF_4]$, **3.3**; $[Ni^{II}(p\text{-}NO_2Ph\text{-}imid)_2][BF_4]_2$, **3.4**; and $[Ni^{II}(Me\text{-}imid)_2][BF_4]_2$, **3.5**. Standard spectroscopic and analytical techniques were used to characterize the complexes. Both the NHC-copper complex, **3.3** and the corresponding NHC-nickel complex **3.5** are derived from the same NHC precursor salt 3-(2-(3,5-dimethyl-1H-pyrazol-1-yl) ethyl)-1-methyl-1H-imidazol-3-ium tetrafluoroborate; **2.1b** and it is noted that both complexes were highly unstable. Complexes are **3.1**, **3.2** and **3.4** are relatively more stable.

3.2. GENERAL INTRODUCTION

Selective alkane oxidation is still a major challenge in synthetic chemistry. Over the years, many important breakthroughs have been reported in biomimetic catalysis such as, the first copper-based catalyst consisting of additives such as oxidants, pyridine, and acetic acid to increase the activity reported by Barton *et al*.[73] Metals such as copper and iron can be found in the active sites of enzymes such as methane monooxygenases in the family of cytochrome P450, which offer excellent activities for the selective oxidation of C-H bonds.[56] It is for this reason that first row transition metals such as nickel and cobalt (these possess very similar properties to iron) are considered to have a great deal of potential as selective alkane oxidation catalysts, under the right conditions and with the appropriate additives.

Although iron and copper complexes may be considered the most promising alkane oxidation catalysts because of their biomimetic properties, other metals such as Mn[74], Os[75], and Ru[59] have been studied successfully and reported as good alkane oxidation catalysts. Some studies show that Ni(II) can replace Fe(II) in some catalytic systems. Similarly, in some instances, Ni(II) based catalysts have shown potential for higher turnover numbers (TON) than Fe(II), Co(II) and Mn(II) based catalysts given that they all had contained the same ligand.[56]

The type of ligand coordinated to the metal centre is as important as the metal centre itself. Chelated ligands or polydentate ligands have resulted in more stable and more active complexes. Polydentate *N*-heterocyclic carbene ligands that have been reported are mainly bidentate, and tridentate-*mer* (*pincer*) type ligands first coordinated to palladium, and then later other metals in the platinum group series that include Rh, Ru and Ir.[76] The strong bonds between NHCs and transition metals (TMs) have sparked an interest in these ligands for applications in organic transformations through catalysis, molecule activation, and biomimetic chemistry.[77] The compatibility of NHCs as ligands for TM catalysis due primarily to the distinctive σ-donor ability with an unpaired lone pair of electrons (sp^2 hybridized) available for donation into the empty σ-accepting orbital of the transition metal.[37] However, despite the strong interactions between NHCs and transition metals, major complications still exist for such complexes. For example, the NHCs' electronic and structural factors are known to generate conditions wherein the ligands become particularly susceptible to reductive elimination.[51]

For thermodynamic stability of NHC-TM complexes; a square planar geometric arrangement is preferred. Other geometric arrangements such as a tetrahedral geometry, result in minimal interactions between the orbitals which leads to decomposition of the catalyst, in some instances even before effective catalysis can occur.[37, 56] The impact of this unwanted reaction can be reduced by increasing the dihedral angle between the plane of the carbene ligand and that of the coordination plane, thus increasing the overlap of interacting orbitals, hence, improving the stability of the complex.[51] One obvious way to achieve this would be the use of relatively inflexible chelating NHC-based ligands.[51]

The vast majority of catalytic studies involving donor functionalized NHC-metal complexes have focused on palladium-catalysed C–C coupling reactions, such as Heck and Suzuki.[17] NHCs as organocatalysts have high activity in the construction of C-C and C-X bonds (X= O or N) under relatively mild conditions. Other examples include complexes of Ni(II) in olefin polymerization reactions.[78] Donor functionalized NHCs are ligands consisting of at least one

other anionic or neutral two electron donor atom (*e.g.* C, N, P, O, or S) which can act as a polydentate ligand once coordinated to the metal.[51] N-donor compounds are different from NHCs because they form much weaker and more labile metal-ligand bonds.[26] The lability of the ligand can result in the reductive elimination of the ligand under favourable conditions leading to catalyst decomposition. However, when the weaker labile ligand is tethered to the stable NHC it results in hemilability. That means upon coordination, the ligand partially behaves in a bidentate fashion with the strong σ-donating NHC anchored to the metal centre and weaker N-donor able to selectively dissociate from the metal centre.[41, 51] In the family of N-donor functionalized NHCs, pyrazolyl functionalized NHCs have attracted the most research interest because of the versatility in the coordination chemistry of pyrazole based ligands and the high catalytic activity of their complexes.[46] In addition to this, pyrazole and its derivatives have proved to be very good dinucleating ligands (this allows for the formation of shorter and stronger metal-metal bonds), leading to bimetallic complexes.[79] Much like *N*-heterocyclic carbenes, the electronic and steric effects of pyrazolyl functionalized ligands can be fine-tuned by changing the substituents on the pyrazole ring.[46]

Complexes containing hemilabile ligands have been successfully applied as hydrogenation catalysts[26] (with the platinum group metals), in C-C coupling reactions[17] and most recently as oxidation catalysts (using transition metals such as Ni, Co, and Cu)[18, 80]. Studies such as these validate that chelating ligand systems can provide a degree of stability against the facile reductive elimination process previously noted for monodentate NHC or N-donor functionalized ligands.

Most published articles on donor functionalized NHCs (NHC-X donor ligands) where X is N, P, C, O or S, are reported with the platinum group metals (PGM) or other precious metals as the central atom. This is because they provide more stable and active catalysts. It is possible that by changing the metal centre and maintaining the same architecture, the new complex synthesized may function as a catalyst for a whole different type of reaction. For example, a hemilabile pyrazolyl functionalized NHC complex of palladium (Pd^{2+}) functions as an excellent catalyst for both Suzuki and Heck cross-coupling reactions in ionic liquids,[17] while a rhodium complex of the same ligand functions as an excellent hydrogenation catalyst.[26] However, one major disadvantage of precious metals is that they are costly and often toxic. For those reasons, researchers are increasingly considering first row transition metals such as nickel (Ni), copper (Cu), and cobalt (Co) as alternatives because they are cheaper and less toxic.[47-48, 81]

Cu-NHC complexes have a wide range of applications in organic synthesis, such as hydrosilylation, conjugate additions, allylic alkylation reactions, and cyclopropanation. Yet, very few Cu-NHC complexes have been reported to be successfully synthesized and isolated due to their highly unstable nature in air or solution.[82] Amongst the reported Cu-NHC complexes, the most well-defined examples were prepared by reacting free carbenes with an appropriate copper source using strong bases under inert conditions.[83] Other reported successful synthesis of the Cu-NHC complexes was via the transmetalation of an intermediate NHC-Ag to the desired copper.[47]

For practical reasons, the Ag_2O route is favoured for the synthesis of precious metal-NHC complexes. The main advantage in the use of Ag-NHC intermediate complex for transmetalation lies in the selectivity of the Ag_2O to the imidazolium C_2 proton. Hence, other acidic protons that might be within the framework of the NHC precursor are excluded in the basic deprotonation by Ag_2O, and retain their forms in the intermediate Ag-NHC generated.[84] Although first row transition metal-NHC complexes can be prepared using either the free carbene and transmetalation routes depending on the sensitivity of other donor groups to strongly basic condition, it has been reported that synthesis using the free carbene route resulted in better yields.[47]

3.3. SYNTHESIS AND CHARACTERIZATION OF PYRAZOLYL FUNCTIONALIZED NHC COBALT(II) COMPLEX

3.3.1. METHODS AND MATERIALS

Unless stated otherwise, all solvents and reagents used in this section of the study were HPLC grade and dried using the appropriate methods for solvent drying. The ligand precursors used in this study showed better stability. The free carbene route was used to synthesize all complexes under inert conditions (N_2 atmosphere), using standard Schlenk techniques. All glassware was washed with water and soap thoroughly and then rinsed with crude methanol and dried in an oven at 110 °C before use. All Schlenk tubes and other glassware are cleaned and dried in the oven at 105 °C. They are then cooled under N_2 before the addition of reactants.
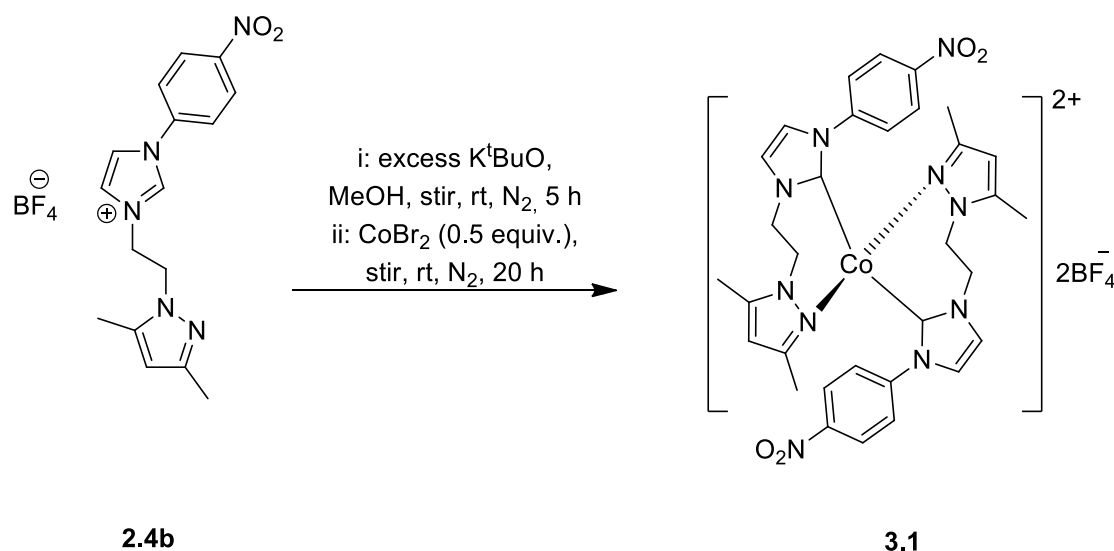
Scheme 3.1: Synthesis of Co(II)-NHC complex **3.1**

1. Synthesis of $[Co^{II}(p\text{-}NO_2Ph\text{-}imid)_2][BF_4]_2$, (**3.1**)

To an orange methanolic solution of **2.4b** (0.260 g, 0.651 mmol) in a degassed Schlenk tube was added 4 mol equivalent of potassium *tert*-butoxide (0.293 g, 2.606 mmol) with continues stirring at room temperature. The resulting bright purple solution that indicated rapid deprotonation taking place was then stirred at room temperature for 5 h, after which anhydrous $CoBr_2$ (0.0712 g, 0.326 mmol) was added, and the solution turned cloudy brown almost immediately with the formation of a precipitate. The reaction was refluxed overnight for 20

hours, and at expiration of the reaction time, the colour of the mixture was thick dark brown, indicating more precipitation had occurred over time.

The solution was filtered, and while the precipitate expected to be a mixture of corresponding displaced potassium salt or unwanted side products are trapped on the bed of Celite. The filtrate is thus concentrated to about 2 mL, and diethyl ether (10 mL) was then added, and the complex precipitated out immediately. It was then washed with more diethyl ether (3×10 mL) until the washing became clear and then vacuum dried. The product showed physical paramagnetic property as it adheres to the magnetic stirrer bar and was obtained as a highly hygroscopic reddish-brown free-flowing powder that melts at 280 °C and decomposes after that. Yield: 0.08 g, 32 %; Mp: 279 – 281 °C. LRMS = ~373.1 m/z (TOF MS ES⁻) fragment belongs to one half of the complex *i.e.* one part of salt **2.4b** coordinated to the cobalt metal centre. The complex is doubly-charged in MS with a mass to charge of 681/2, this accounts for the peaks observed at ~681 and ~340 m/z. Poorly resolved ^{1}H and slightly less poorly resolved ^{13}C NMR, an indication of paramagnetic nature of the complex. ^{13}C NMR (600 MHz, DMSO-d_6): δ 139.82, 136.99, 135.18, 129.41, 129.19, 128.52, 123.53, 122.95, 105.46, 49.168, 47.509, 13.693, 10.479

Thus only the ^{13}C NMR was reported for this complex. The disappearance of the carbene carbon signal is due to a longer relaxation time in the collection of FID, which is common for such NHC-metal complexes.[69]
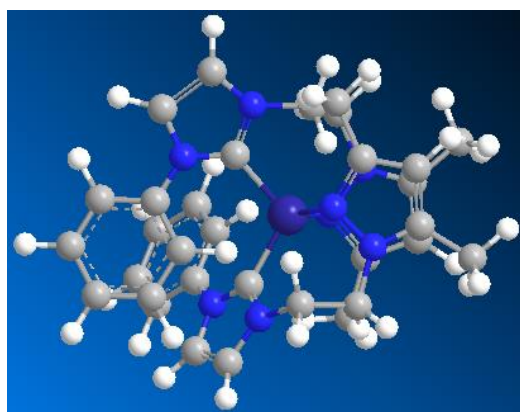
White = H atoms
Grey = C atoms
Blue = N atoms
Navy = Co

Figure 3.1: 3D structural representation of complex **3.1**

3.3.2. RESULTS AND DISCUSSIONS

This study was aimed at synthesizing and characterizing a pyrazolyl functionalized NHC cobalt(II) complex. The complex was synthesized by direct deprotonation of the most acidic proton in the ligand precursor which is the imidazolium C_2-H. The procedure involved the use of strong base, tBuOK (potassium *tert*-butoxide) in methanol, before introducing the metal source, and then allowing the reaction to complete over a period of 20 h. The time frame for the reaction to reach completion was chosen based on studies conducted during the synthesis of complex **3.1** to determine when the highest yield of the desired complex was obtainable, and information from related literature[85-87]. The maximum yield was observed at around 16 – 20 with no further conversion of the reactants thereafter. The choice of methanol as the solvent was because all the starting materials and the base are highly soluble in it.

The coordination of cobalt(II) to salt **2.1b** was attempted via direct deprotonation with the aid of tBuOK as the strong base and by transmetalation of an intermediate Ag-NHC complex. However, the latter route was discontinued due to longer time frame of the reaction and the sensitivity of the Ag-NHC to UV light. With the free carbene route, all side products of the reactions formed after each stage precipitated out of solution, leaving only the desired product in the solution which made its purification very simple.

The observation of colour changes as each reactant was added at different stages of the reaction was the first indicator that a reaction was occurring. Cobalt(II) complex **3.1**, derived from **2.4b** was isolated as a solid powder with a reddish colour, typical of cobalt(II)-NHC complexes.[77] The complex is highly hygroscopic upon exposure to air and decompose upon prolonged exposure to air. The reddish micro crystalline solid particles also stuck to the magnetic stirrer after purification was completed. However, several attempts to grow crystals suitable for single crystal X-ray analysis were futile.

3.3.2.1. NMR analysis

NMR was used as the first tool to investigate whether the integrating complexes were successfully synthesized. Both ^{1}H and ^{13}C NMR analysis were conducted. In the proton NMR, the disappearance of the most downfield signal ($\delta \sim 10$, singlet integrating for 1H) which belongs to the most acidic proton of the imidazolium C_2-H, would indicate that the deprotonation was successful. Theoretically, a downfield chemical shift would be observed for

the aryl and alkyl structural groups in the complexes in comparison to the ligand precursor(s). This would indicate a reduction in the electron density of the complex, which is evidence that the coordination was successful.[88] The ^{1}H and ^{13}C NMR of complex **3.1** supported this as, shown in Figure 3.2 and Figure 3.3.
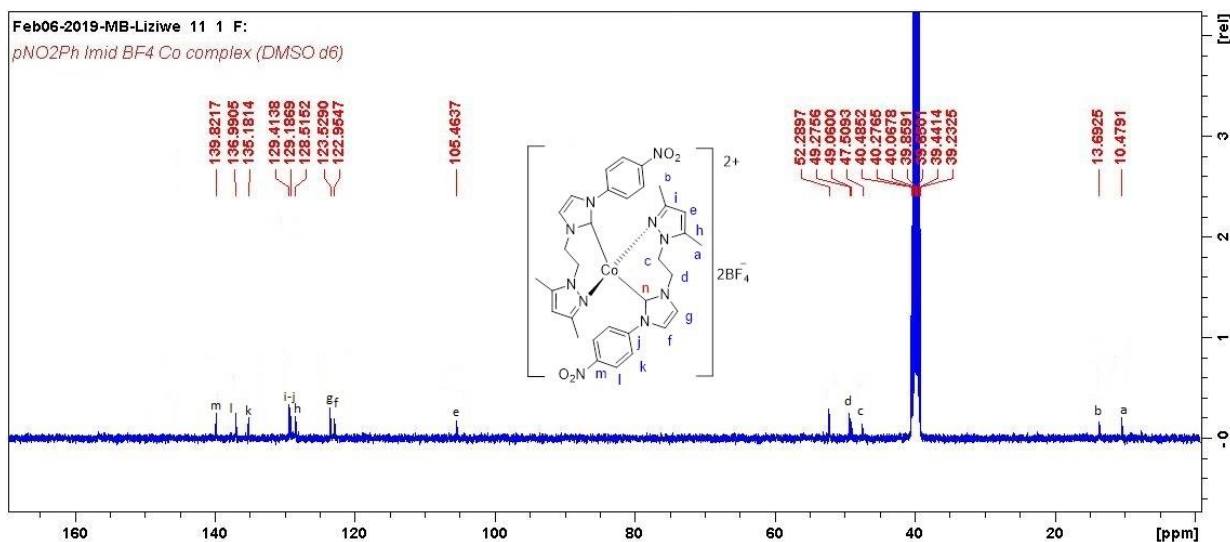
Figure 3.2: ^{13}C NMR spectrum of complex **3.1**
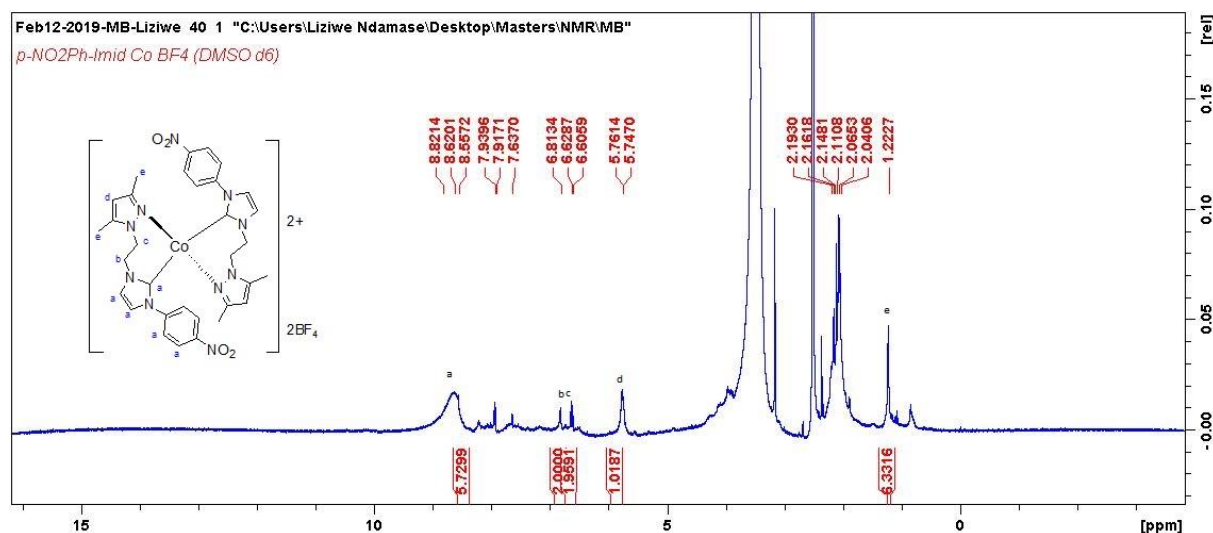
Figure 3.3: ^{1}H NMR for complex **3.1**

The ligand is neutral, and the Co(II) centred complex contained high spin d7 metal ions in a tetrahedral arrangement. The NMR experiment had to be run multiple times on the 600 Hz NMR to obtain a reasonably resolved spectrum due to the paramagnetic nature of the Co(II)

complex. The NMR spectra for **3.1** indicated that the complex was symmetrical with two molecules of the ligand coordinated to the Co(II) metal centre. The ^{13}C NMR resonance signals for the carbons in the heterocyclic rings were the most poorly resolved, and the signal for the carbene carbon disappeared into the baseline. This situation is similar to what was reported for other Co-NHC complexes and was attributed to decomposition during the collection of FID.[69]

3.3.2.2. *Coordination geometry*

Cobalt(II) results in a tetrahedral or square planar geometrical arrangement.[89] In the cobalt complex reported herein, i.e. **3.1,** the bis-ligated (C,N) NHC ligand promotes a symmetric (CN-Co-NC) arrangement. The coordination number in the complex is 4, and thus permits either tetrahedral or square planar geometries. The broadness of ^{1}H NMR for **3.1** (Figure 3.3) with the complimentarily, lack of the expected far downfield carbene signal in its ^{13}C NMR spectrum (Figure 3.2), suggest that the complex exhibits behaviour typical of paramagnetic high–spin Co(II) ions in a tetrahedral geometry.[90] A downfield chemical shift of the ethylene linker signal can be observed. This is due to the electron density of the ethylene linker being pulled by the electron deficient metal centre, leaving the linker deshielded. The colour of **3.1** was a vibrant reddish-orange.

Figure 3.4 shows the predicted partial dissociation of the N-donor atom of CN donor ligand based on literature.[43] The hemilability of a ligand has shown excellent properties that have vastly improved the catalytic activity of the complexes. When the weakly bound donor atom of the ligand dissociates from the metal centre, it leaves open a vacant site for the catalysis to take place. This allows for the metal centre to interact with the substrate and activate it while stabilizing the intermediate species. The first successful hemilabile complex was first reported for Ir(I) catalysts for hydrogenation by Korbinian *et al.*[43] The salts used were very bulky heteroaryl imidazolium salts that did not contain any free rotating *sp³* alkyl linkers which made them more stable and rigid. This possibility for free C-C bond rotation by the ethylene linker between the pyrazole ring (N-donor) and the imidazole ring (C-donor) in the ligands also contributed to the difficulty in obtaining crystal structural data for the complexes reported in this study.
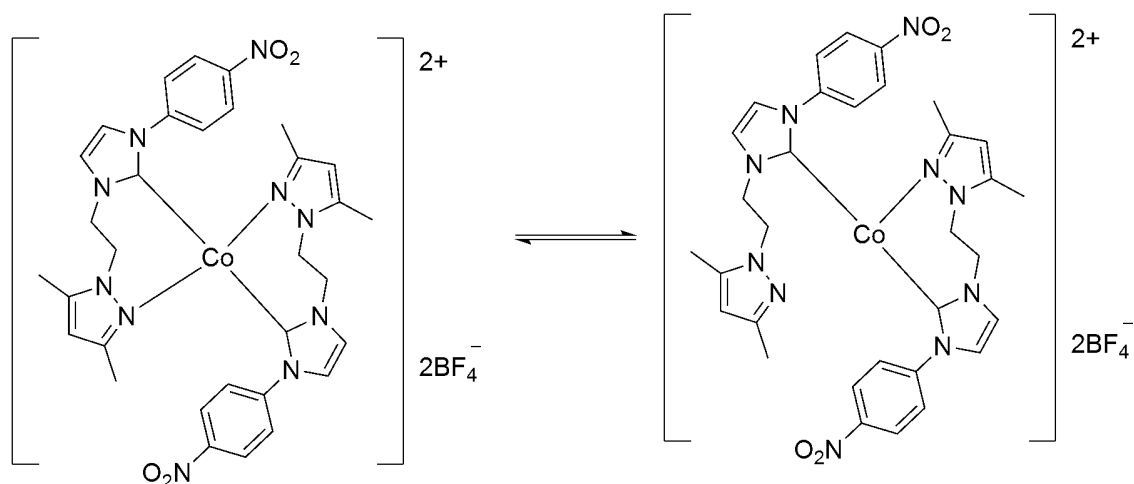
Figure 3.4: Depiction of the anticipated partial dissociation or hemilability of ligand from the cobalt centre in **3.1**.

3.3.2.3. *Mass Spectrometry analysis*

The molecular ion peak mass to charge ratio (m/z) of **3.1** can be characterized as its molecular weight with the exclusion of the counter ion, (m/z) = $[M - BF_4]^{2+}$. The second fragment (base peak), which belongs to the most stable ion and is available in greater abundance and corresponds to the loss of one ligand motif from the molecular ion, i.e. (m/z) = $[M - 2BF_4 - NHC \ ligand]^+$. The base peak shows the most stable fragment of the molecule and was detected more abundantly than other fragments as supported by its peak intensity. The calculated m/z and experimental m/z are comparable. The mass spectrometry data confirmed that complex **3.1** was symmetrical, with mass for half of the molecule observed as shown in fragmentation Scheme 3.2. The base peak of the MS spectrum for **3.1** is (m/z) = 373.1, which is comparable to the calculated base peak of (m/z) = 372.1. The complex is doubly-charged in MS with a mass to charge of 681/2, this accounts for the peaks observed at ~681 and ~340 m/z. The peaks at ~681 and ~340 m/z had relatively low intensities and thus were not labelled by the instrument. Their low intensity is due to the instability of the complex.

(m/z) = [M - 2BF$_4$]$^+$
Molecular ion = 681.2
Experimental: 680 m/z

(m/z/) = [M - 2BF$_4$ - NHC ligand + 2H
Base peak = 372.1
Experimental: 3731 m/z
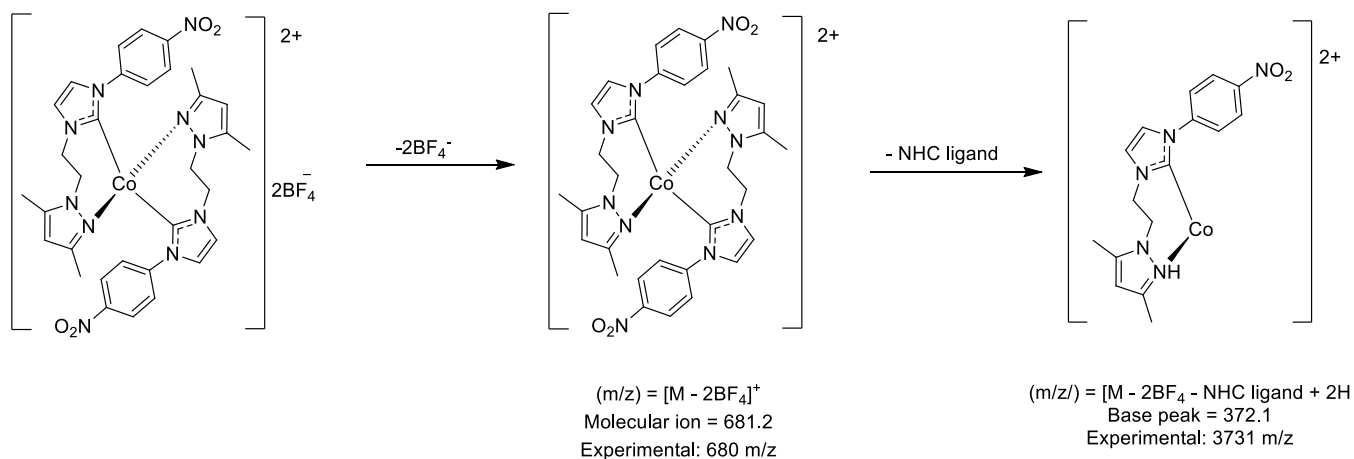
Scheme 3.2: TOF – MS Fragmentation pattern of complex **3.1**

3.3.2.4. FT –IR Spectroscopy Analysis

Fourier-transform infrared spectroscopy was used to investigate the vibrational modes of the functional groups for **3.1**. The alkyl C-H stretching vibration in **3.1** was observed at 2941 cm^{-1} and corresponded to the ethylene linker between the imidazolium and the dimethyl pyrazole moieties.[91] C-H stretching vibrations observed at 3183 cm^{-1} and 3107 cm^{-1} were assigned to the aromatic C-H functional group. NHC precursor **2.4b** has a vibration at 1555 cm^{-1} corresponding to the bending vibration of NO$_2$. However, upon coordination of the ligand motif to the metal, the vibration belonging to the NO$_2$ was observed at about 1602 cm^{-1}. This is similar to the observed shift in reported Co-NHC complexes.[69] A broad weak bending vibration accounting for N-N functionality in pyrazole ring was observed at about 1128 cm^{-1}.[91]

3.4. SYNTHESIS AND CHARACTERIZATION OF PYRAZOLYL FUNCTIONALIZED NHC COPPER(I) COMPLEXES

The oxidation of paraffins under mild conditions and producing the desired products in high yields remains a problem to synthetic chemists to-date. Many metalloenzymes that perform alkane oxidations in nature at high reaction rates and perfect selectivity contain copper and iron ions in their active sites. Many catalytic systems that contain this metal ion have been developed to mimic the performance of enzymes in oxidation reactions. Hence, in this section pyrazolyl functionalized NHC-Cu(I) complexes are presented.

2.1a: R = Me, X = Cl
2.4b: R = p-NO$_2$C$_6$H$_4$, X = BF$_4$

3.2: R = p-NO$_2$C$_6$H$_4$,
3.3: R = Me
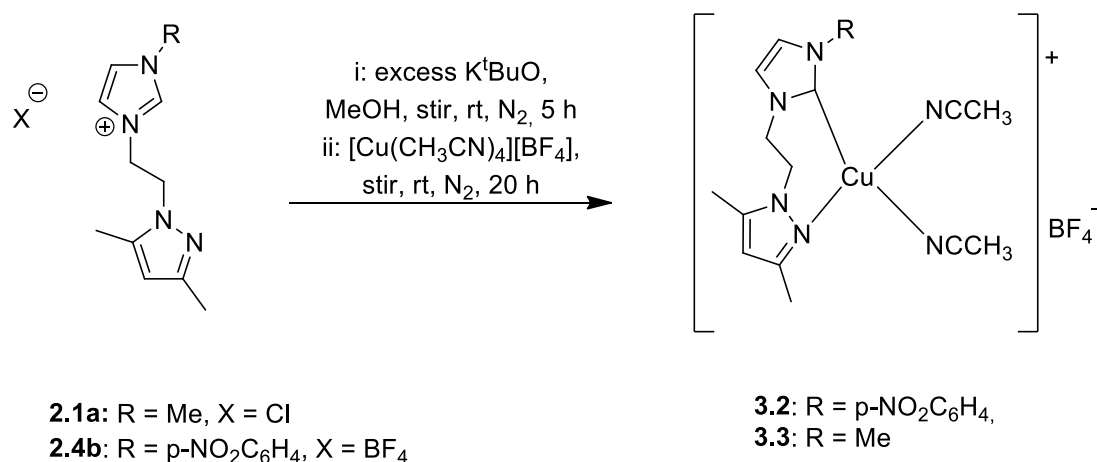
Scheme 3.3: Synthesis of Cu(I)-NHC complexes

3.4.1. METHODS AND MATERIALS

1. Synthesis of [Cu^I (CH$_3$CN)$_2$(p-NO$_2$Ph-imid)][BF$_4$] (**3.2**)

To a methanolic solution of **2.4b** (0.110 g, 0.259 mmol) initially deprotonated with tBuOK (0.120 g, 1.04 mmol) was added dropwise, an acetonitrile solution of Cu(I) precursor, [Cu(CH$_3$CN)$_4$][BF$_4$] (0.0407 g, 0.259 mmol) (Scheme 3.3). The addition caused the initially orange solution to immediately turned cloudy reddish-brown, with formation of a precipitate. The reaction was continued at room temperature overnight for 20 hours. More precipitation occurred over time, while a thick dark brown solution ensued at the end of the reaction. The orange-brown supernatant was filtered over a bed of Celite and concentrated to about 2 mL. The addition of ether prompted the precipitation of red solid which was filtered and washed with more ether (3×10 mL) till the wash was clear. The solid was then vacuum dried to afford

the Cu(I)-NHC complex, **3.2** as a reddish-brown solid. Yield: 0.041 g, 36 %, Mp: 78 – 79 °C and decomposes at 80 °C. LRMS: (m/z) = 475. ^{1}H NMR (400 MHz, DMSO-d$_6$): δ 8.2416 (CH, m, 3H, ^{2}J= 2.6030 Hz), 7.9601 (CH, m, 4H, ^{2}J= 8.4719 Hz), 6.7751 (CH$_2$, t, 2H), 6.6087 (CH$_2$, t, 2H, ^{2}J= 8.7924 Hz), 5.7776 (CH, s, 1H), 1.231 (2CH$_3$ s, 6H), 0.8510(CH$_3$, s, 3H).^{13}C NMR data was not available due to possible decomposition during the collection of FID.[69]

2. Synthesis of [Cu^I (Me-imid)(NCCH$_3$)$_2$][BF$_4$], (**3.3**)

Complex **3.3** was synthesized using the same method as complex **3.2**, by reacting deprotonated **2.1a** (0.7 g, 2.397 mmol) with the Cu precursor (0.1077 g, 2.397 mmol). The product was a highly hygroscopic brown amorphous solid. Mp: 80 - 85 °C Yield: 0.336 g, 32 %. LRMS: (m/z) = 355 m/z. ^{1}H NMR (400 MHz, DMSO-d6): δ ^{1}H NMR (400 MHz, DMSO-d$_6$): δ 8.5016 (CH, s, 1H), 5.7460 (CH, s, 1H), 4.0778 (CH$_2$, t, 2H, ^{2}J= 12.3268 Hz), 3.8149 (CH$_2$, t, 2H, ^{2}J= 12.4068 Hz), 3.1589 (CH, s, 1H), 3.0956 (CH, s, 1H, ^{3}J= 2.7215) 1.9972 (CH$_3$ s, 3H), 1.6152 (CH$_3$, s, 3H), 0.8510(CH$_3$, s, 3H). ^{13}C NMR (DMSO-d$_6$): δ 166.721, 152.95, 146.77, 139.56, 111.92, 110.87, 105.03, 48.900, 47.070, 30.244, 13.788, 10.542.

3.4.2. RESULTS AND DISCUSSIONS

This section of the study was aimed at synthesizing and characterizing pyrazolyl functionalized NHC copper complexes. These complexes were synthesized by way of direct deprotonation which entails the generation of free carbenes. This was achieved by deprotonating the ligand precursors using a strong base in a suitable solvent under inert (air and moisture-free) conditions. In this study, potassium *tert*-butoxide in dried methanol was used.[49] Each salt was first dissolved in dry methanol and stirred at room temperature under an atmosphere of nitrogen gas, and then the strong base was added (Scheme 3.3). This resulted in immediate colour changes suggesting deprotonation was rapid. The reaction was stirred for about five hours. The resulting free carbene was then be reacted with an appropriate metal source [Cu(NCCH$_3$)$_4$][BF$_4$] to obtain the desired corresponding complexes. Colour change was one of the first indicators that a reaction was taking place.

The copper complexes were all highly hygroscopic and were characterized by NMR, IR, and MS spectroscopies. Both complexes showed solubility in DMSO in high dilution. This makes their yield low (< 50%) and further characterization like SCXD analysis difficult.

3.4.2.1. NMR analysis

Proton NMR analysis was used to determine the deprotonation of the base to form the free carbene, this was confirmed by the disappearance of the most acidic proton C_2-H. A downfield chemical shift was observed for the aryl and alkyl functional groups in the complexes compared to the ligand precursors indicating a reduction in the electron density of the complex. This was observed for all the complexes.

By virtue of the counter-ion on the Cu precursor, both **2.1a** and **2.1b** are expected to give the same Cu-NHC complexes bearing a BF_4^- counter ion. Although, a preliminary synthesis was conducted using **2.1b**, the resulting complexes were very unstable and difficult to characterize. Hence, the use of the ligand precursor **2.1b** was discontinued for the synthesis of the Cu-NHC complexes. The corresponding Cu complex, **3.3** synthesized from salt **2.1a** was much more stable and provided enough spectroscopic data for characterization. A downfield chemical shift of the aryl carbons was observed; this indicated that the electron density of the aromatic rings had decreased due to the electron-withdrawing effect of the metal. Two additional signals were observed in the ^{13}C NMR; these signals were consistent with the presence of the $NCCH_3$ ligand in the complex. Figure 3.5 and Figure 3.6 compares the ^{13}C and ^1H NMR spectra of both ligand precursor, **2.1a** and the corresponding Cu-NHC **3.3** respectively.
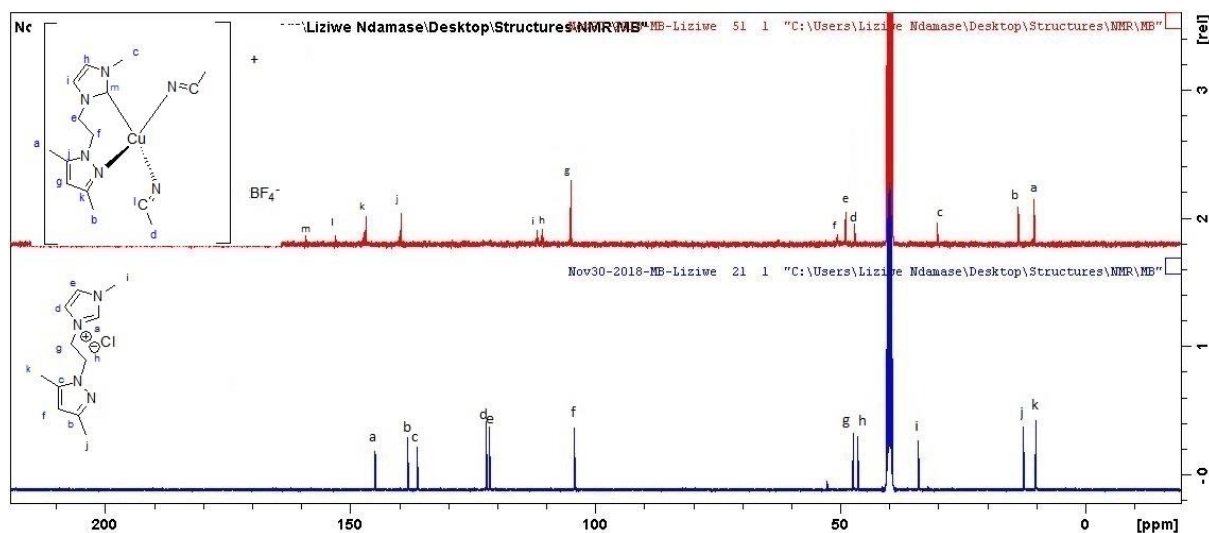
Figure 3.5: ^{13}C NMR spectra comparison of complex **3.3** vs Salt **2.1a**
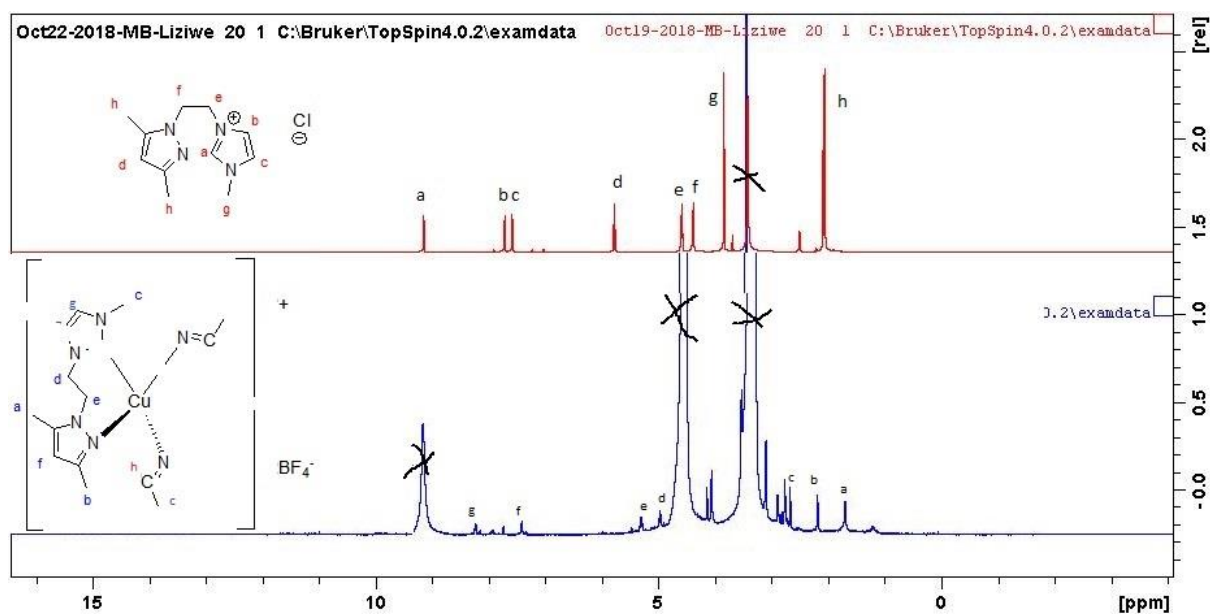
Figure 3.6: ^{1}H NMR spectra comparison of complex **3.3** vs Salt **2.1a**

The effect on the electron density of the carbons before and after coordination was greatest on the aryl carbons. After coordination, the two (a and b) of the five aryl carbons shifted downfield, indicating that the electron density around these carbon atoms had decreased. One of the aryl carbon (c) remained at its position while the other two (d and e) shifted upfield, indicating that the electron density around those carbons had increased. Although these chemical shifts were slight, they were an indication that coordination was successful. In both the ^{1}H and ^{13}C NMR, the signals in the complex spectrum are further apart than the signals in the ligand spectrum. This is due to the metal-ligand coordination.[92]

To understand the effect of different metal centres coodinating to NHC ligand derived from **2.4b,** a comparison was made between the ^{1}H NMR spectra of **3.1** and **3.2** (Figure 3.7). In both complexes a downfield chemical shift of the ethylene linker ($-CH_2-CH_2-$) can be observed and in both complexes the ethylene linker can be observed at approximately the same position. The same can be said for the methyl groups on the pyrazole ring. According to the spectrochemical series for metals, copper and cobalt have very similar effects on ligands.
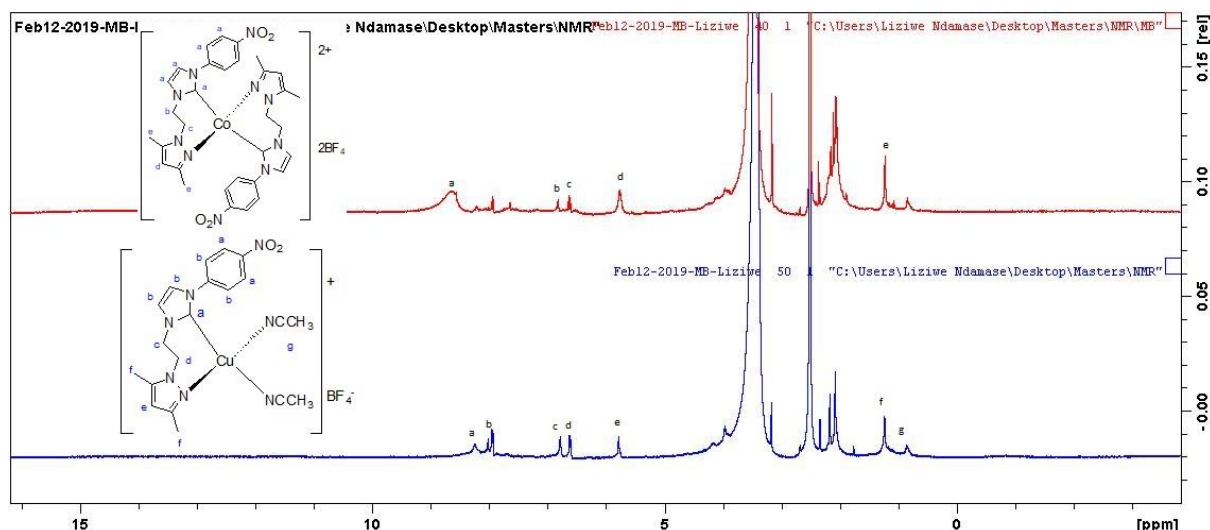
Figure 3.7: ^{1}H NMR comparison between Co-NHC complex **3.1** and Cu-NHC **3.2** bearing same ligand motif

3.4.2.2. Coordination geometry

Copper was chosen as a metal centre because it is one of the earth's most abundant metals.[93-95] Copper complexes have been renown as catalysts for mimicking nature in some oxidation reactions.[96] Some enzymes that play key roles in the oxidation reactions of many organic compounds contain copper as the metal in their active sites.[55] However, less is known about copper complexes catalysing oxidation reactions of saturated hydrocarbons.[96]

The coordination and geometry of copper complexes depends on the oxidation state of the metal. The complexes synthesized here are Cu[I] complexes, thus the geometry of these complexes can range from trigonal planar, tetrahedral, square planar *etc*.[97] The coordination number of the complexes reported in this study is four, indicating that **3.2** and **3.3** have tetrahedral or square planar geometry. The reddish-brown and brown colours for **3.2** and **3.3** respectively, are typical colours for such Cu(I) complexes.[98]

3.4.2.3. Mass Spectrometry analysis

Mass spectrometry data was collected for complexes **3.2** and **3.3**. The MS signals reported here belong to the major fragments of both Cu(I) complexes studied. A peak was observed at ~ 457 m/z on the spectrum belonging to **3.2**. This peak corresponds to the molecular weight of the complex. A peak at ~ 416 m/z consistent with the loss of one NCCH$_3$ ligand and another one at ~ 373 m/z consistent with the loss of both NCCH$_3$ ligands were observed. Further fragmentation corresponding to the salt **2.4** and the loss of the dimethylpyrazole group from

salt **2.4** were observed, with the most intense peak belonging the remaining 1-ethyl-3-(4-nitrophenyl)-2,3-dihydro-1H-imidazole.   The values obtained are comparable to the calculated one within acceptable limits. Schemes 3.4 and 3.5 show the fragmentation patterns for both Cu(I) complexes.

3.2
Chemical Formula: $C_{20}H_{24}CuN_7O_2$
m/z: cal. 457.1287
Experimental: 457

$[M - NCCH_3]^+$
Chemical Formula: $C_{18}H_{21}CuN_6O_2$
m/z:cal. 416.1022
Experimental: 416

$[M - BF_4 - NCCH_3]$
Chemical Formula: $C_{16}H_{18}CuN_5O_2$
m/z: cal. 375.0757
Experimental: 373.1109
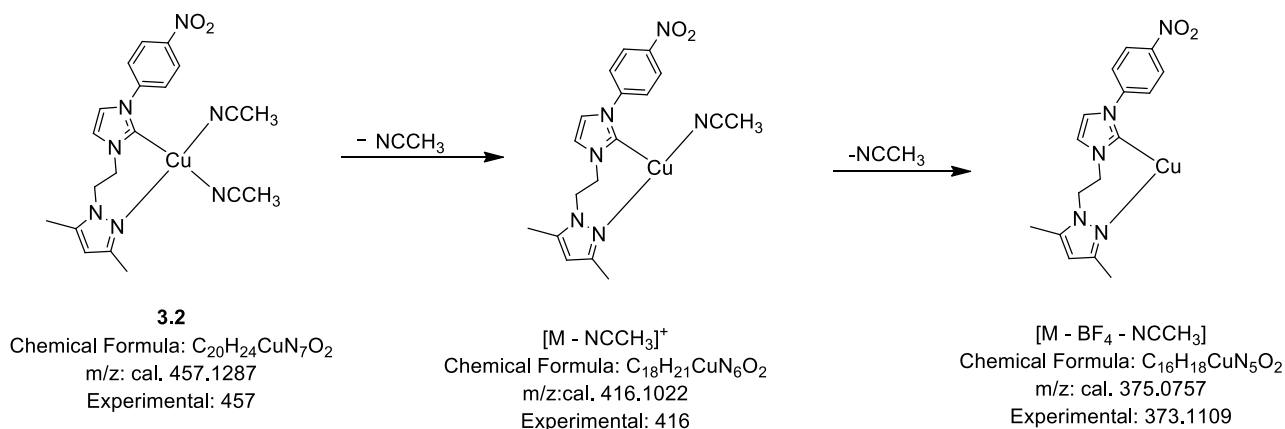
Scheme 3.4: MS fragmentation for **3.2**

The signal on the MS spectrum at ~355 m/z corresponds to the molecular mass of **3.3**. This indicates successful formation of the complex. The base peak was observed at 308 m/z and corresponded to the loss of $NCCH_3$ ligand from the complex. Further fragmentation was also observed at ~267 m/z corresponding to the loss of the second $NCCH_3$ ligand.

3.3
Chemical Formula: $C_{15}H_{23}CuN_6$
m/z: 350.1280
Experimental: 355.1877

$[M - NCCH_3]^+$
Chemical Formula: $C_{13}H_{20}CuN_5$
m/z: 308.10
Experimental: 309.1278

$[M - NCCH_3 - NCCH_3]$
Chemical Formula: $C_{11}H_{17}CuN_4$
m/z: 268.0749
Experimental: 267.0688
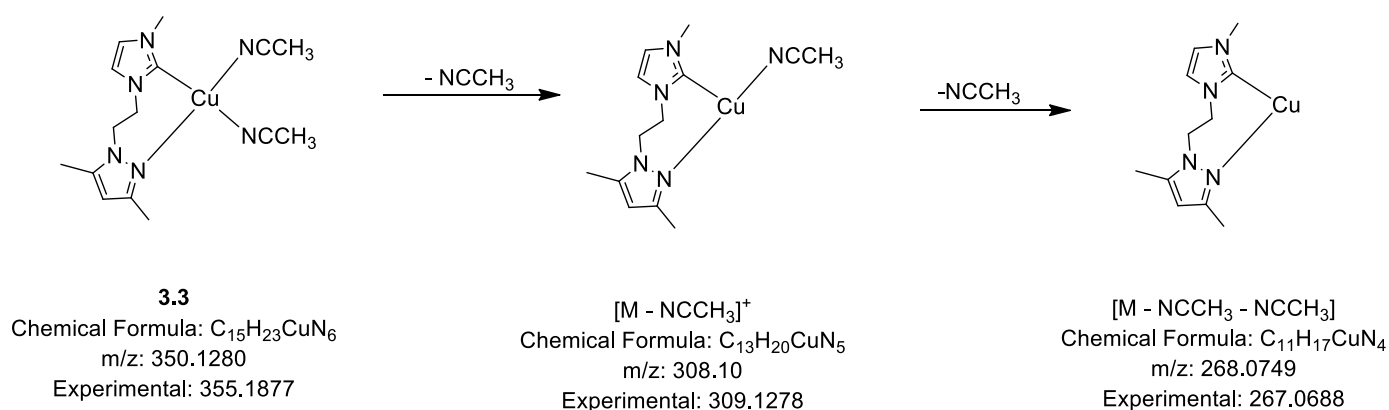
Scheme 3.5: MS fragmentation of **3.3**

3.4.2.4. FT –IR Spectroscopy

Fourier-transform infrared spectroscopy was used to investigate the vibrational modes of the functional groups of complexes **3.2** and **3.3** by obtaining the spectrum of absorption and emission. Both complexes were solids; however complex **3.3**, was very sensitive to air and absorbs moisture from the air on exposure. This caused some difficulties in obtaining a more resolved FTIR spectrum for the complex.

Both complexes contained an ethylene linker between the imidazolium and the dimethyl pyrazole, this alkyl C-H stretching vibration was observed at about 2939 cm^{-1}. On the other hand, the corresponding aromatic C-H stretching vibration was observed at about 3184 – 3104 cm^{-1}. When salt **2.4b** coordinated to copper in the formation of **3.1**; the strong bending vibration frequency belonging to the nitro (NO_2) functional group bound at the para position on the phenylimidazolyl group was observed at about 1601 cm^{-1}. This is also similar to that observed via FTIR analysis for Cu-NHC complex, **3.2.** This was also indication of a successful metalation. A weak and broad N-N bending vibration belonging to the pyrazole ring was observed at about 1128 cm^{-1}. A strong bending vibration was observed at about 1342 cm^{-1} on the spectra of both complexes, and this vibration belongs to the aromatic amine functional group (C-N). Table 3.1 shows the significant vibrational frequencies and their corresponding functional groups for each complex.

Table 3.1: Main vibrational frequencies and their corresponding functional groups for complexes **3.2** and **3.3**

Complex	Aromatic C-H/ cm^{-1}	Alkyl C-H stretch/ cm^{-1}	Alkyl C-H bend/cm^{-1}	Aromatic C-C bend/cm^{-1}	Aromatic C-N bend/ cm^{-1}	Aromatic N-N/ cm^{-1}
3.2	3177, 3105	2779	1478	1557	1317	1068
3.3	3184, 3104	2939, 2786, 2705	1460, 1431	1590	1381, 1347, 1322	1055

3.5. SYNTHESIS AND CHARACTERIZATION OF PYRAZOLYL FUNCTIONALIZED NHC NICKEL(II) COMPLEXES

2.1b: R = Me
2.4b: R = p-NO$_2$C$_6$H$_4$

3.4: R = p-NO$_2$C$_6$H$_4$, X = BF$_4$
3.5: R = Me, X = BF$_4$
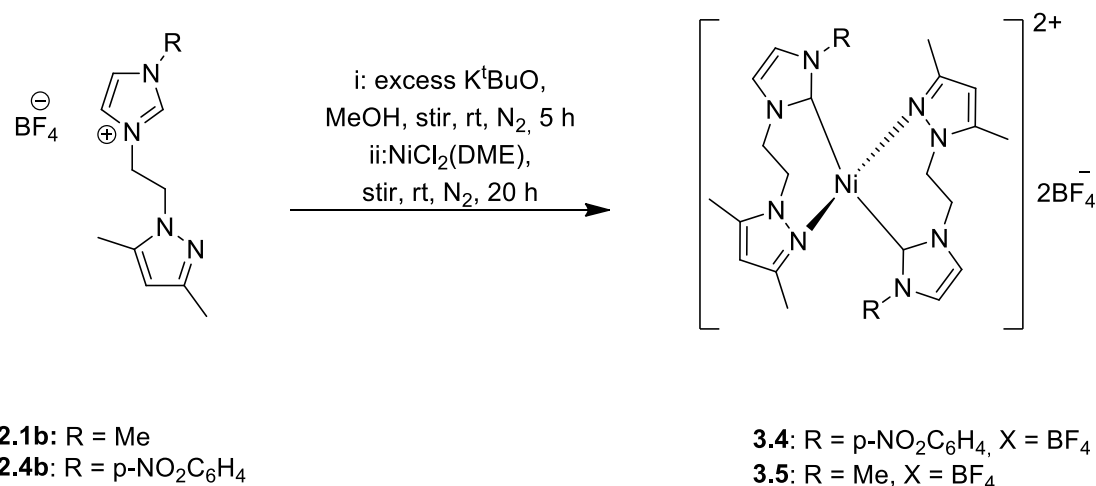
Scheme 3.6: Synthesis of NHC-Ni(II) complexes

3.5.1. METHODS AND MATERIALS

1. Synthesis of 3-(2-(3,5-dimethyl-1H-pyrazol-1-yl) ethyl)-1-(4-nitrophenyl)-1H-imidazol-3-ium Ni(II) BF$_4$ (**3.4**)

Nickel(II)-NHC complex was synthesized using the same method as complex **3.1** by reacting deprotonated **2.4b** with NiCl$_2$(DME) in dry methanol (Scheme 3.6). **3.4** was obtained as a hydroscopic reddish-orange solid. Yield: 55%, Mp: 75 – 78 °C. Yield = 0.0306 g, 55 %. LRMS: (m/z) = 590. ^{1}H NMR (400 MHz, DMSO): δ 8.5187 (CH, s, 2H,), 7.9630 (CH, s, 2H, ^3J= 9.1234 Hz), 6.7555 (CH, s, 2H), 6.6065 (CH, m, 1H, ^2J= 9.1626 Hz), 5.7779 (CH, s, 1H), 3.9508 (CH$_2$, m, 4H, ^2J= 12.9499 Hz), 1.6223 (CH$_3$, s, 3H), 1.2317 (CH$_3$, s, 3H). ^{13}C NMR data was not available due to possible decomposition in the collection of FID.[69]

2. Synthesis of 3-(2-(3,5-dimethyl-1H-pyrazol-1-yl) ethyl)-1-methyl-1H-imidazol-3-ium Ni(II) BF$_4$ (complex **3.5**)

Complex **3.5** was synthesized using the same method as complex **3.2** with the ligand precursor being **2.1b**. The complex was isolated as a hydroscopic pale-yellow powder. Yield: 1.54 g, 29%. Mp: 58 – 60 °C. LRMS = 470 m/z. ^{1}H NMR (400 MHz, DMSO): δ 5.5330 (CH, s, 2H), 4.7179 (CH, s, 1H), 4.1477 (CH$_2$, m, 4H, ^2J= 123.6647 Hz), 1.8838 (CH$_3$, s, 3H), 1.6055 (CH$_3$, s, 3H), 1.2341 (CH$_3$, s, 3H). ^{13}C NMR data was not available due to possible decomposition in the collection of FID.[69]

3.5.2. RESULTS AND DISCUSSIONS

This study was aimed to synthesize and characterize pyrazolyl functionalize NHC-Ni(II) complexes for the catalytic activation of alkanes. Nickel was one of the three transition metals selected for this study due to its similarities in catalytic activity with copper.[99]

Most reported nickel(II)-NHC complexes were synthesized using the transmetalation route, where the ligands were weakly coordinated to Ag. The intermediate Ag-NHC could be stable for isolation and possible characterization, while in most cases, it is used in situ to transfer the ligand to the desired metal.[21] The synthesis of both **3.4** and **3.5** were attempted via the transmetalation of corresponding intermediate Ag-NHC complexes. However, the end products in the preliminary synthesis of the Ag-NHC had very low yields, and were also contaminated by impurities. The metal source (Ag$_2$O) was light (UV) sensitive, making the resulting intermediate species UV sensitive as well. Hence, the adapted direct deprotonation (in situ free carbene) synthetic route was used for the synthesis of the Ni(II)-NHC complexes.

3.4 was isolated as a rod-shaped micro crystalline solid. Its physical form looked very similar to the cobalt(II) complex **3.1** and the copper(I) complex **3.2**, which were both synthesized from the same ligand precursor, **2.4b**. Complex **3.5** is a hygroscopic pale-yellow powder obtained in low yields (29%). The sharp melting point of 58 – 60 °C, is an indication of its purity, and both complexes are soluble in DMSO in high dilution.

3.5.2.1.NMR analysis

NMR was used as the first tool to investigate whether the complexes were successfully synthesized. Both **3.4** and **3.5** are paramagnetic Ni(II) complexes, however, the ^{1}H NMR spectra for both complexes were fairly sufficiently resolved to assign the signals. A comparison was made between each complex and its ligand precursor to correspond common features. This,

coupled with FTIR and MS data were sufficient to decide on the structure of each complex synthesized. ^{13}C NMR was not available due to possible decomposition in the collection of FID.[69] In the ^{1}H NMR, an upfield chemical shift was observed for all the protons with the exception of the proton on the pyrazole ring. The complete disappearance of the C_2 proton (labelled 'a' in Fig. 3.8 (top)) is confirmation of the deprotonation. Figure 3.8 shows a comparison between the NMR data of salt **2.4** and its corresponding nickel complex (**3.4**).
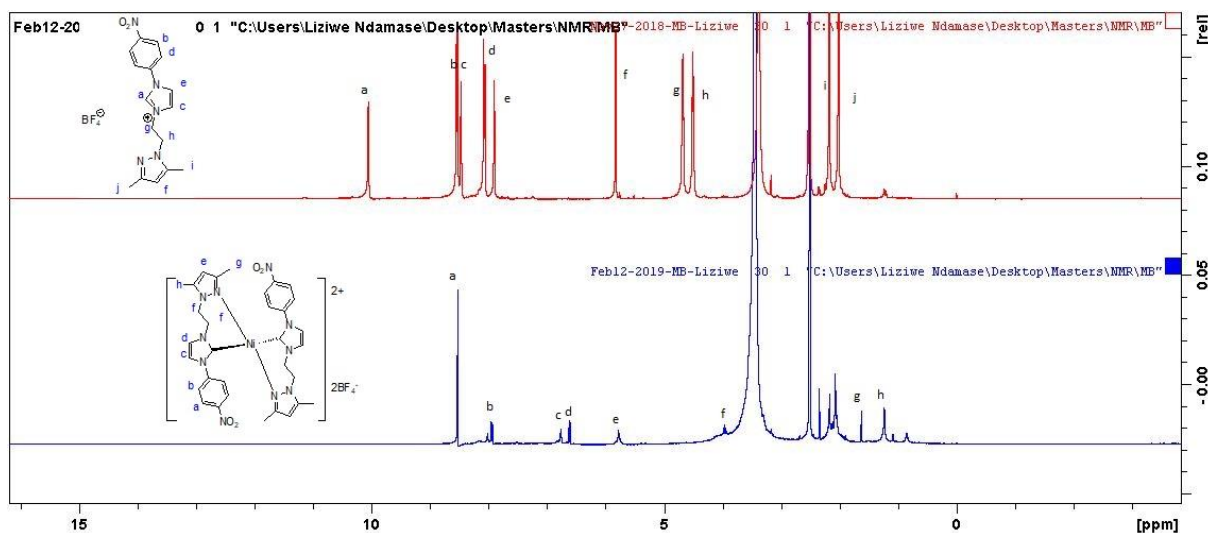
Figure 3.8: ^{1}H NMR comparison between **2.4** and its corresponding nickel complex (**3.4**)

Complex **3.4** was also successfully synthesized. However, it is highly sensitive to air as it decomposes upon a few minutes of exposure to air. The proton NMR spectrum of **3.4** revealed that the complex had imbibed considerable quantity of moisture. The ligand's hygroscopic nature could also account for the rapid decomposition after exposure to air. All the solvents used in the synthesis of the complexes were HPLC grade solvents of high purity ($\geq 99.9\%$). In addition, they were also dried using the suitable methods prior to use. Thus, the water molecules detected in the complex by NMR were absorbed by the complex from the moist air (Fig. 3.9).
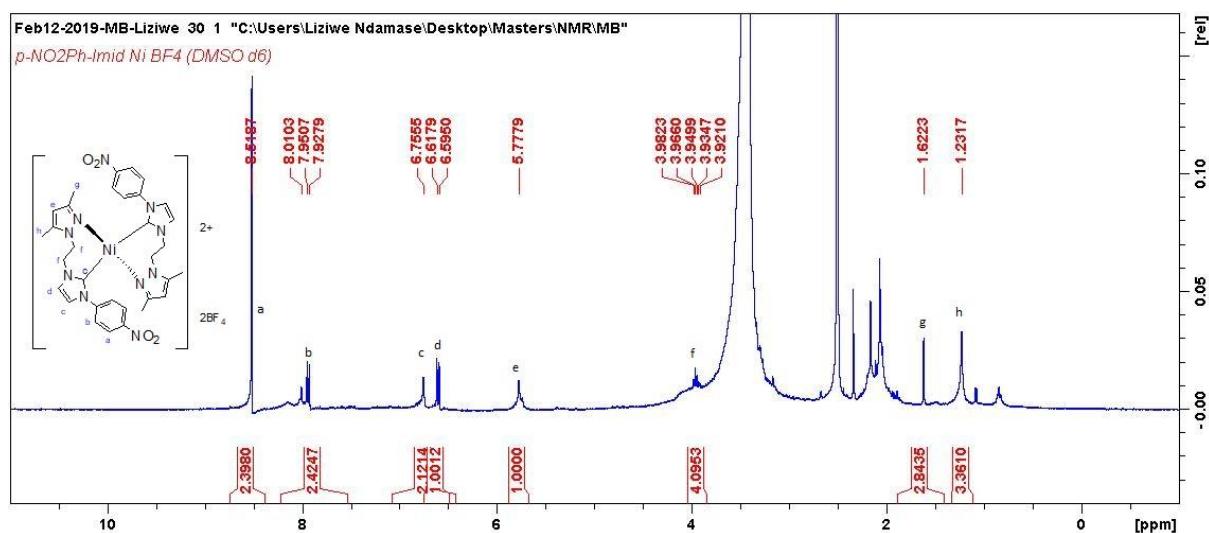
Figure 3.9: ^{1}H NMR of complex **3.4**

3.5.2.2. Coordination geometry

Nickel based catalysts have attracted attention mainly because nickel is cheap and highly abundant. Nickel-NHC complexes have been reported in numerous organic transformations that include C-C and C-N bond formations.[69, 100] Recent studies have reported on the use of nickel–NHC complexes in the activation or functionalization of hydrocarbons. These organic transformations include alkylation, alkenylation, *etc*. however, most of these transformations are for *sp^2* hybridised hydrocarbons, and relatively much less is reported on organic transformation of *sp^3* hybridised hydrocarbons.[101]

The coordination and geometry of transition metal complexes depend on the oxidation state of the metal ion. The complexes synthesized here are Ni(II) complexes, and thus the geometry of these complexes could be tetrahedral or square planar. This type of symmetry limits the number of reaction pathways possible and consequently increases the selectivity of the complex as a catalyst.[102]

3.5.2.3. Mass Spectrometry analysis

The molecular ion peak of **3.4** is (m/z) = 590, and this value corresponded to the loss of the nitro (NO$_2$) groups from both ligand motifs tethered to the Ni centre as shown in Scheme 3.7. The complex is highly hygroscopic and unstable; it might have started decomposing during the MS analysis. The

3.4
Chemical Formula: $C_{32}H_{36}N_{10}NiO_4$
m/z 683/2= 341 m/z
Experimental= ~343 m/z

[M-2NO₂]²⁺ z=2
Chemical Formula: $C_{32}H_{38}N_8Ni$
m/z 592
Experimental: 590 m/z

Chemical Formula: $C_{11}H_{12}N_4Ni$
m/z 263
Experimental: 263 m/z
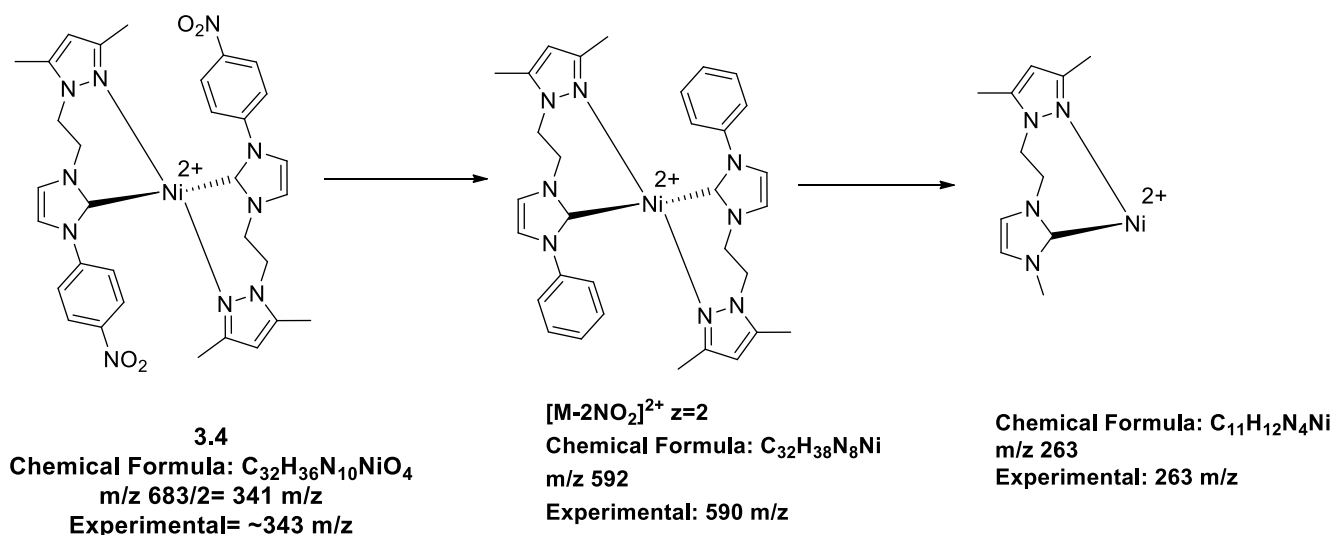
Scheme 3.7: Fragmentation pattern of complex **3.4**

Among all the complexes synthesized so far, those derived from **2.4b** tends to be more stable than others. The steric bulk of the ligand precursor and the electronic nature of the substituents or the generated ligand motif, might be the underlying advantage that led to the relatively higher stability of the corresponding complexes when compared to others. This complex is also doubly charged. The molecular ion peak is at 470 m/z and the base peak is at 235 m/z. These values are comparable with the theoretical values as indicated in the Scheme 3.8.

3.5
Chemical Formula: $C_{21}H_{32}N_8Ni$
m/z 466/2=233
Experimental Molecular ion Peak:
470m/z
Experimental Base Peak = 470/2 =235
m/z

Chemical Formula: $C_{11}H_{16}N_4Ni$
m/z 263
Experimental: 263 m/z

Chemical Formula: $C_{11}H_{17}N_4Ni$
m/z 206
Experimental: 205 m/z
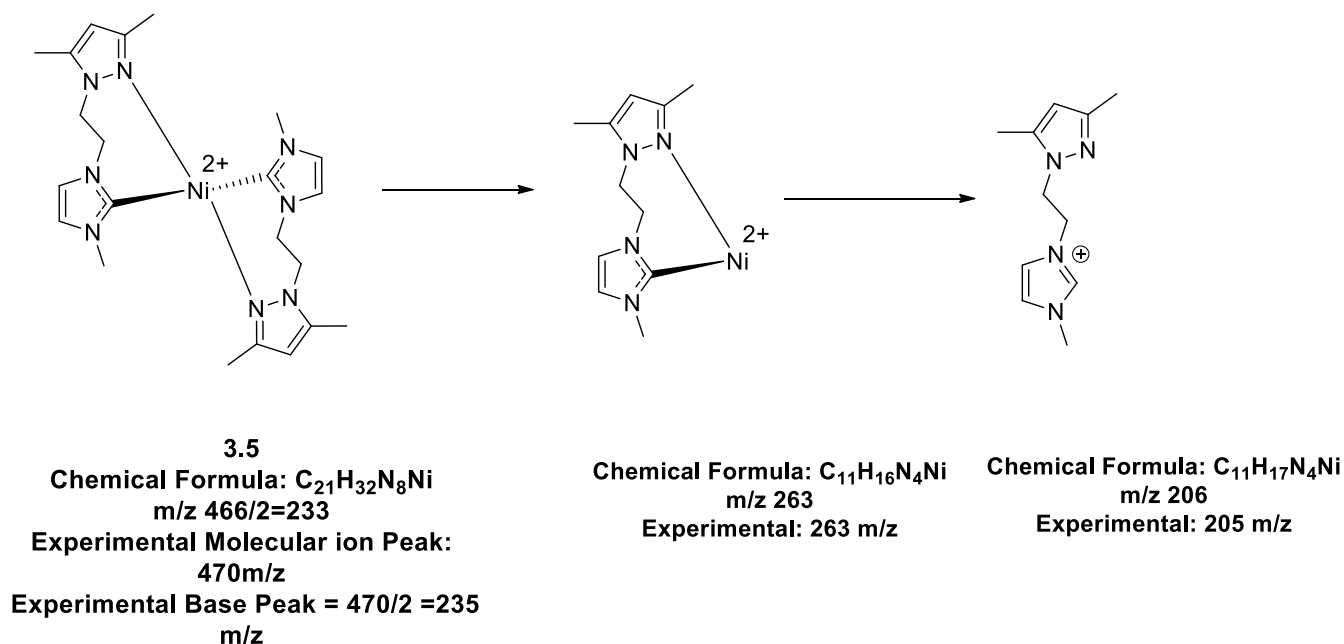
Scheme 3.8: Fragmentation pattern of complex **3.5**

3.5.2.4. FT –IR Analysis

Fourier-transform infrared spectroscopy was used to investigate the vibrational modes of the functional groups of complex **3.4** and complex **3.5** by obtaining the spectrum of absorption and emission. Both complexes contained an ethylene linker between the imidazolium and the dimethyl pyrazole, this alkyl C-H stretching vibration was observed at a range 2950-2750 cm[1]. The stretching vibration observed at ~3150 cm^{-1} corresponds to the aromatic C-H functional group. Bending vibration for the para NO_2 group on the ligand motif coordinated to **3.4** was observed at 1585 cm^{-1}. Similarly, a broad bending vibration at about 1055-1085 cm^{-1} accounted for the N-N functionality in both complexes. Table 3.2 summarizes the FTIR vibrational frequencies of major the functional groups in the Ni(II)-NHC complexes.

Table 3.2: Main vibrational frequencies and their corresponding functional groups for complexes **3.4** and **3.5**.

Complexes	Aromatic C-H/ cm^{-1}	Alkyl C-H stretch/ cm^{-1}	Alkyl C-H bend/cm^{-1}	Aromatic C-C bend/cm^{-1}	Aromatic C-N bend/ cm^{-1}	Aromatic N-N/ cm^{-1}
3.4	3167, 3102	2941, 2887, 2817, 2712	1413	1558, 1511	1355, 1317	1055
3.5	3200	2943, 2828, 2715	1428	1619, 1598, 1557	1355,1336	1058

3.6. SUMMARY AND CONCLUSION

This chapter was aimed to present the data on the synthesis and characterization pyrazolyl functionalized *N*-heterocyclic carbene transition metal complexes of cobalt(II), copper(I) and nickel(II). The most stable ligands discussed in chapter 2 were chosen and coordinated to each of the transition metals. In total, five complexes were synthesized; one cobalt complex from salt **2.4b**; two copper complexes from salts **2.1b** and **2.4b**; and two nickel complexes from salts **2.1b** and **2.4b**.

In comparison, amongst the five compounds, **3.1** and **3.2**, synthesized from salt **2.4b** were the most the stable complexes. The hygroscopic nature of the ligands was transferred to the complexes, and was magnified in some complexes. Copper complexes have been reported to be highly efficient catalysts for the oxidation of hydrocarbons and other organic compounds such as aromatics.[55] This is because some oxidizing enzymes available in nature contain copper ions in their active sites.[10, 55] Consequently, some copper complexes have some biomimetic properties.[18] NHC-nickel complexes have been reported as successful Suzuki catalysts and also for olefin polymerisation.[47] Cobalt, being part of the "iron triad" has similar physical and chemical properties to iron and nickel. Very little data has been reported on the use of such complexes as oxidation catalysts, making this work novel.

NMR, MS and FTIR were used to characterise each complex. The Co(II) and Ni(II) complexes are paramagnetic; hence, their NMR spectra were poorly resolved. Owing to their hygroscopic nature, some complexes would decompose in solution if even a trace amount of H_2O molecules was present. This explains the unidentified signals in the ^1H NMR of the complexes. The decomposition pattern was similar in complexes containing the same metal centre.

CHAPTER 4: PRELIMINARY OXIDATION OF CYCLOHEXANE

4.1. SUMMARY

Two complexes, $[Co^{II}(p\text{-}NO_2Ph\text{-}Imid)_2][BF_4]_2$ (**3.1**) and $[Cu^{I}(p\text{-}NOPh\text{-}Imid)(NCCH_3)_2][BF_4]_2$ (**3.2**) containing the same hemilabile bidentate ligand (**2.4b**) were used as model compounds to test the catalytic applicability of the pyrazolyl functionalized NHC-metal complexes for the oxidation of cyclohexane to cyclohexanol and cyclohexanone in acetonitrile. **3.1** was more active with a TON of 104. However, the complex had significantly lower chemoselectivity towards cyclohexanol in comparison to **3.2** which has a lower TON of 18. The chemoselectivity to cyclohexanol by **3.2** was at 83%, implying a K/A ration of 0.2. The effect of reaction time on product distribution was investigated as well as effect of reaction time on conversion and it was revealed that an induction period was required before a significant increase in conversion could be observed. Cyclohexanol was observed to be the major product throughout the reaction. The concentration of cyclohexanol gradually decreased over time due to over oxidation, this resulted in an increase in the concentration of the correspond ketone. A proposed mechanism for the oxidation of cyclohexane mediated by complex **3.2** is discussed.

4.2. INTRODUCTION

Paraffins have become desirable substrates for chemical transformation. This is because they are readily available; hence, they are used as principal feedstock in many chemical processes. Although chemical transformations of alkanes have been reported for a long time, these transformations involve the combustion of hydrocarbons in air at elevated temperatures (>300 °C), usually characterized by lack of selectivity. Thus, even though this route is highly valuable, the harsh conditions and low selectivity are its main drawback.

Although the chemical inertness of alkanes can be overcome under harsh reaction conditions, issues like low selectivity, low yields and unwanted environmental waste have forced chemists to find new ways for alkane conversion into valuable products (unsaturated hydrocarbons or oxygenated products) under mild conditions.[18] In the last few years, new reactions of saturated hydrocarbons under mild conditions have been reported, *e.g.* alkane transformations in superacid media, interactions with metal atoms and ions, and reactions with some radicals and carbenes.

To the best of our knowledge, no work been reported on the use of pyrazolyl functionalized imidazolium copper complexes as catalysts for paraffin oxidation. However, various copper complexes have been found to be highly efficient catalysts in alkane oxidation and oxidation of other organic compounds, such as alcohols and aromatics.[55] Copper and iron based metalloenzymes were used as models in the synthesis of efficient C-H oxidation catalysts that have offered high selectivity. One of the first copper catalysed alkane oxidation catalytic systems operated under mild conditions was reported by Barton *et al.* and composed of copper powder, acetic acid, pyridine and hydrogen peroxide as the oxidant.[103] The process of alkane oxidation was said to take place via a radical chain reaction via a Fenton-type reaction mechanism. However, the product yield was significantly low at less than 5 %. The most recent studies done by Pérez and co-workers using a trispyrazolylborate ligand coordinated to mononuclear copper complex showed high selectivity with a moderate product yield.[104]

In this study, new pyrazolyl-functionalized NHC transition metal complexes were synthesized and reported in chapter 3. In addition, some of these NHC-metal complexes that are stable enough are tested as catalysts in alkane oxidation.

4.3. METHODS AND MATERIALS

All the oxidation reactions were conducted with cyclohexane as the substrate, cyclohexanone as the internal standard and, hydrogen peroxide (H_2O_2) as the oxidant in the solvent acetonitrile. Copper(II) chloride ($CuCl_2$) was used as the reference catalyst for alkane oxidation. The reactions were performed in duplicate using two-neck pear-shaped flasks (25 mL capacity), which were equipped with a condenser. The solvent and oxidant are HPLC grade.

All the reactions were performed using the same method, unless stated otherwise. The components were added in the following manner: acetonitrile (solvent), cyclohexanone (internal standard), cyclohexane (substrate), hydrogen peroxide (oxidant) and, the complex followed by more acetonitrile if required so that the total volume equated to 5 ml. The complexes were introduced in the form of stock solutions with the number of moles constant at 9.56×10^{-6} mol. The complex to substrate ratio was kept constant at 1:100 and a substrate to oxidant ratio of 1:9 was used. The reaction was then refluxed at 65 °C under an atmosphere of nitrogen gas for 24 h. The temperature was maintained using an oil bath on a hot plate connected to a thermocouple. After the 24 h had lapsed, a small volume (about 2 mL) of the

solution was treated with PPh$_3$ and filtered with the aid of Celite and thereafter both samples (treated and untreated with PPh$_3$) were subjected to GC analysis.

A volume of 0.5 μL of each sample was injected into the GC for product analysis and quantification. A PerkinElmer Auto System Gas Chromatograph with an FID (flame ionisation detector) was used. The detector temperature used for product analysis was set at 280 °C. The injector temperature was set at 250 °C and a DB 5 column with a length of 30 m was used to effectively separate the product stream. The GC method used was: starting temperature 50 °C, hold for 1 minute, ramp at 2 °C/minute to 80 °C, hold at 80 °C for 5 minutes and ramp at 2 °C/minute to 100 °C, hold at 100 °C for 2 min and then ramp to 200 °C at 15 °C/minute.

Yields were calculated based on the total moles of products formed as a function of the initial moles of substrate added into the reaction mixture and was expressed as a percentage, while the selectivity was expressed as moles of each product as a function of the total moles of all products in the stream.

4.4. RESULTS AND DISCUSSION

4.4.1. General Discussion

A series of preliminary studies were carried out to obtain the optimum reaction conditions. Standards were used to calibrate the instrument prior to analysis. Calibration curves are displayed in the appendix E. A multicomponent standard was prepared and used to calculate the response factor for each of the components using the formula,

$$\frac{Ax}{Cx} = F \frac{As}{Cs}$$

where 'Ax' is the peak area of the analyte, 'Cx' is the known concentration of the analyte, 'F is the response factor, 'As' is the peak area of the internal standard, and 'Cs' is the concentration of the internal standard. The response factor was then used to calculate the concentration of the analytes from the catalysis.

Blank studies were prepared before each complex was tested. Three blank studies were conducted in duplicates for each complex, this was done to test the reproducibility of the results

obtained and to determine the role of each reagent and additives (metal complex, oxidant) on the catalytic process.

Complexes **3.1** and **3.2** were utilised as model catalysts for the oxidation process. Cyclohexane was selected as the substrate because its product stream has (*i*) two possible products, which are cyclohexanol and cyclohexanone, (*ii*) both of the products are highly valuable on an industrial scale, this is a value addition to the starting material (industrial uses range from rubber chemicals, dyes, plasticizers to pharmaceuticals).[105]

Two oxidants namely; hydrogen peroxide (H_2O_2) and tert-butylhydroperoxide (TBHP) were tested to determine which one was better suited for catalytic systems similar to those used in this report. Both of these oxidants are commonly used because they are environmentally friendly, cheap and readily available. H_2O_2 was used for this study.

The influence of temperature on the conversion of alkanes to oxygenated products was investigated by Mncube[106] and the conversion was reported to increase with an increase in temperature. However, at 80 °C, the rate of conversion started decreasing. This was due to the decomposition of hydrogen peroxide (Scheme 4.1). The optimal temperature range for the oxidation of cyclohexane was established to be 60 – 70 °C. Thus, all the oxidation studies reported herein were carried out at 70 °C.

$$2H_2O_2 \xrightarrow[\triangle]{} 2H_2O + O_2$$
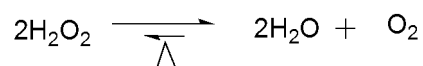
Scheme 4.1: Thermal decomposition of hydrogen peroxide

4.4.2. Analysis of complex 3.1

Complex **3.1** was analysed under the same reaction conditions as complex **3.2** and very different results were observed. The substrate was completely consumed in the catalysis process using complex **3.1**, as indicated in Figure 4.1 which shows the concentrations of the product stream after 24 hours of catalysis before treatment with PPh₃.
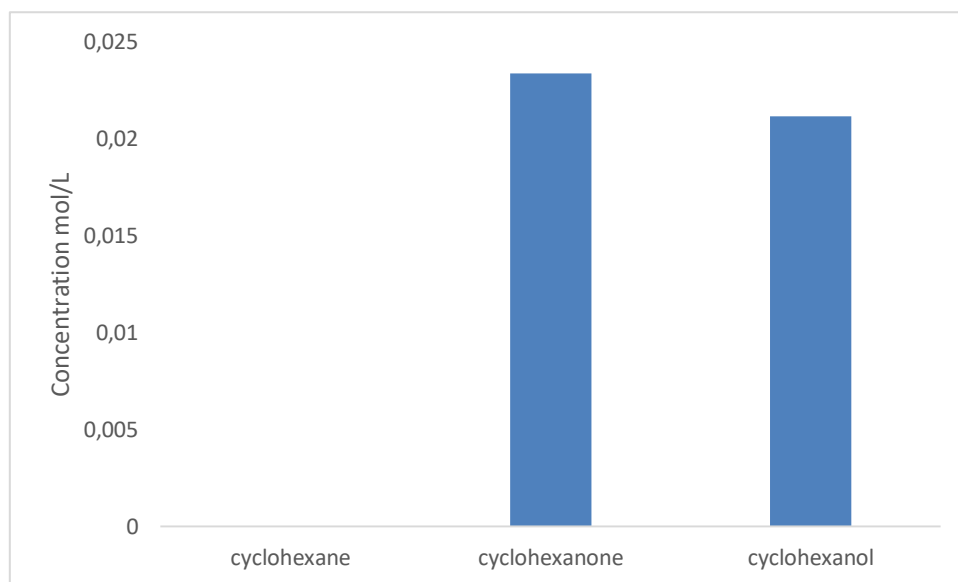
Figure 4.1: Concentrations of cyclohexane and its oxygenated products before treatment with PPh$_3$ from complex **3.1**

A conversion of 38% was obtained for complex **3.1**, which was much higher than the 19 % conversion obtained for complex **3.2**. This indicates that **3.1** was more active as catalyst for oxidation of cyclohexane than **3.2**. However, the chemoselectivity of **3.1** towards alcohols was significantly lower at 47 % in comparison to 83 % obtained for **3.2**. This was expected as the highly active catalyst will eventually be efficient in the secondary oxidation of cyclohexanol to cyclohexanone.[107] Poor catalyst control was also observed by Tordin *et. al.* who reported on the effect of the solvent on the activity of a copper and a cobalt complex in the oxidation of cyclohexane.[56] A higher activity and consequently a higher TON was observed when the solvent's polarity was high for the cobalt complex; the copper complex had very low TON but a high selectivity. However, when the polarity of the solvent was decreased the opposite trend was observed for both complexes. The calculated TON for **3.1** was 104 which is higher than the TON for **3.2** calculated as 19. The high TON supported the conclusion that **3.1** was more active than **3.2**.

4.4.3. *Analysis of complex 3.2*

Copper complexes have been reported to be very efficient catalysts in the oxidation of alkanes.[55] **3.2**, was a copper complex synthesized using salt **2.1b**. This complex was used as a catalyst in the oxidation of cyclohexane to cyclohexanol and cyclohexanone as represented in reaction Scheme 4.2. Cyclohexyl hydroperoxide is the intermediate primary product, which is reduced to cyclohexanol. Cyclohexanone is the secondary product of the oxidation reaction. Shul'pin *et al.* reported that the addition of triphenyl phosphine (PPh$_3$) to the primary product results in the quantitative reduction of the cyclohexyl hydroperoxide to the desired alcohol product.
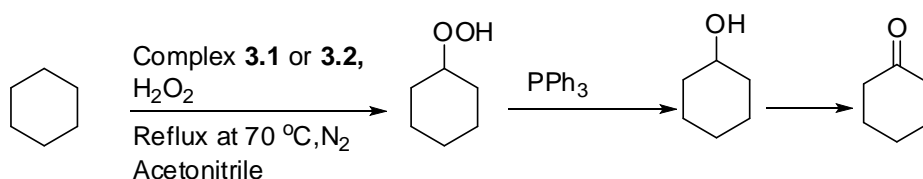
Scheme 4.2: Oxidation of cyclohexane

The gas chromatograms obtained before PPh$_3$ is added differ significantly from those obtained after PPh$_3$. This is because PPh$_3$ reduces the cyclohexyl hydroperoxide to cyclohexanol, consequently leading relatively to an increase in the amount of alcohol product and a decrease in the relative amount of the ketone product.[108, 55] This is supported by the higher concentration of cyclohexanol as shown in Figure 4.2. The analysis before and after sample treatment with PPh$_3$ allows for a quantitative analysis of each component at any given time.
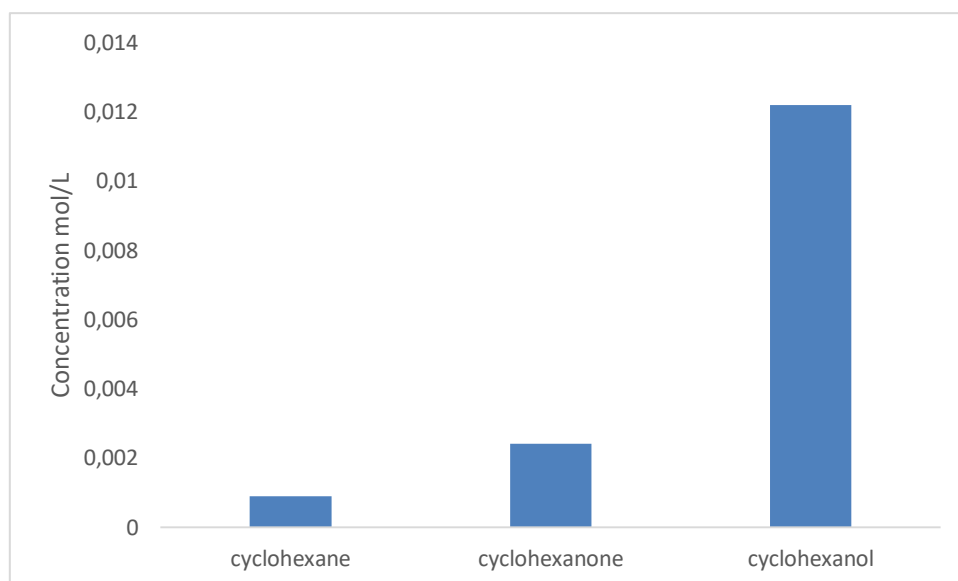
Figure 4.2: Concentrations of cyclohexane and its oxygenated products before treatment with PPh$_3$ from **3.2**

The turnover number (TON) calculated for the oxidation of cyclohexane using **3.2** was low at 19. This means the complex is a poor catalyst for this catalytic system. The inefficiency of the Cu-NHC complex as a catalyst for this oxidation reaction might be due to the oxidant used in this reaction, *i.e.* hydrogen peroxide, which produces water as a by-product of the oxidation process. The moisture is a distinct disadvantage as it attacks the complexes leading to their gradual decomposition of **3.2**.

Acetonitrile was used as the solvent for the oxidation studies because many related works of literature including Shul'pin have reported that it is the most suitable solvent for the catalytic reaction due to its stability during the oxidation reaction. Other common solvents such as THF, ethers and alcohols are all unsuitable due to their reactivities.[55] However, both complexes i.e. **3.1** and **3.2** applied as catalysts for the oxidation of cyclohexane are only partially soluble in the acetonitrile. This could also account for the low TONs observed in this study.
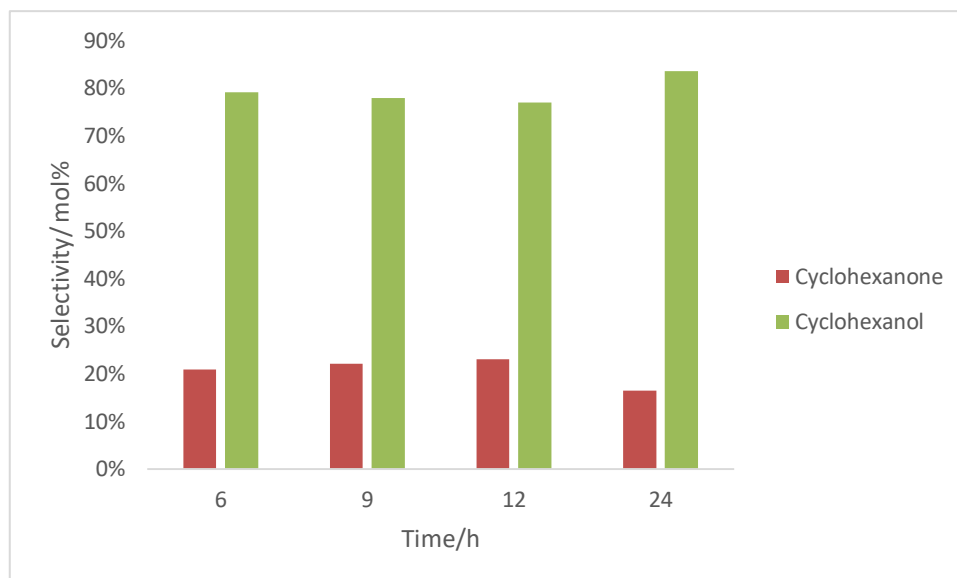
4.4.4. *Effect of time*

Analysis of conversion over time graph (Figure 4.3) revealed that an induction period was required before a significant increase in conversion was observed. The most significant increase in conversion was observed in the first 12 h, and thereafter a modest gradual increase

was observed until 24 h. A similar trend was observed by Ribeiro *et al*. when the oxidation was performed in an ionic liquid.[108]
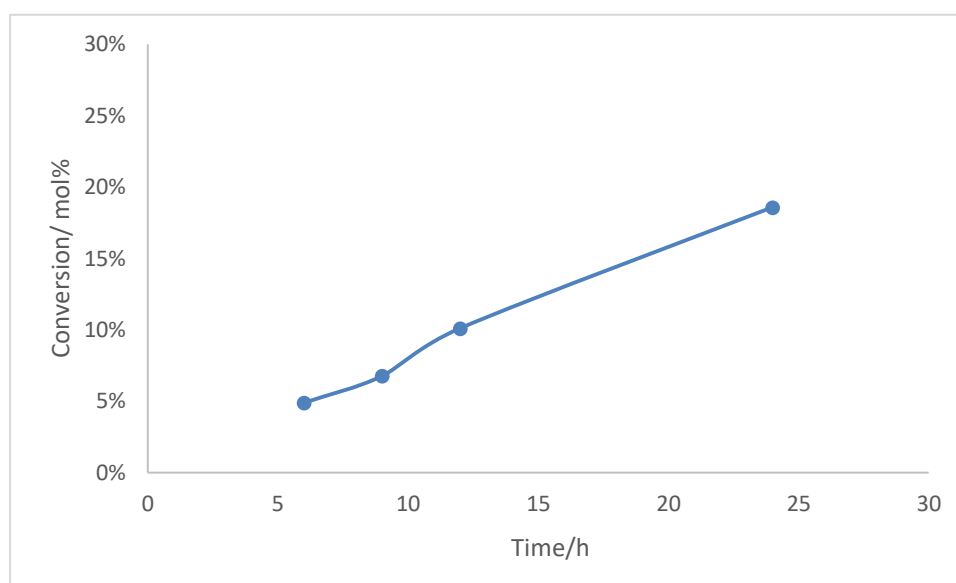

Figure 4.3: Effect of reaction time on conversion

The effect of time on the product distribution was also investigated with the aim of determining the optimum reaction time. The reactions were monitored at 3, 6, 9, 12 and 24 h intervals and were carried out at 70 °C under inert conditions, as shown in Figure 4.4. The results indicated that cyclohexanol is the major product throughout the reaction. The highest concentration of cyclohexanol was observed at 24 h. The concentration of cyclohexanol was observed to gradually decrease within the first 12 h while the concentration of cyclohexanone in the product stream increased gradually. This phenomenon is due to the over oxidation of cyclohexanol resulting in an increase in the corresponding ketone.[109] A slight decrease in the concentration of cyclohexanone was observed at 24 h which is most likely due to the gradual formation of adipic acid from cyclohexanone.[108]

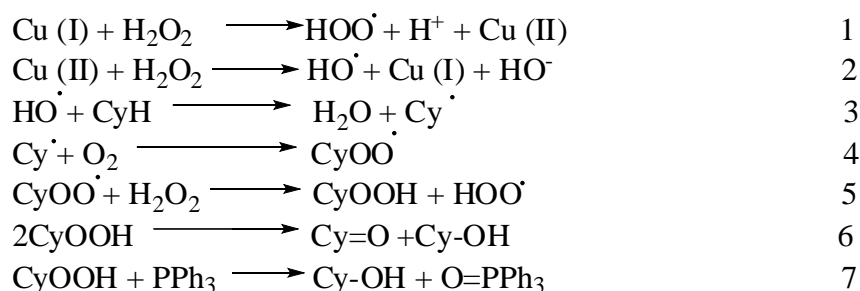**Figure 4.4**: Effect of reaction time on product distribution

Trace amounts of adipic acid were observed in the GC trace of the product stream of the oxidation of cyclohexane using both complexes. Adipic acid can be formed directly from cyclohexane during the oxidation process and/or when the oxygenated products of cyclohexane *i.e.* cyclohexanol and cyclohexanone are over oxidised in the presence of nitric acid (Fig. 4.5).[110-111] Vang reported that *N*-heterocyclic carbenes bound to a labile transition metal centre could induce ring-opening polymerization of cyclohexane.[112] Adipic acid is used in the synthesis of nylon-6,6, polyurethane, lubricants and plasticizers, and thus has a higher value than both cyclohexanol and cyclohexanone.[113]
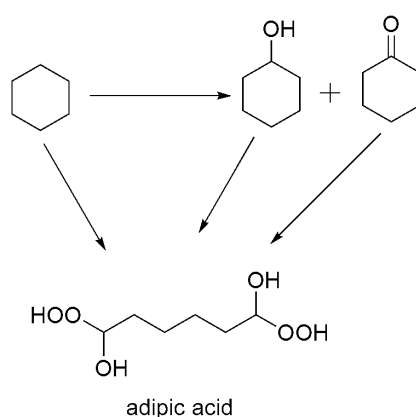
Figure 4.5: Formation of adipic acid from cyclohexane

4.4.5. *Mechanism of the catalytic reaction*

To date, no information is available to propose that there is initial coordination of cyclohexane to copper or cobalt ions (catalyst centre) during the stages of catalytic oxidation of its inert C-H bond. Hence, the activation of the substrate (cyclohexane) CyH, takes place via a chain reaction of free radicals (free radical mechanism). Scheme 4.3 is a proposed reaction mechanism for the oxidation of the CyH activated by a Cu(I) centre such as **3.2**, based on Fenton reaction reported by Ribeiro *et al.* [18, 108] Compound **3.2** catalytically activates the oxidant hydrogen peroxide to oxygenated free radicals (HOO• and HO•) (step 1 and 2). The HO• is then used to abstract H from cyclohexane resulting in a cyclohexyl radical (step 3).[108, 114-115] The reaction of the cyclohexyl radical with dioxygen from the decomposition of HOO• radical forms CyOO• (step 4), cyclohexyl hydroperoxide is then formed when CyOO• deprotonates H_2O_2 (step 5). Catalyst assisted decomposition of cyclohexyl hydroperoxide (step 6) then leads to the formation of cyclohexanol and cyclohexanone. The alcohol produced can also be readily obtained by the addition of a suitable reducing agent such as PPh_3 (step7).

$$Cu\ (I) + H_2O_2 \longrightarrow HOO^{\cdot} + H^+ + Cu\ (II) \qquad\qquad 1$$
$$Cu\ (II) + H_2O_2 \longrightarrow HO^{\cdot} + Cu\ (I) + HO^- \qquad\qquad 2$$
$$HO^{\cdot} + CyH \longrightarrow H_2O + Cy^{\cdot} \qquad\qquad 3$$
$$Cy^{\cdot} + O_2 \longrightarrow CyOO^{\cdot} \qquad\qquad 4$$
$$CyOO^{\cdot} + H_2O_2 \longrightarrow CyOOH + HOO^{\cdot} \qquad\qquad 5$$
$$2CyOOH \longrightarrow Cy{=}O + Cy{-}OH \qquad\qquad 6$$
$$CyOOH + PPh_3 \longrightarrow Cy{-}OH + O{=}PPh_3 \qquad\qquad 7$$

Scheme 4.3: Proposed reaction mechanism for the activation of cyclohexane using a Cu(I) ions *i.e.* complex **3.2**

4.5. CONCLUSION

This chapter aimed to test the catalytic activity of two complexes, complexes **3.1** and **3.2**, synthesized and characterized as reported in chapter 3. This was done by applying the complexes as catalysts in the oxidation of cyclohexane using well-established procedures. The primary catalytic product from this reaction is cyclohexyl hydroperoxide which was then catalytically reduced by the addition of PPh_3 to produce cyclohexanol and cyclohexanone. Both complexes had the same bidentate ligand, with **3.1** as a cobalt complex and **3.2** as a copper

complex. Compound **3.1** showed higher TON of 104 and had a higher conversion of 38% after 24 h reaction time. Hence, **3.1** is the better catalyst for this reaction.

In conclusion, the prepared complexes have demonstrated moderate catalytic activities for the oxidation of the cyclohexane substrate under mild reaction conditions. However, more studies still need to be conducted to investigate the effect of other bidentate CN ligands on the activity and selectivity of the catalysts.

CHAPTER 5

CONCLUSIONS AND RECOMMENDATIONS
FOR FURTHER RESEARCH

5.1. GENERAL INTRODUCTION

Organic transformations such as the oxidation of alkanes are the initial steps for many industrial chemical syntheses. However, the inertness of the C-H bond in saturated hydrocarbons is why most reported transformations require very harsh condition such as high temperatures, strong oxidants *etc.* and often require long reaction times while characterized with low product selectivity. An efficient catalytic system that is green, with high selectivity towards the desired products, and under mild conditions at room temperature, is still to date a challenge.

NHCs are now considered one of the most versatile ligands in transition metal catalysts. Donor functionalized NHC ligands such as NHC-N chelates have been reported to possess hemilabile property. The NHC is strongly bonded to the metal centre, almost anchored, while the N-donor is loosely bonded to the metal centre. When these two ligands are tethered together and anchored to the metal centre, the loosely bound N-donor allows for partial dissociation of the ligand from the metal. This increases the accessibility of the metal centre to the substrate for oxidation to occur and such is among desired properties of more stable catalysts with high activities. Thus, the synthesis and characterization of new pyrazolyl functionalized NHC ligand precursor salts reported in Chapter 2 is topical.

5.2. SYNTHESIS AND CHARACTERIZATION OF PYRAZOLYL FUNCTIONALIZED NHC PRECURSORS

Two methods for the synthesis of the salts were developed from 2-(3,5-dimethyl-1H-pyrazol-1-yl) ethanol. Salt **2.1** (3-(2-(3,5-dimethyl-1H-pyrazol-1-yl) ethyl)-1-methyl-1H-imidazol-3-ium) (for both **2.1a** and **2.1b**) was synthesized using both methods. The first method involved 1-(2-(1H-imidazol-1-yl) ethyl)-3,5-dimethyl-1H-pyrazole nucleophilic attack by the lone pair of electrons on the nitrogen on the polar covalent Me-I bond, thereby displacing iodide, and forming salt **2.1a** with iodide as the counter-ion. Method two involved a bimolecular nucleophilic substitution reaction, where the halide was displaced from 1-(2-chloroethyl)-3,5-

dimethyl-1H-pyrazole resulting in the formation of a primary carbocation intermediate molecule which is then substituted by *N*-methyl imidazole forming a salt **2.1a** with chloride as the counter ion. Route one resulted in a salt that contained many impurities, thus requiring further purification. This was done using column chromatography, since washing the salt with ethyl acetate (a solvent that all the starting material and impurities are soluble in) resulted in the loss of some of the salt as it was partially soluble in the solvent as well. Method two resulted in a higher yield, 100% conversion with no unreacted starting material and thus no need for purification; that is why it was chosen as the method for the synthesis of the rest of the salts.

A few challenges were encountered when synthesizing the salts, the first was by correctly adjusting the pH of the 1-(2-chloroethyl)-3,5-dimethyl-1H-pyrazole. Progress of the reaction was monitored using litmus paper. An acidic pH meant that hydrochloric acid was present in solution with 1-(2-chloroethyl)-3,5-dimethyl-1H-pyrazole, and if left unneutralized, could eventually react with the alkyl imidazole quicker than the 1-(2-chloroethyl)-3,5-dimethyl-1H-pyrazole, resulting in the formation of a *H*-imidazolium chloride salt instead of the desired product. The second challenge was encountered in the synthesis of salt **2.4a**. All the other salts were successfully synthesized using a solvent-free method, and however, when **2.4a** was synthesized using the same method, no reaction took place. This is most likely directly linked to steric hindrance from the bulky nitrophenyl wingtip substituent on the imidazole, making it difficult for the nucleophilic attack of imidazole to the 1-(2-chloroethyl)-3,5-dimethyl-1H-pyrazole. Or, because the melting point of 1-(4-nitrophenyl)-1H-imidazole which is 309 – 311°C, is much higher than that of 1-(2-chloroethyl)-3,5-dimethyl-1H-pyrazole, meaning that by the time 1-(4-nitrophenyl)-1H-imidazole melts into solution the 1-(2-chloroethyl)-3,5-dimethyl-1H-pyrazole had decomposed resulting in no reaction occurring. Thus, DMSO was used to dissolve 1-(4-nitrophenyl)-1H-imidazole into solution, and the reaction took place at 110 °C. After that, all the salts were subjected to anion metathesis to increase the stability and induce crystallization. None of the salts crystallize out despite numerous attempts using a variety of crystal growth techniques. The hygroscopic nature of the salts also made handling much more difficult.

Suggested further studies include an investigation into decreasing the ethylene linker to a methylene linker to increase rigidity and decrease the free rotation in the molecule backbone. This is hypothesized to also contribute to the enhancing stability of the ligand precursors. In

addition, investigating the effect of bulky substituents on the stability of the salts is also important.

5.3. SYNTHESIS AND CHARACTERIZATION OF PYRAZOLYL FUNCTIONALIZED NHC TRANSITION METAL COMPLEXES

Five complexes were synthesized from salts **2.1b**, and **2.4b**. These complexes were synthesized using in situ free carbene route. The free carbene was prepared in the reaction flask via direct deprotonation of the imidazolium proton with a base (*t*BuOK) in a protic solvent (MeOH) at room temperature. Characterization was done using ^{1}H and ^{13}C NMR, MS and FTIR. The complexes inherited the hygroscopic nature of the ligand precursors. This made handling the complexes very difficult. Consequently, only two of the five complexes were stable enough to be tested as catalysts in the oxidation of alkanes. A comparison was made between the most stable complexes of cobalt and copper *i.e.* complexes **3.1** and **3.2**.

A study on reducing the length of the alkyl linker between the pyrazole and imidazole rings with the aim of increasing rigidity and consequently, the stability of the complexes still needs to be carried out.

5.4. OXIDATION OF CYCLOHEXANE

Both **3.1** and **3.2** were used as catalysts for the oxidation of cyclohexane. The primary product from the method used in the catalytic oxidation is cyclohexyl hydroperoxide which was then reduced to produce cyclohexanol. Also, the oxidation of cyclohexanol produced during the catalytic process yielded the ketone, cyclohexanone. Complex **3.1** had a higher TON of 104 and had a higher conversion of 38 % after a reaction time of 24 h. However, after 24 h reaction time, catalyst **3.1** produced 53 % of cyclohexanone, and the K/A ratio is 1.11. On the other hand, **3.2** had a lower TON of 18 and a low conversion of 19 % after 24 h. The complex also showed better production of cyclohexanol of 83 %.

More studies still need to be conducted to investigate the effect of structural variation on the activity of the catalysts. Studies into the effect of additives on the catalytic activity and selectivity of the complexes, and the effect of solvent polarity on selectivity and reaction time should also be carried out.
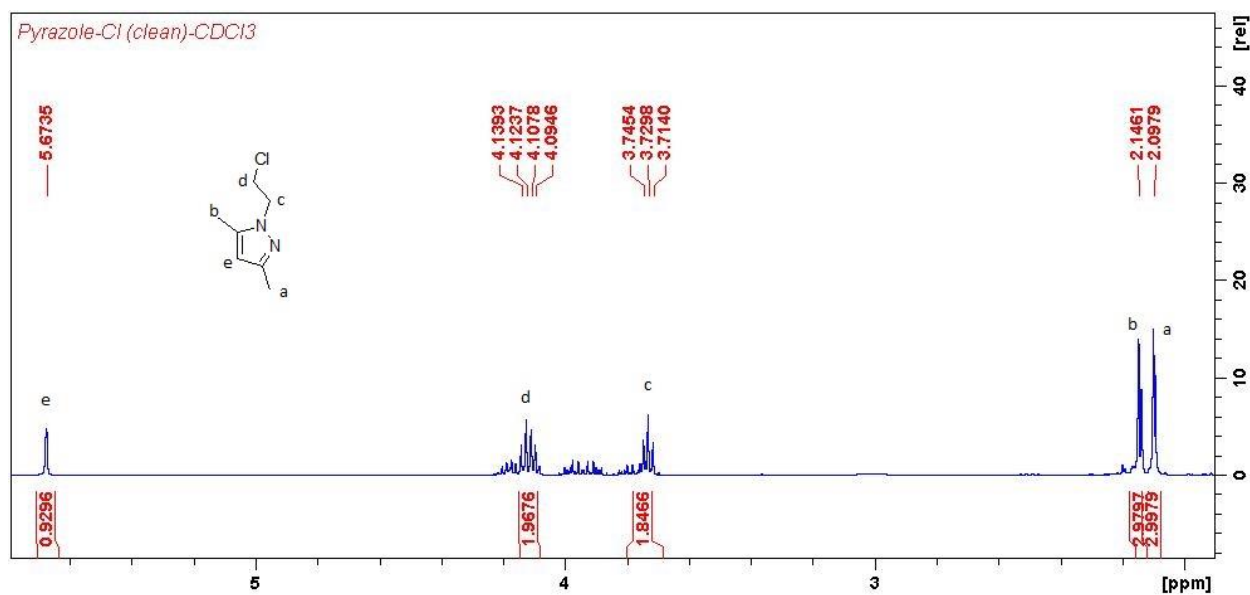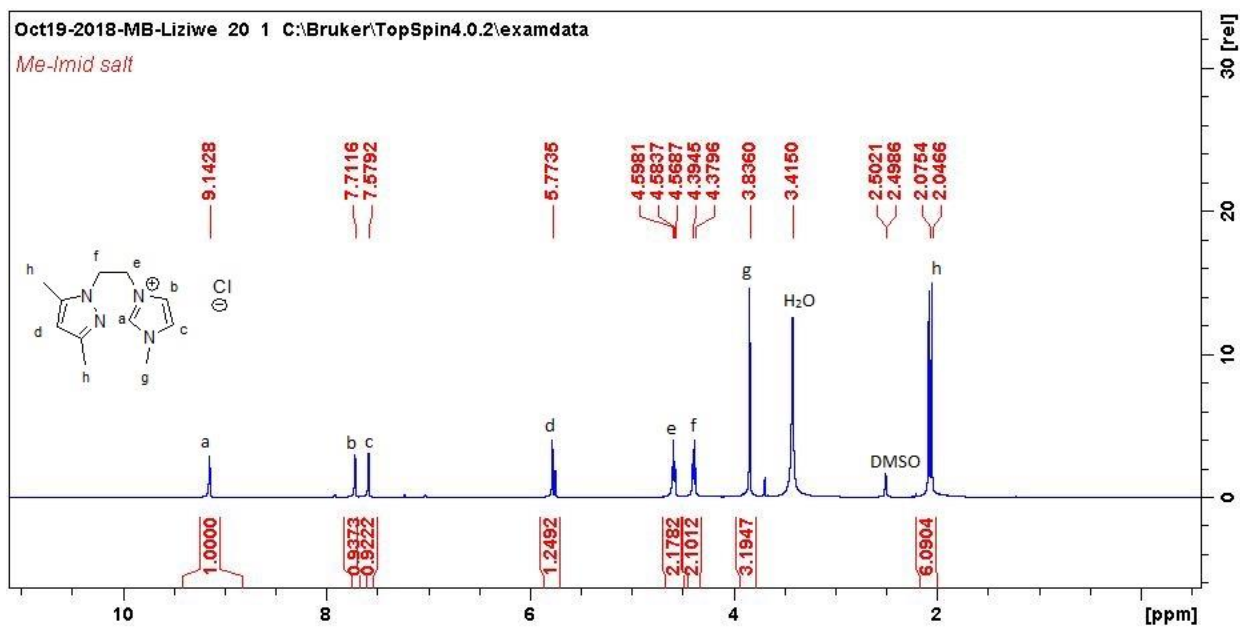
¹H and ¹³C NMR spectra of :-
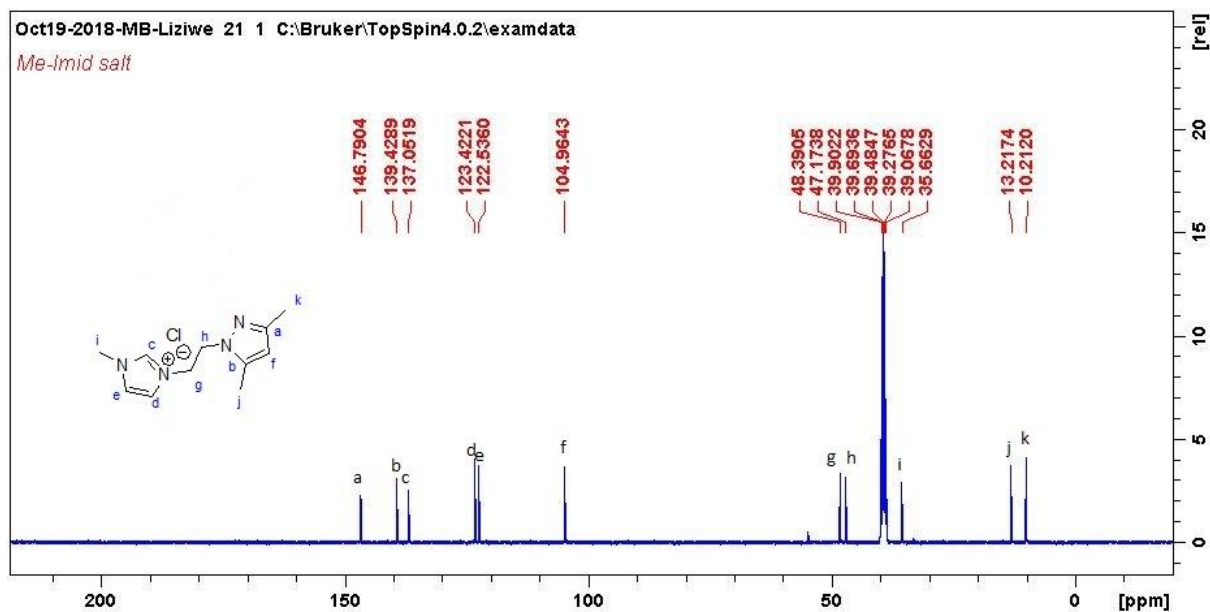
1. 2-(3,5-dimethyl-1H-pyrazol-1-yl)ethanol
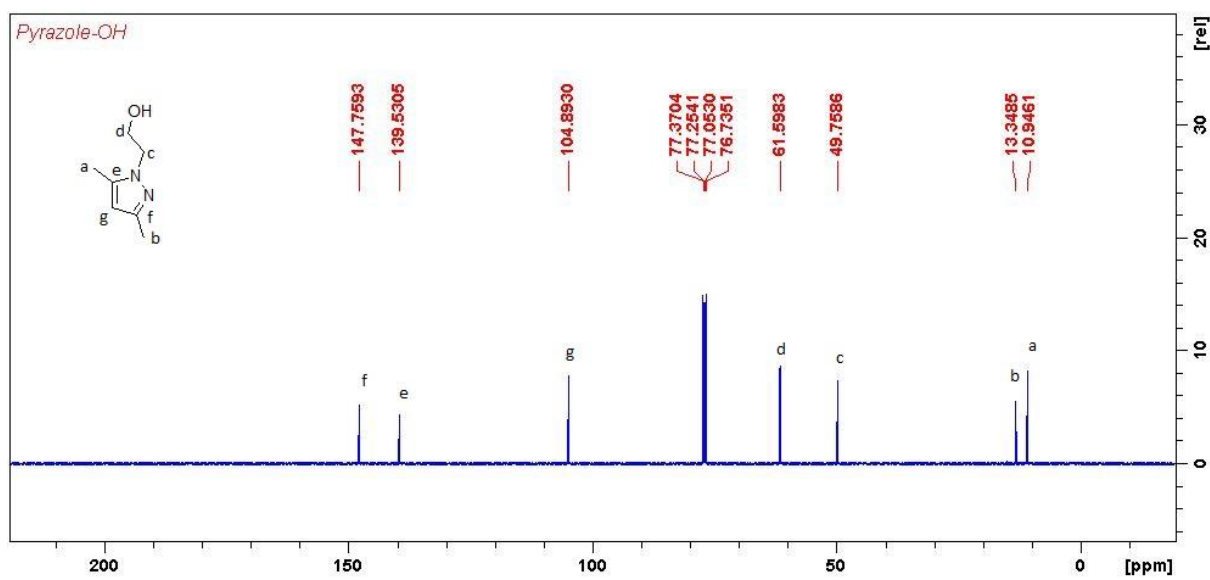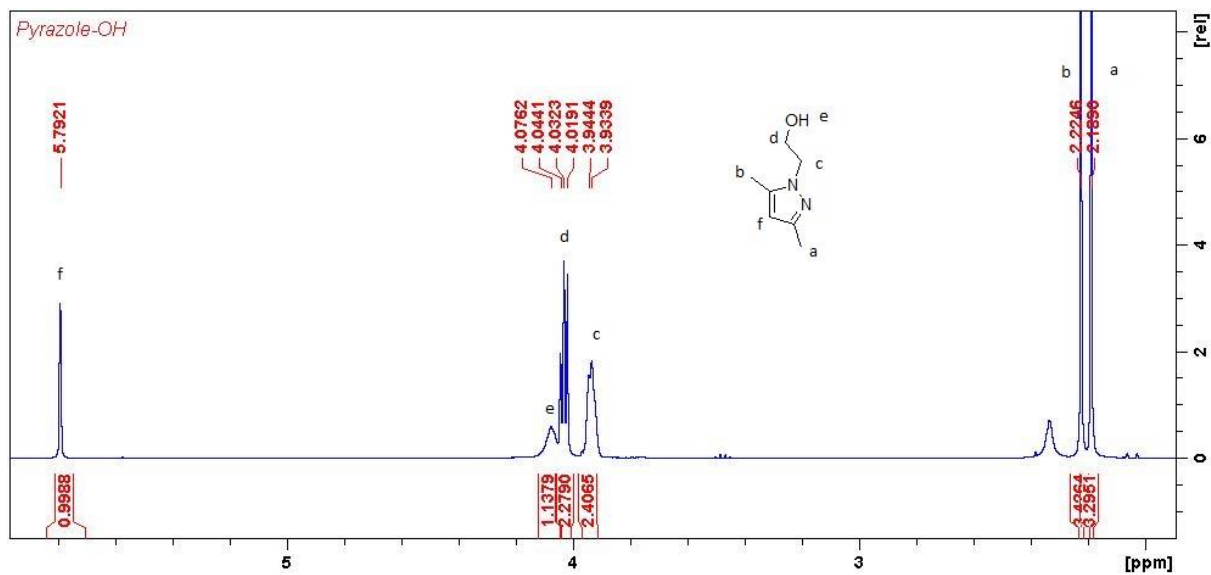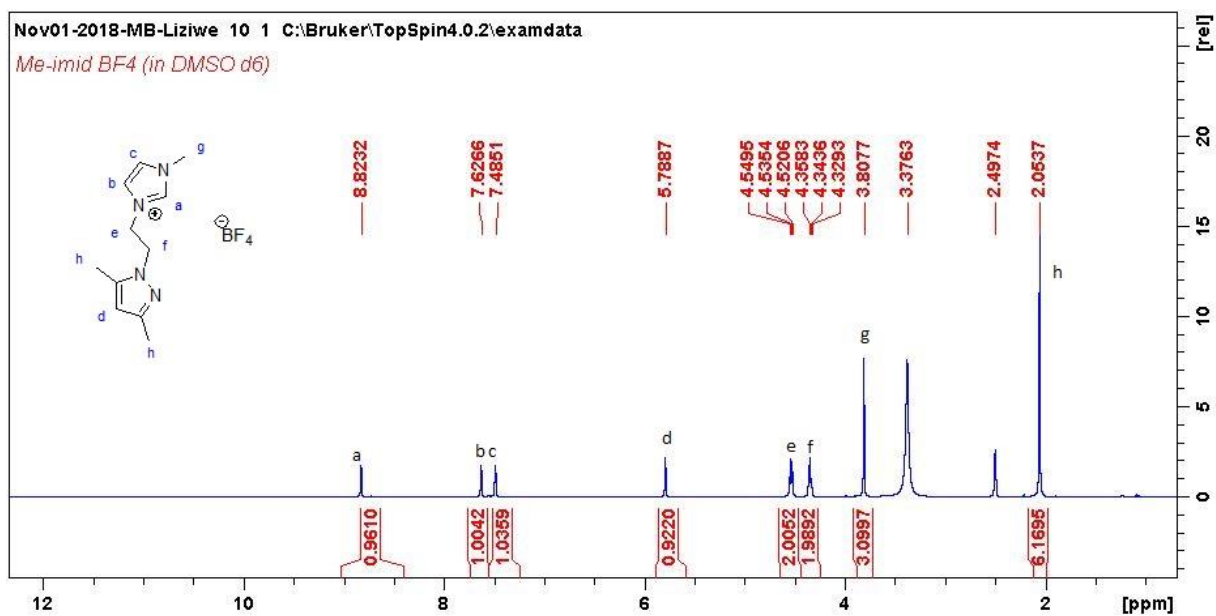
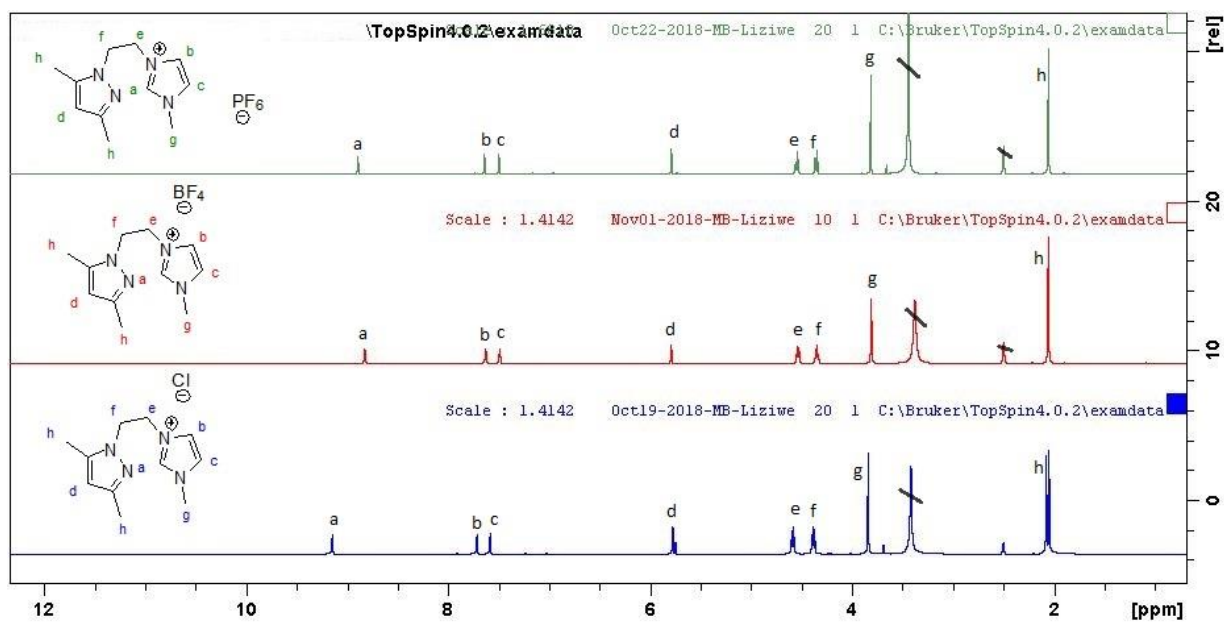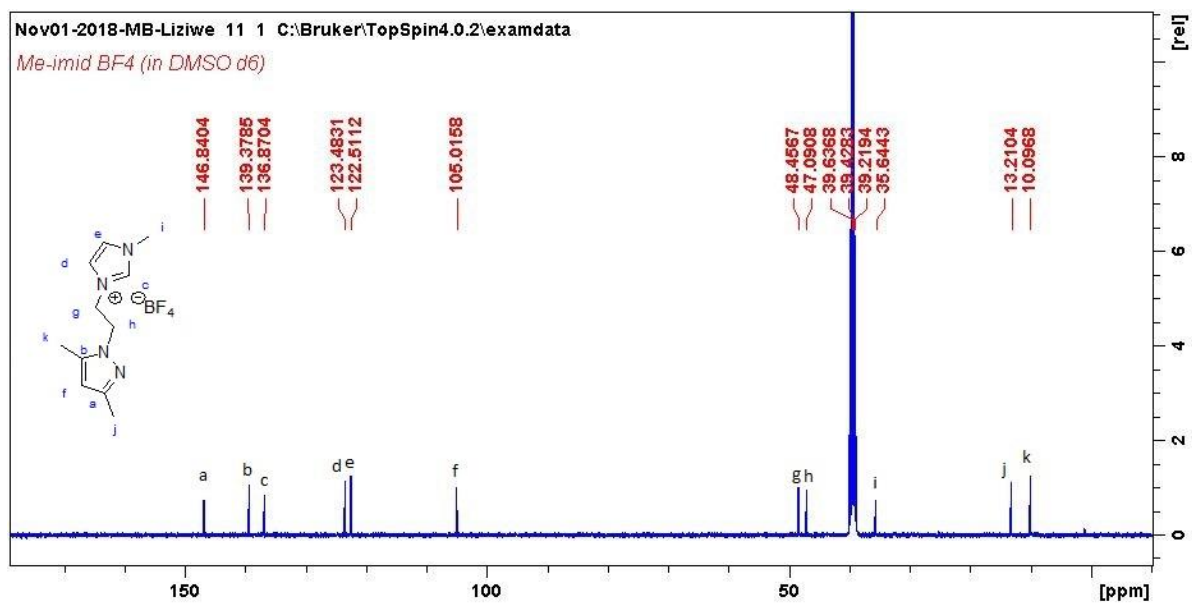2. 1-(2-chloroethyl)-3,5-dimethyl-1H-pyrazole

3. Salt **2.1a** (3-(2-(3,5-dimethyl-1H-pyrazol-1-yl)ethyl)-1-methyl-1H-imidazol-3-ium chloride)

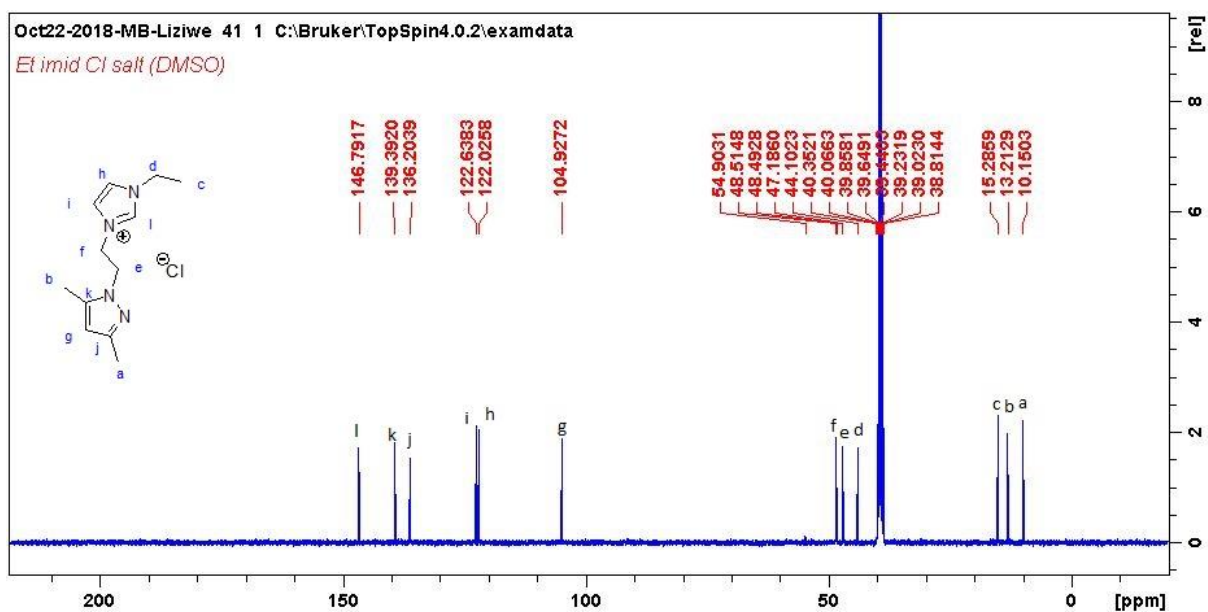Oct19-2018-MB-Liziwe 21 1 C:\Bruker\TopSpin4.0.2\examdata
Me-Imid salt

4. Salt **2.1b** (3-(2-(3,5-dimethyl-1H-pyrazol-1-yl)ethyl)-1-methyl-1H-imidazol-3-ium tetrafluoroborate)

Nov01-2018-MB-Liziwe 10 1 C:\Bruker\TopSpin4.0.2\examdata
Me-imid BF4 (in DMSO d6)

Comparison on the ^{1}H NMR spectra of salt **1** with Cl$^-$, BF$_4^-$ and PF$_6^-$ counterions

5. Salt **2.2a** (3-(2-(3,5-dimethyl-1H-pyrazol-1-yl) ethyl)-1-ethyl-1H-imidazol-3-ium chloride)
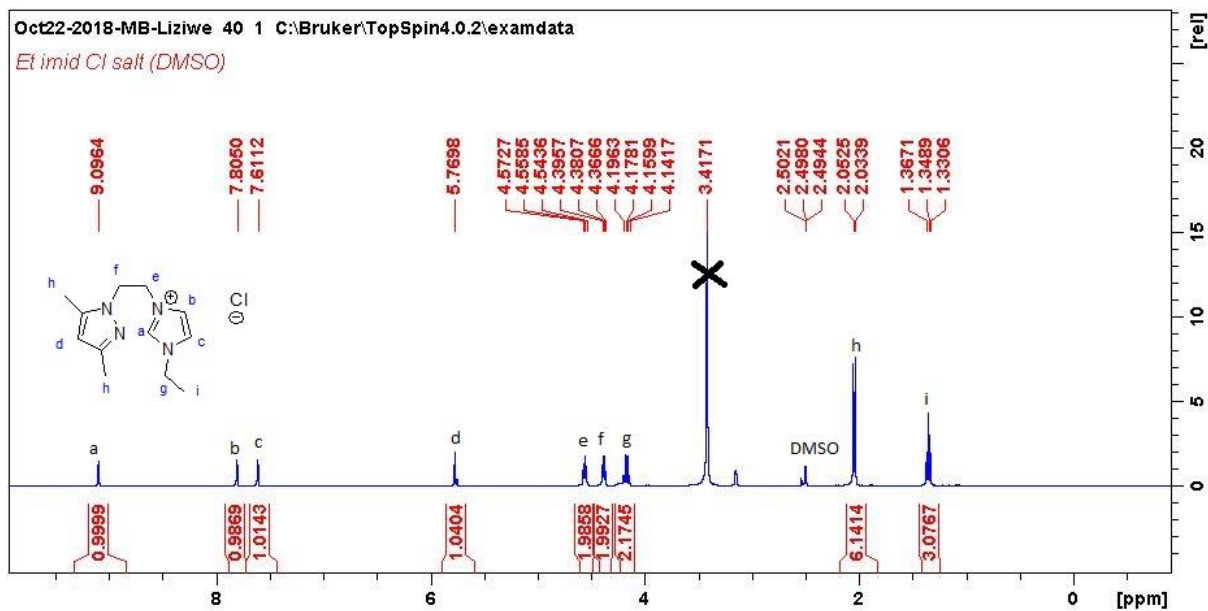
6. Salt **2.2b** (3-(2-(3,5-dimethyl-1H-pyrazol-1-yl) ethyl) - 1 – ethyl - 1H - imidazol-3-ium tetrafluoroborate)

7. Salt **3a** (1-benzyl-3-(2-(3,5-dimethyl-1H-pyrazol-1-yl) ethyl)-1H-imidazol-3-ium chloride)

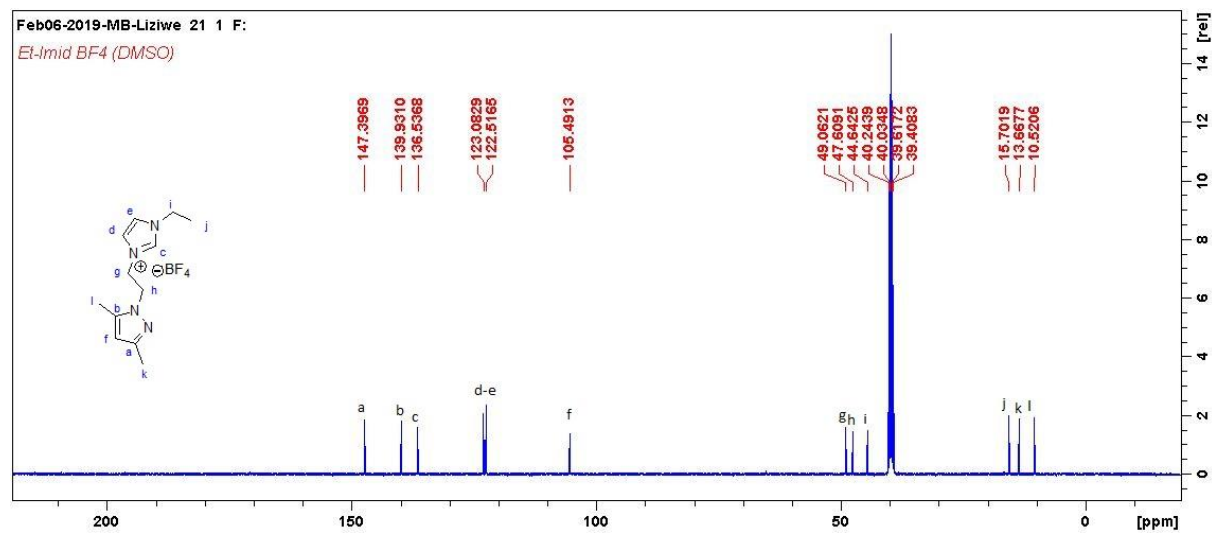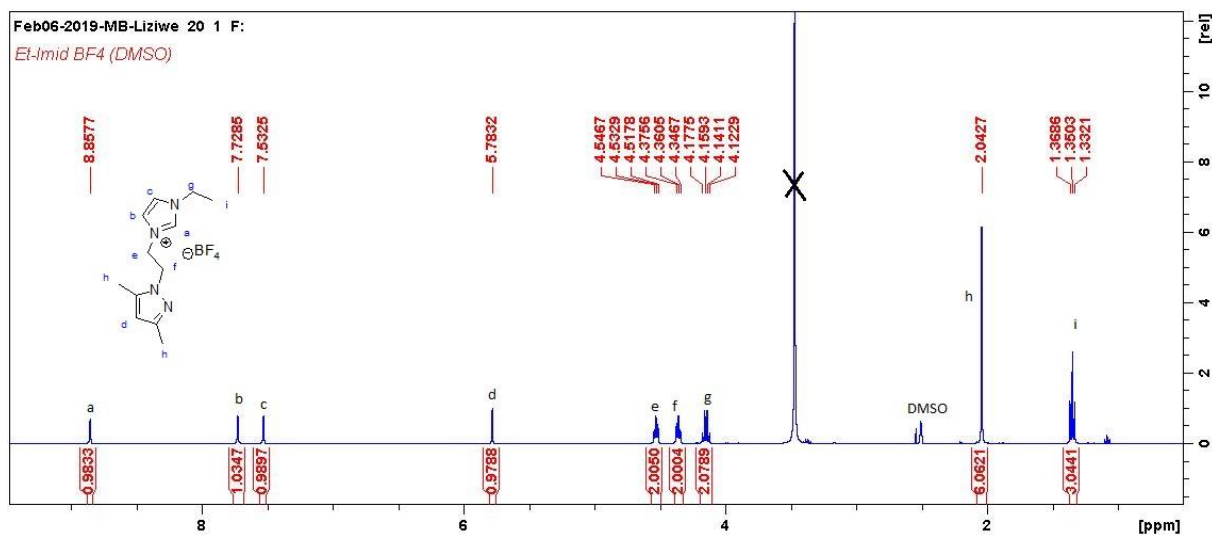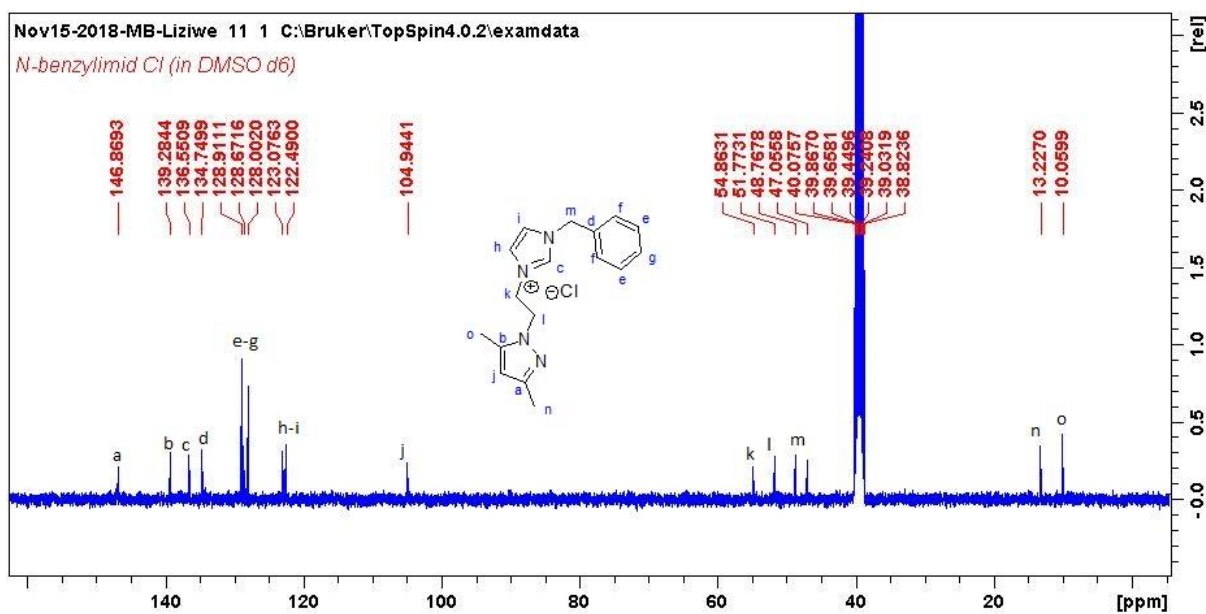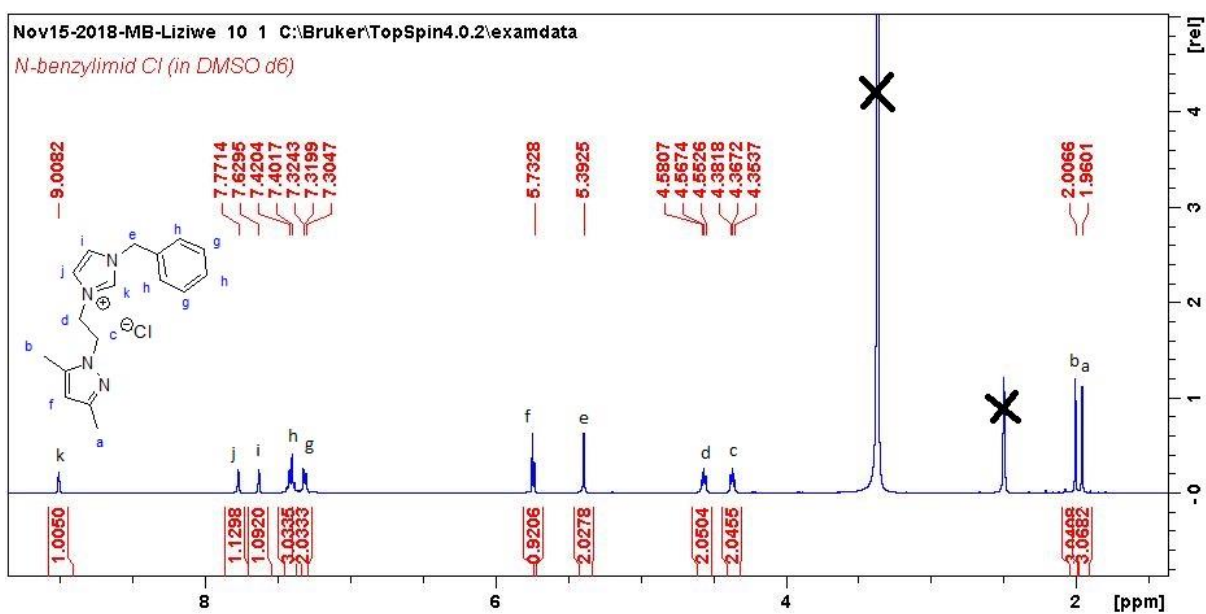8. Salt **3b** (1-benzyl-3-(2-(3,5-dimethyl-1H-pyrazol-1-yl) ethyl)-1H-imidazol-3-ium tetrafluoroborate)
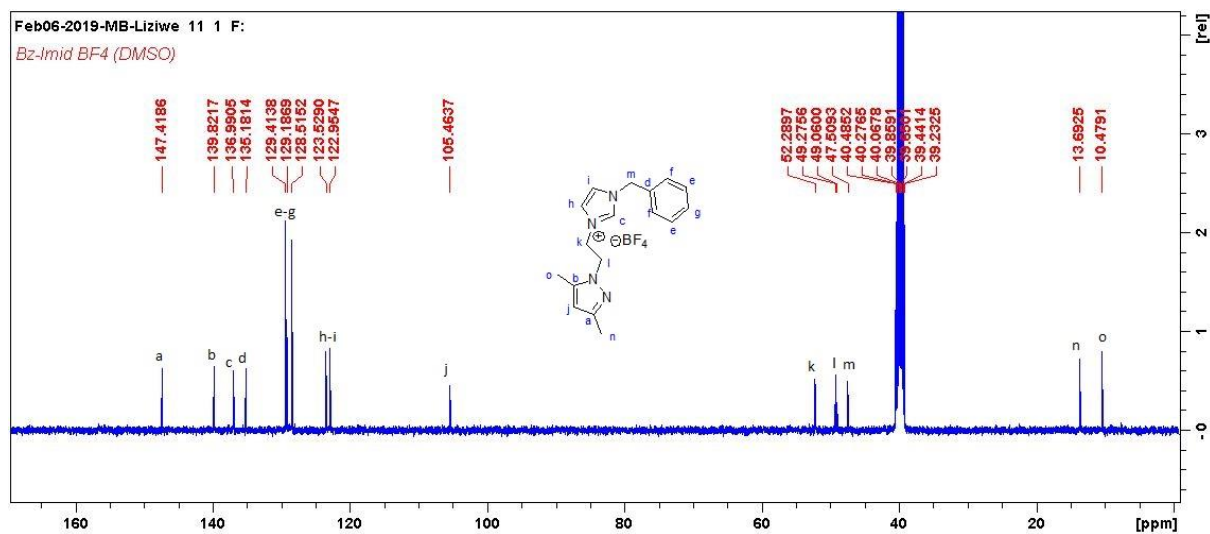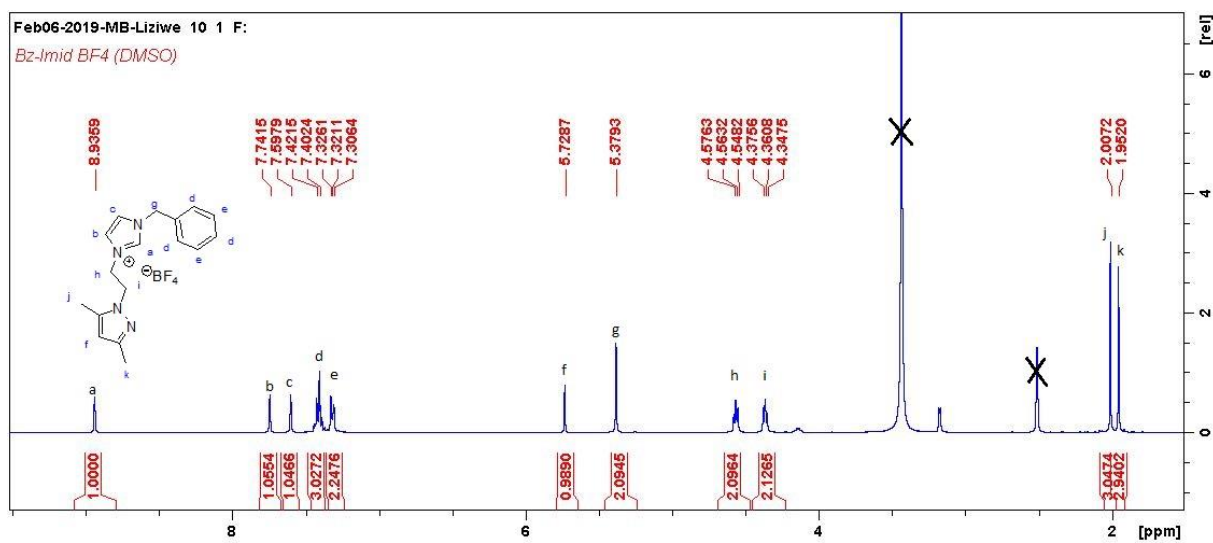
Feb06-2019-MB-Liziwe 10 1 F:
Bz-Imid BF4 (DMSO)

Feb06-2019-MB-Liziwe 11 1 F:
Bz-Imid BF4 (DMSO)

9. Salt **4a** (3-(2-(3,5-dimethyl-1H-pyrazol-1-yl) ethyl)-1-(4-nitrophenyl)-1H-imidazol-3-ium chloride)

Oct19-2018-MB-Liziwe 10 1 C:\Bruker\TopSpin4.0.2\examdata

p-NO2 Phenyl imid salt

10. Complex **3.1**

Feb12-2019-MB-Liziwe 40 1 "C:\Users\Liziwe Ndamase\Desktop\Masters\NMR\MB"

p-NO2Ph-Imid Co BF4 (DMSO d6)
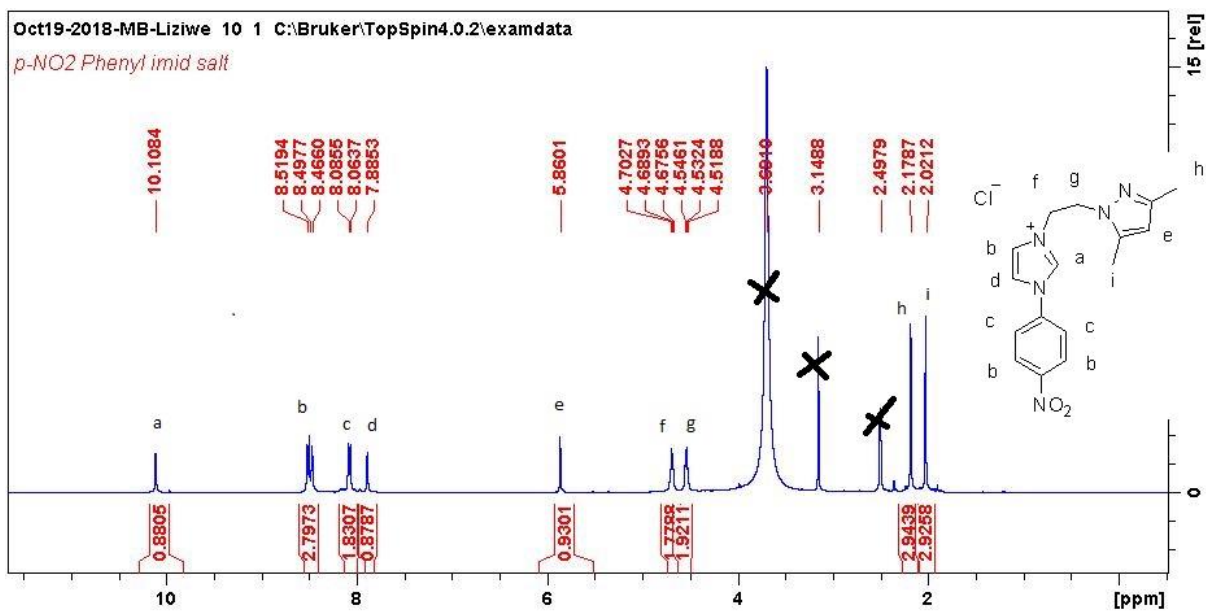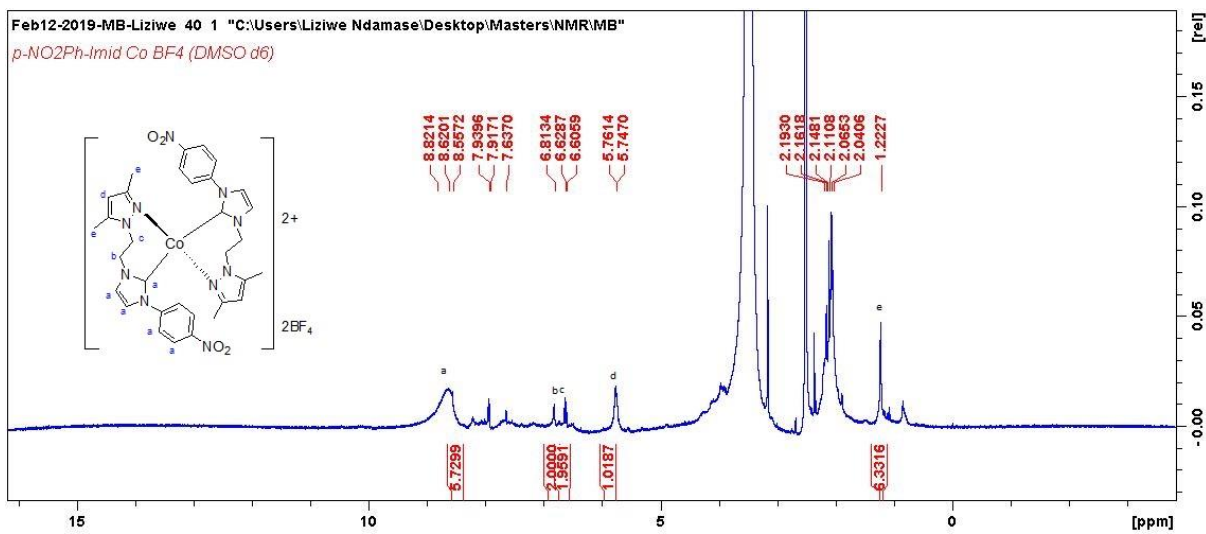
11. Stacked ^{1}H NMR of complexes **3.1** and **3.2**
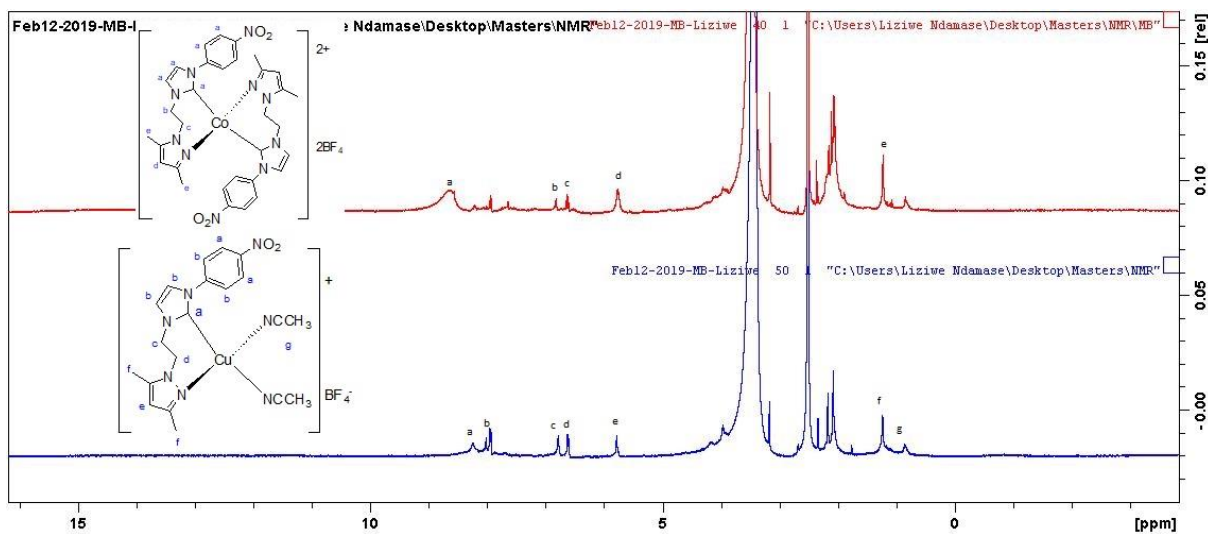
12. Complex **3.2**

13. Complex **3.3**

Me-Imid Cu BF4 (DMSO d6)

Me-Imid Cu Cl (DMSO d6)
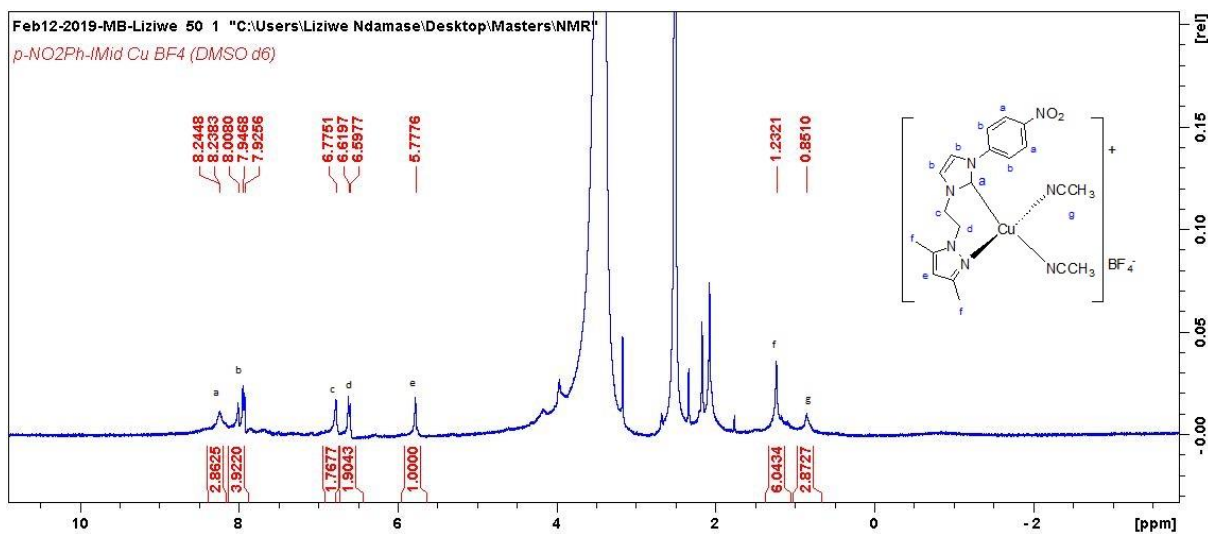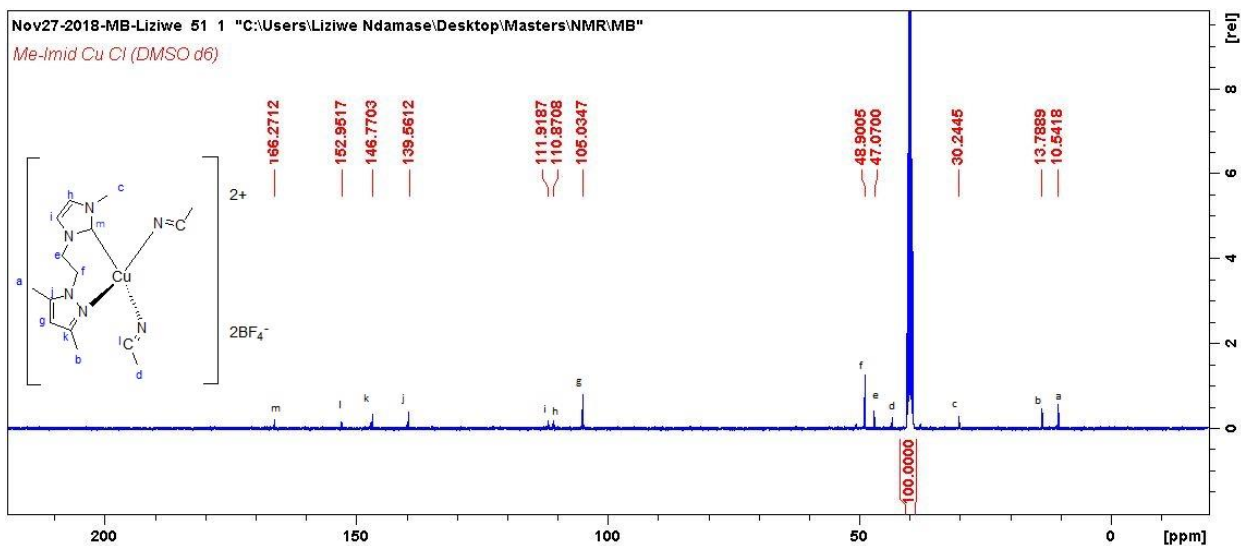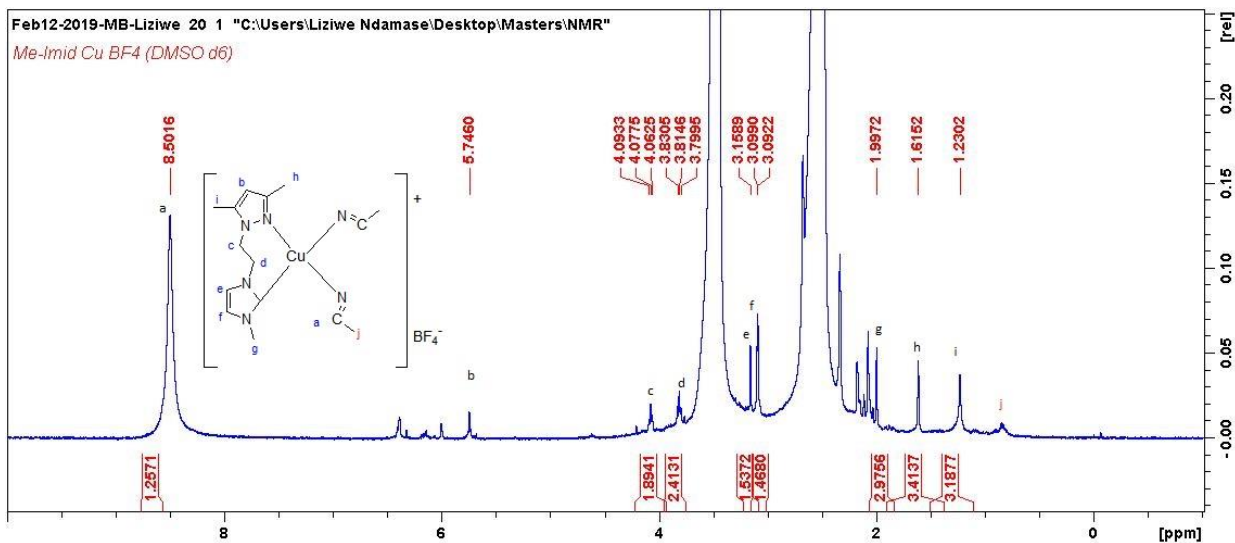
14. Complex **3.4**

15. Complex **3.5**

Feb12-2019-MB-Liziwe 10 1 "C:\Users\Liziwe Ndamase\Desktop\Masters\NMR\MB"
Me-Imid Ni BF4 (DMSO d6)
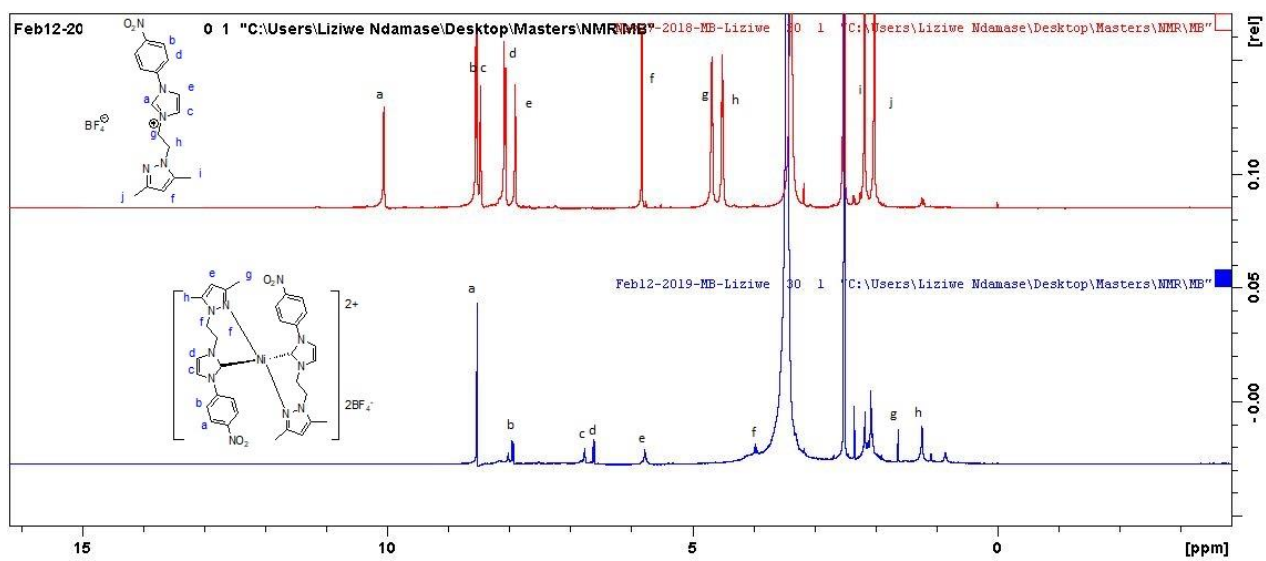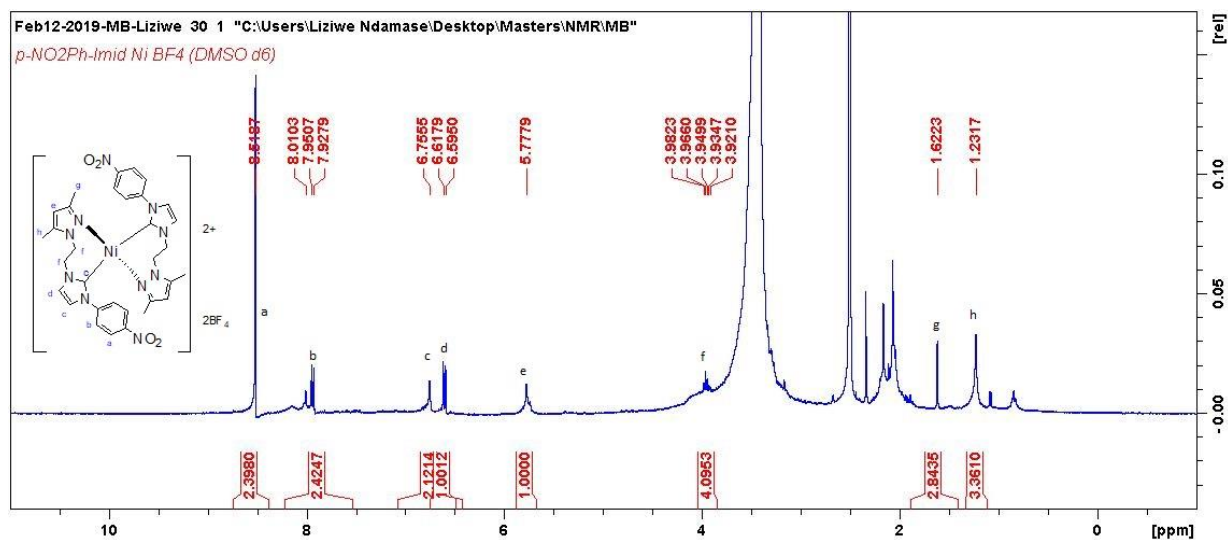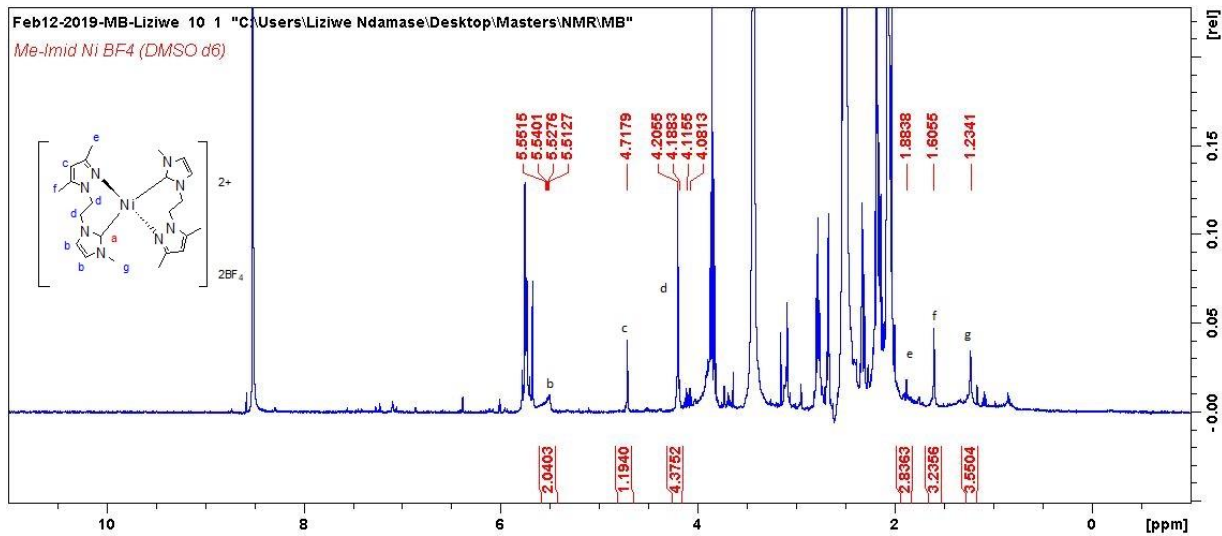
APPENDIX B: FOURIER TRANSFORM INFRARED SPECTROSCOPY

1. Stacked FT-IR spectra of pyrazole-OH (blue) and pyrazole-Cl (black)
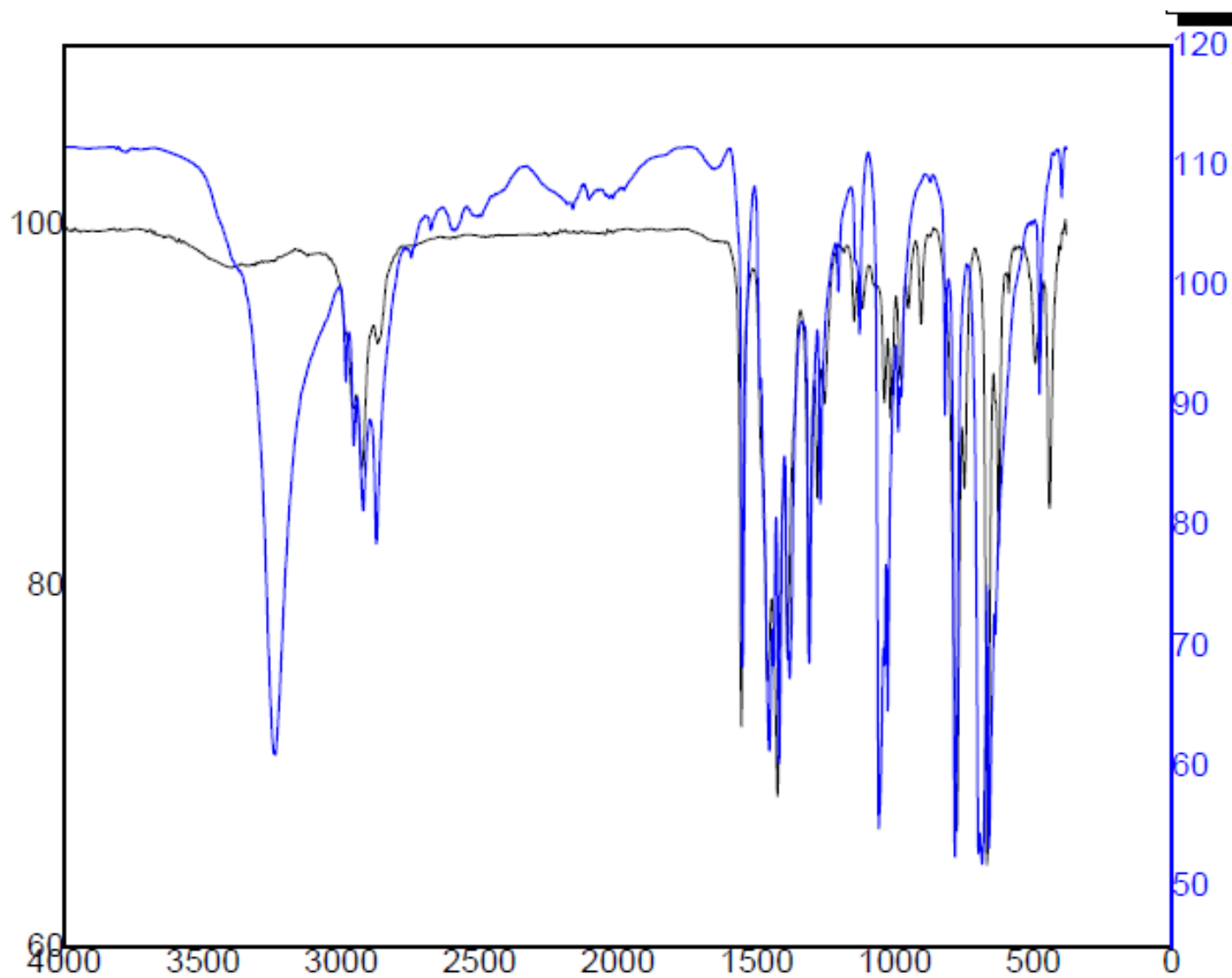
2. Salt **2.1b**
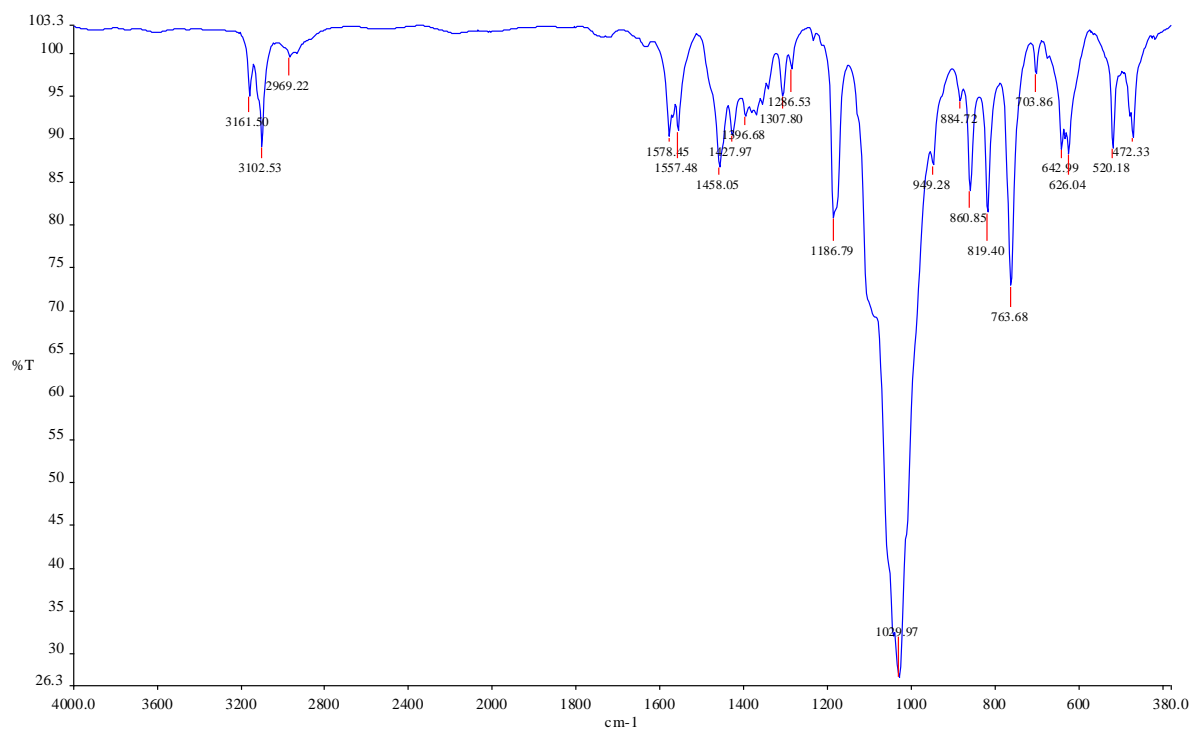
3. Salt **2.1a**
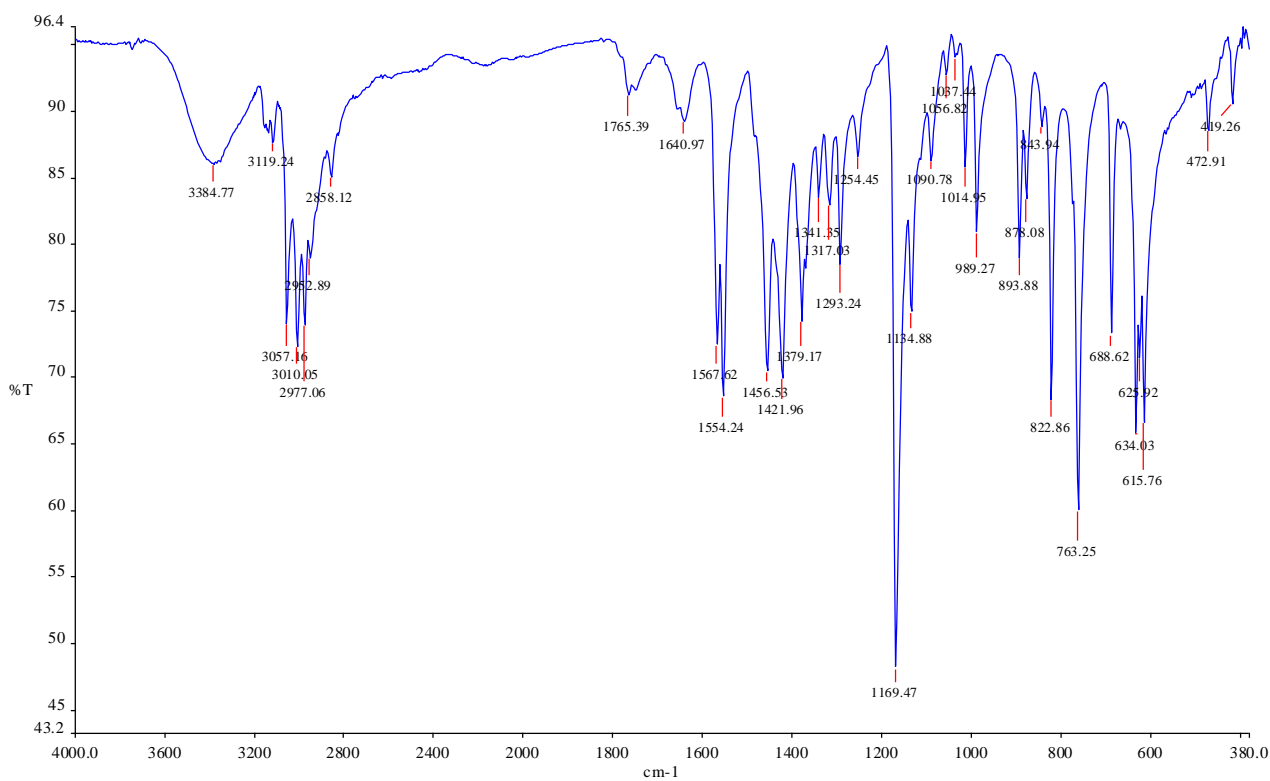
4. Salt **2.1a** (black) vs Salt **2.1b** (blue)
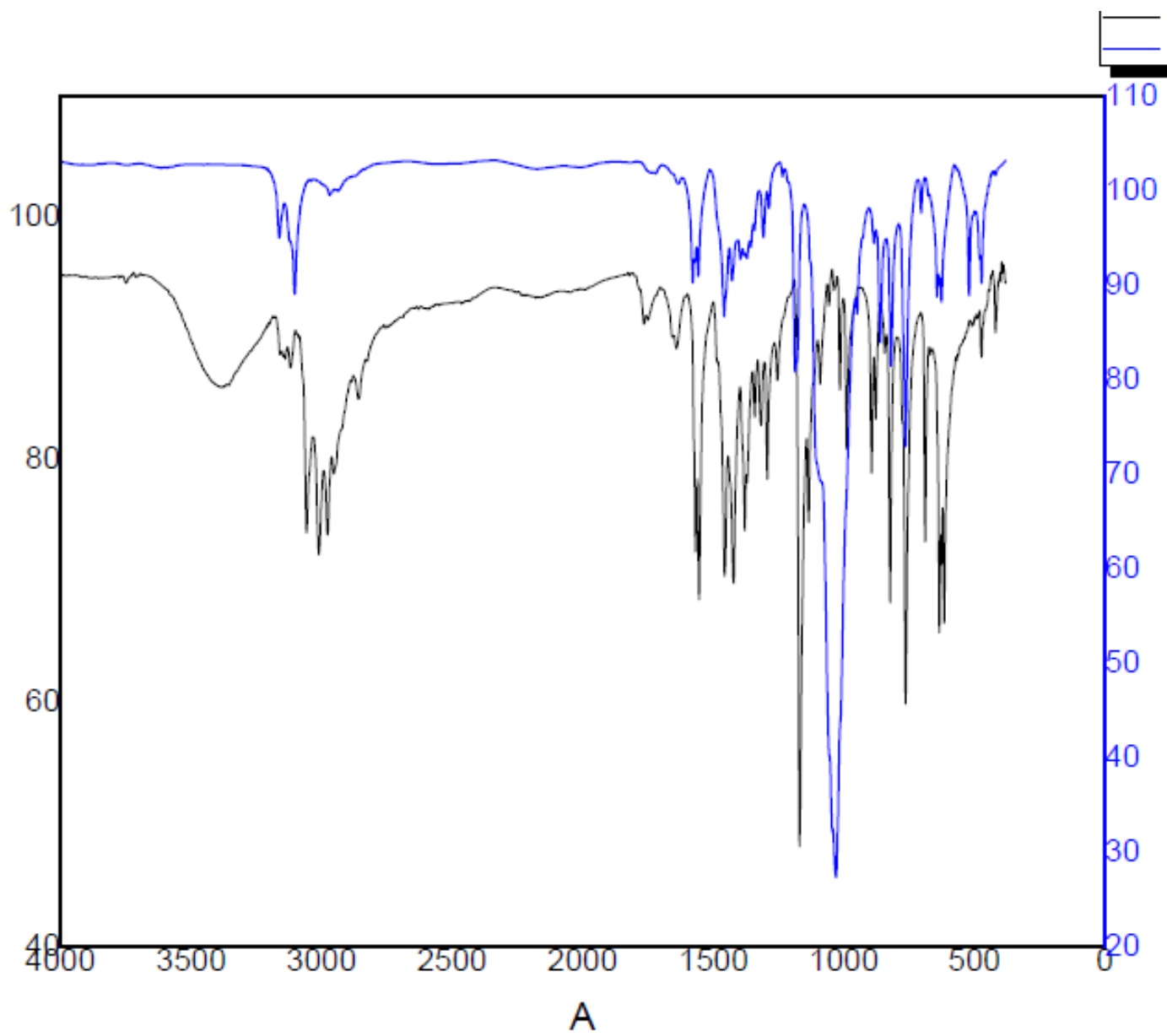
5. Salt **2.3a**
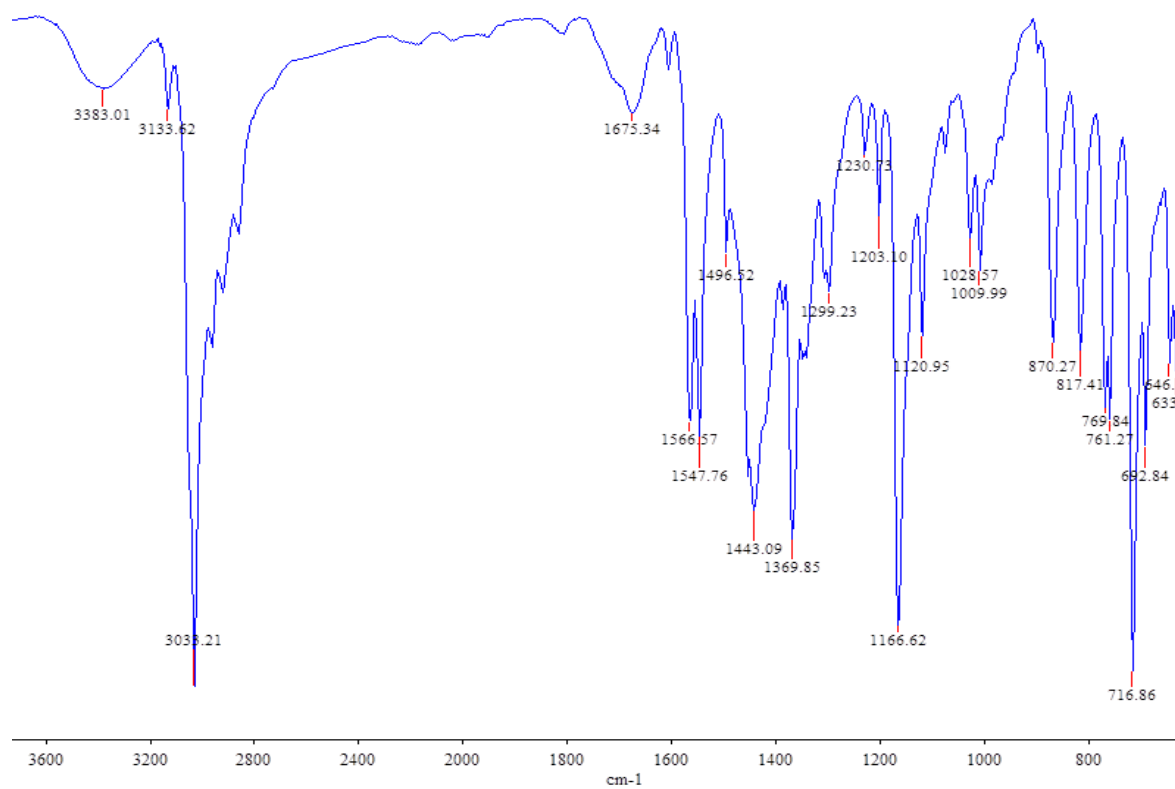
6. Salt **2.4b**
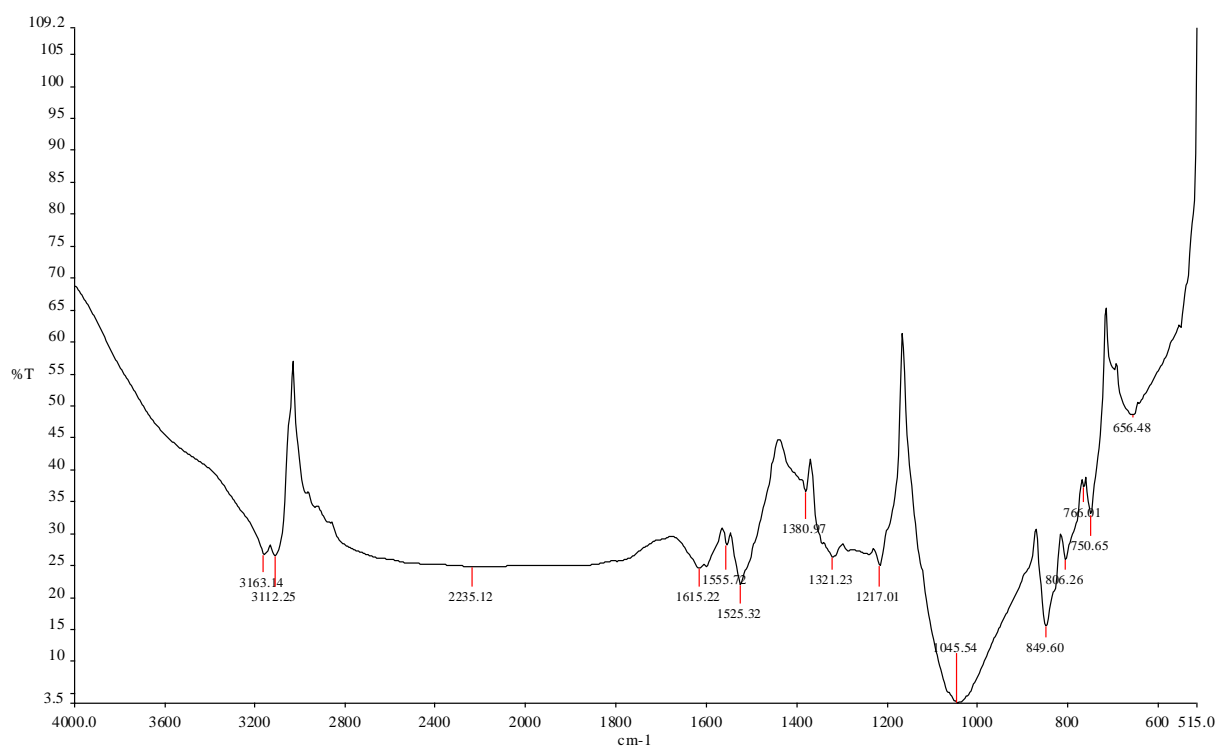
7. Complex 3.1

8. Complex 3.2

9. Complex **3.3**

IR spectrum peaks: 3184.31, 3104.14, 2939.61, 2786.63, 2705.08, 1907.01, 1590.85, 1460.78, 1431.97, 1381.21, 1347.45, 1322.07, 1195.28, 1130.10, 1055.28, 1020.37, 920.67, 886.79, 835.04, 785.08, 755.84, 700.02, 675.39, 642.48, 593.78, 544.53

10. Complex **3.4**

IR spectrum peaks: 3167.21, 3102.33, 2941.84, 2887.63, 2817.10, 2712.67, 1585.44, 1558.04, 1511.83, 1413.77, 1355.01, 1317.07, 1288.92, 1216.26, 1195.42, 1129.78, 1084.79, 1055.64, 1020.48, 888.44, 830.07, 765.91, 755.17, 699.52, 677.23, 641.05, 557.89, 484.12, 415.99, 391.49

11. Complex **3.5**

APPENDIX C: MASS SPECTROSCOPY SPECTRA

All the spectra are attached as PDF documents

APPENDIX D: ELEMENTAL ANALYSIS SPECTRA

All spectra are attached as PDF documents

APPENDIX E: CALIBRATION CURVES, FORMULAE FOR CALCULATIONS AND GC SPECTRA

Calibration curve for cyclohexanol
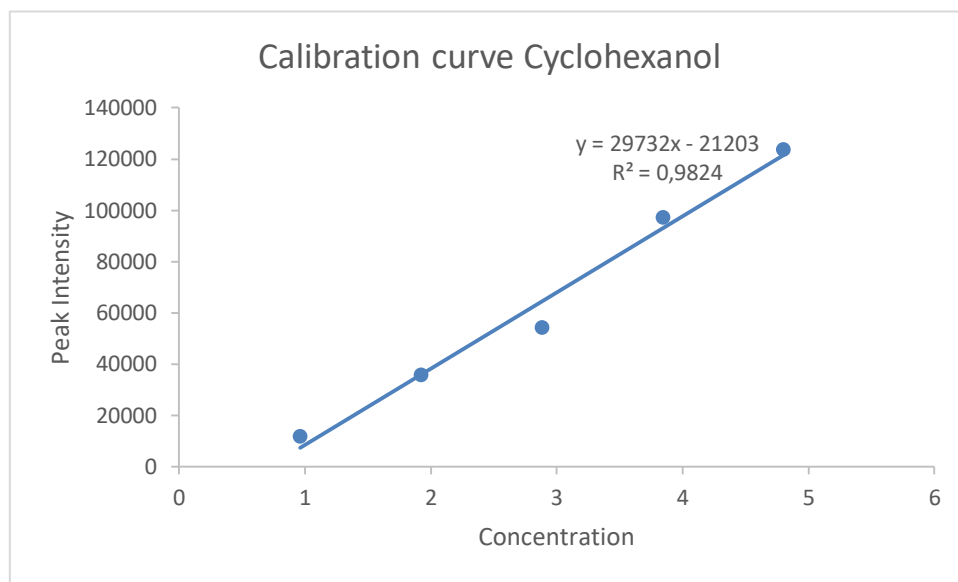
Calibration curve of cyclohexanone
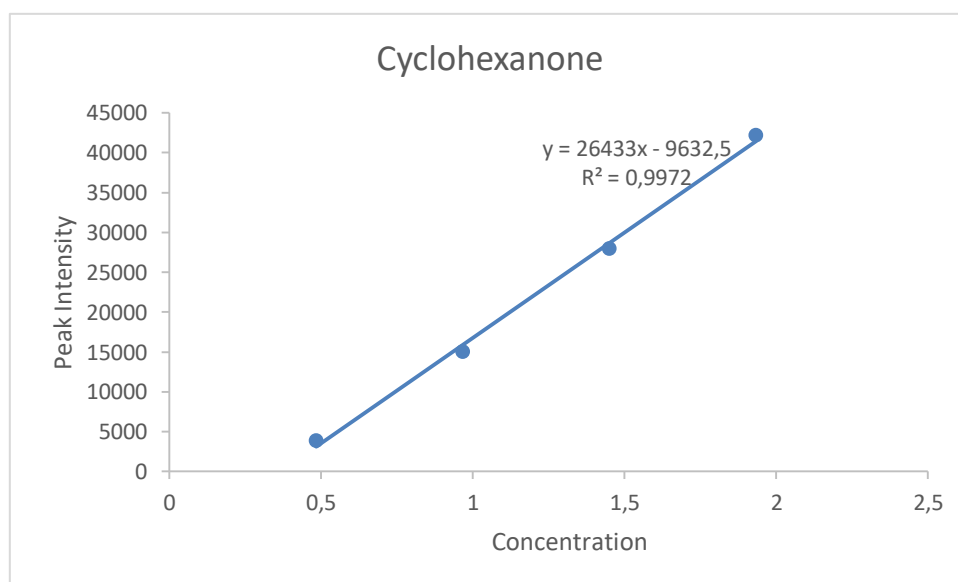
$$Conversion = (Initial\ moles\ of\ substrate)/(Total\ moles\ of\ product)\ \times 100\%$$

$$Selectivity = (Moles\ of\ product)/(Total\ moles\ of\ products)\ \times 100\%$$

$$Response\ Factor = (Ci \times Ax)/(Ai \times Cx)$$

*GC spectra is attached as PDF documents.

APPENDIX F: SUPPLEMENTAL INFORMATION

Although the methanol used was 99.8% pure methanol, the salts decomposed when it anion metathesis was attempted. An NMR spectrum showed that the methanol contained H_2O as indicated in Figure A shows the peak for H_2O was more intense than that of methanol suggesting even higher than that of methanol which reacted with the salts and consequently decomposed them. This prompted for the further drying of the methanol by pouring ~200 mL of HPLC grade methanol into a 500 mL round bottom flask and then adding magnesium turnings (10g) and ~1g of iodine and refluxing at 65 °C until all the magnesium has reacted and distilled off under nitrogen and stored in container with activated molecular sieves (Fig. B and C). [116] The dry solvent was used immediately or within 24 hours of drying to avoid contamination or reabsorption of moisture.
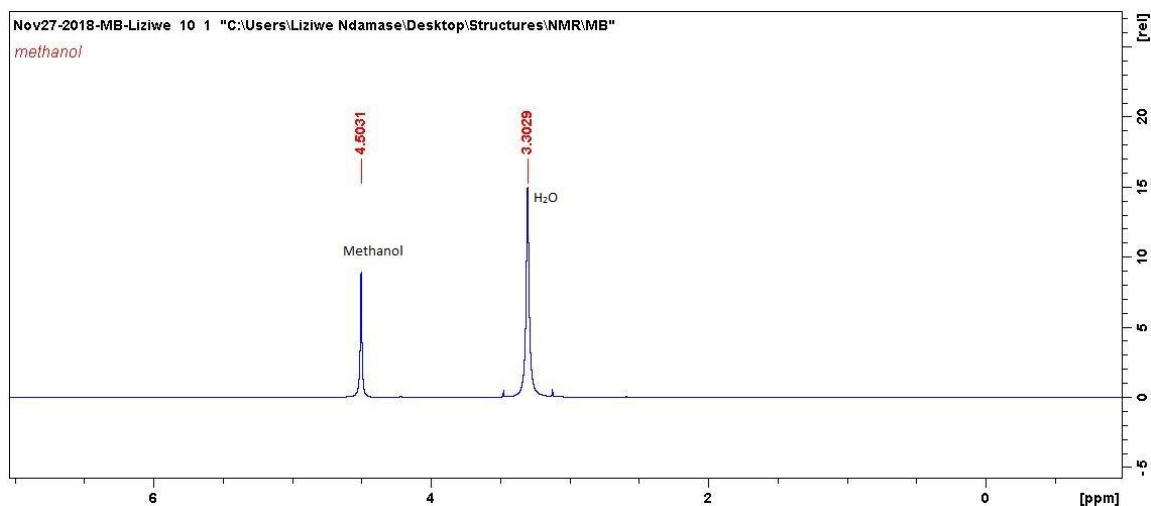
Figure A: NMR spectrum showing HPLC grade methanol contaminated with water
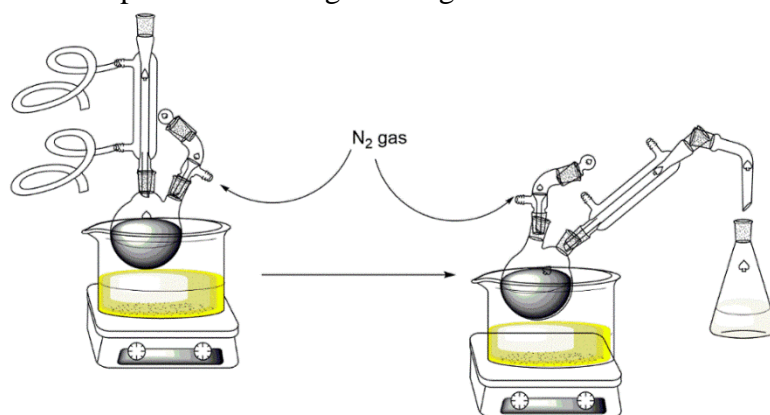
Figure B: Schematic diagram of the drying and distillation process of methanol

Figure C: Methanol drying using Mg turnings and distillation

Colum chromatography was used to purify salt **2.2a** as other methods proved to be less efficient for this process

Figure D: Purification of Salt **2.2a** using Column chromatography silicon bed

REFERENCES

1.   Tang, X.; Jia, X.; Huang, Z., Challenges and opportunities for alkane functionalisation using molecular catalysts. *Chem Sci* **2017,** *9* (2), 288-299.
2.   Sivaramakrishna, A.; Suman, P.; Veerashekhar Goud, E.; Janardan, S.; Sravani, C.; Sandeep, T.; Vijayakrishna, K.; Clayton, H. S., Review: active homogeneous reagents and catalysts in n-alkane activation. *Journal of Coordination Chemistry* **2013,** *66* (12), 2091-2109.
3.   Shilov, A. E. e.; Shul'pin, G. B., *Activation and catalytic reactions of saturated hydrocarbons in the presence of metal complexes*. Springer Science & Business Media: 2001; Vol. 21.
4.   Crabtree, R. H., Alkane C–H activation and functionalization with homogeneous transition metal catalysts: A century of progress—A new millennium in prospect. *Journal of the Chemical Society, Dalton Transactions* **2001,** (17), 2437-2450.
5.   Schardt, C. L. H. a. B. C., Activation and functionalization of alkanes. *American Chemical Society* **1989,** *102* (20), 6374-6375.
6.   AtulDev, A. K. S., Surajit Karmakar, New Generation Hybrid Nanobiocatalysts: The Catalysis Redefined *Handbook of Nanomaterials for Industrial Applications* **2018**, 217-231.
7.   Olivo, g., Cusso, O., Borrell, M., et al., Oxidation of alkane and alkene moieties with bilogically inspired nonheme iron catalysts and hydrogen peroxide: from free radicals to stereoselective transformations. *journal of Biological Inorganic Chemistry* **2017,** *22*, 425-452.
8.   Marchetti, L.; Levine, M., Biomimetic Catalysis. *ACS Catalysis* **2011,** *1* (9), 1090-1118.
9.   Breslow, R., Biomimetic chemistry, centenary lecture. *Chem. Soc. Rev* **1972,** *1*, 553-580.
10.   Breslow, R., Biomimetic Chemistry and Artificial Enzymes: Catalysis by Design. *Accounts of Chemical Research* **1995,** *28* (3), 146-153.
11.   Tabushi, I., BIOMIMETIC CHEMISTRY. In *Frontiers of Chemistry*, Laidler, K. J., Ed. Pergamon: 1982; pp 275-286.
12.   T., G. J., Models and mechanisms of Cytochrome P450 action *Cytochrome P450* **2005**.
13.   Herrmann, W. A., N-heterocyclic carbenes: a new concept in organometallic catalysis. *Angewandte Chemie International Edition* **2002,** *41* (8), 1290-1309.
14.   S. Julia, C., Martinez-Martorell and J. Elguero, Heterocycles. *Wiley Analytical Science* **1986,** *24*.
15.   Buendia, J.; Grelier, G.; Dauban, P., Dirhodium (II)-Catalyzed C (sp3)–H Amination Using Iodine (III) Oxidants. In *Advances in Organometallic Chemistry*, Elsevier: 2015; Vol. 64, pp 77-118.
16.   Hofmann, A., Study of the coniin group. *Ber. Dtsch. Chem. Ges.* **1885,** *18*, 109-131.
17.   Wang, R.; Twamley, B.; Shreeve, J. n. M., A Highly Efficient, Recyclable Catalyst for C−C Coupling Reactions in Ionic Liquids: Pyrazolyl-Functionalized N-Heterocyclic Carbene Complex of Palladium(II). *The Journal of Organic Chemistry* **2006,** *71* (1), 426-429.
18.   Garcia-Bosch, I.; Siegler, M. A., Copper-Catalyzed Oxidation of Alkanes with H2O2 under a Fenton-like Regime. *Angewandte Chemie International Edition* **2016,** *55* (41), 12873-12876.
19.   Wanzlick, H., Aspects of nucleophilic carbene chemistry. *Angewandte Chemie International Edition in English* **1962,** *1* (2), 75-80.
20.   Vyboishchikov, S. F.; Frenking, G., Structure and Bonding of Low-Valent (Fischer-Type) and High-Valent (Schrock-Type) Transition Metal Carbene Complexes. *Chemistry–A European Journal* **1998,** *4* (8), 1428-1438.
21.   Bertrand, G., *Carbene chemistry: from fleeting intermediates to powerful reagents*. CRC Press: 2002.
22.   Wanzlick, H. W.; Schönherr, H. J., Direct synthesis of a mercury salt-carbene complex. *Angewandte Chemie International Edition in English* **1968,** *7* (2), 141-142.
23.   Arduengo III, A. J.; Harlow, R. L.; Kline, M., A stable crystalline carbene. *Journal of the American Chemical Society* **1991,** *113* (1), 361-363.

24.   Hopkinson, M. N.; Richter, C.; Schedler, M.; Glorius, F., An overview of N-heterocyclic carbenes. *Nature* **2014,** *510* (7506), 485.

25.   Cavallo, L.; Correa, A.; Costabile, C.; Jacobsen, H., Steric and electronic effects in the bonding of N-heterocyclic ligands to transition metals. *Journal of organometallic chemistry* **2005,** *690* (24-25), 5407-5413.

26.   Page, M. J.; Wagler, J.; Messerle, B. A., Pyrazolyl-N-heterocyclic carbene complexes of rhodium as hydrogenation catalysts: The influence of ligand steric bulk on catalyst activity. *Dalton Transactions* **2009,** (35), 7029-7038.

27.   Herrmann, W. A.; Koecher, C., N-Heterocyclic carbenes. *Angewandte Chemie International Edition in English* **1997,** *36* (20), 2162-2187.

28.   Díez-González, S.; Nolan, S. P., Stereoelectronic parameters associated with N-heterocyclic carbene (NHC) ligands: a quest for understanding. *Coordination chemistry reviews* **2007,** *251* (5-6), 874-883.

29.   Dorta, R.; Stevens, E. D.; Scott, N. M.; Costabile, C.; Cavallo, L.; Hoff, C. D.; Nolan, S. P., Steric and electronic properties of N-heterocyclic carbenes (NHC): a detailed study on their interaction with Ni (CO) 4. *Journal of the American Chemical Society* **2005,** *127* (8), 2485-2495.

30.   Brovarets, V.; Lobanov, O.; Kisilenko, A.; Kalinin, V.; Drach, B., Conversions of Substituted Phosphinomethylenes Containing 2-Alkyl-(Aryl)-4, 5-dihydro-5-thioxo-4-oxazolylidene Fragments. *ChemInform* **1987,** *18* (6), no-no.

31.   Wen, L. R.; Men, L. B.; He, T.; Ji, G. J.; Li, M., Switching Regioselectivity of β-Ketothioamides by Means of Iodine Catalysis: Synthesis of Thiazolylidenes and 1, 4-Dithiines. *Chemistry–A European Journal* **2014,** *20* (17), 5028-5033.

32.   Navarro, M.; Wang, S.; Müller-Bunz, H.; Redmond, G.; Farràs, P.; Albrecht, M., Triazolylidene metal complexes tagged with a bodipy chromophore: Synthesis and monitoring of ligand exchange reactions. *Organometallics* **2017,** *36* (8), 1469-1478.

33.   Grimmett, M. R., *Imidazole and benzimidazole synthesis*. Academic press: University of Otago, 1997; Vol. 1.

34.   Schuster, O.; Yang, L.; Raubenheimer, H. G.; Albrecht, M., Beyond conventional N-heterocyclic carbenes: abnormal, remote, and other classes of NHC ligands with reduced heteroatom stabilization. *Chemical reviews* **2009,** *109* (8), 3445-3478.

35.   Lavallo, V.; Canac, Y.; Präsang, C.; Donnadieu, B.; Bertrand, G., Stable cyclic (alkyl)(amino) carbenes as rigid or flexible, bulky, electron-rich ligands for transition-metal catalysts: a quaternary carbon atom makes the difference. *Angewandte Chemie International Edition* **2005,** *44* (35), 5705-5709.

36.   Aldeco-Perez, E.; Rosenthal, A. J.; Donnadieu, B.; Parameswaran, P.; Frenking, G.; Bertrand, G., Isolation of a C5-deprotonated imidazolium, a crystalline "abnormal" N-heterocyclic carbene. *Science* **2009,** *326* (5952), 556-559.

37.   Jacobsen, H.; Correa, A.; Poater, A.; Costabile, C.; Cavallo, L., Understanding the M (NHC)(NHC= N-heterocyclic carbene) bond. *Coordination Chemistry Reviews* **2009,** *253* (5-6), 687-703.

38.   Togni, A.; Venanzi, L. M., Nitrogen donors in organometallic chemistry and homogeneous catalysis. *Angewandte Chemie International Edition in English* **1994,** *33* (5), 497-526.

39.   Hopkinson, M. N.; Richter, C.; Schedler, M.; Glorius, F., An overview of N-heterocyclic carbenes. *Nature* **2014,** *510*, 485.

40.   Edwards, P. G.; Hahn, F. E., Synthesis and coordination chemistry of macrocyclic ligands featuring NHC donor groups. *Dalton Transactions* **2011,** *40* (40), 10278-10288.

41.   Messerle, B. A.; Page, M. J.; Turner, P., Rhodium (I) and iridium (I) complexes of pyrazolyl-N-heterocyclic carbene ligands. *Dalton Transactions* **2006,** (32), 3927-3933.

42.   D. S. SLONE, D. A. W., C. A. Mirkin, The transition metal coordination chemistry of hemilabile ligands. . *Progress in Inorganic Chemistry* **1999,** *48*.

43.   Riener, K.; Bitzer, M. J.; Pöthig, A.; Raba, A.; Cokoja, M.; Herrmann, W. A.; Kühn, F. E., On the Concept of Hemilability: Insights into a Donor-Functionalized Iridium(I) NHC Motif and Its Impact on Reactivity. *Inorganic Chemistry* **2014,** *53* (24), 12767-12777.

44.   Perry, M. C.; Cui, X.; Powell, M. T.; Hou, D.-R.; Reibenspies, J. H.; Burgess, K., Optically active iridium imidazol-2-ylidene-oxazoline complexes: preparation and use in

asymmetric hydrogenation of arylalkenes. *Journal of the American Chemical Society* **2003,** *125* (1), 113-123.

45.   Burling, S.; Field, L. D.; Messerle, B. A.; Vuong, K. Q.; Turner, P., Rhodium (I) and iridium (I) complexes with bidentate N, N and P, N ligands as catalysts for the hydrothiolation of alkynes. *Dalton Transactions* **2003,** (21), 4181-4191.

46.   Cheng, C.-H.; Xu, J.-R.; Song, H.-B.; Tang, L.-F., Synthesis and catalytic activity of pyrazolyl-functionalized N-heterocyclic carbene palladium complexes. *Transition Metal Chemistry* **2014,** *39* (2), 151-157.

47.   Liu, B.; Xia, Q.; Chen, W., Direct Synthesis of Iron, Cobalt, Nickel, and Copper Complexes of N-Heterocyclic Carbenes by Using Commercially Available Metal Powders. *Angewandte Chemie International Edition* **2009,** *48* (30), 5513-5516.

48.   Dötz, K.-H.; Fischer, H.; Hofmann, P.; Kreissl, F.; Schubert, U.; Weiss, K., Transition metal carbene complexes. *Angewandte Chemie* **1983,** *23* (8).

49.   Bo Liu, B. L., † Yongbo Zhou,† and Wanzhi Chen*,†,‡, Copper(II) Hydroxide Complexes of N-Heterocyclic Carbenes and Catalytic Oxidative Amination of Arylboronic Acids. *Organometallics* **2010,** *29*, 1457–1464.

50.   Y. Ohki, T. H., K. Tatsumi, C-H Bond Activation of Heteroarenes Mediated by Half-Sandwich Iron Complex of N-Heterocyclic Carbene. *American Chemical Society* **2008,** *50* (130), 17174-17186.

51.   Normand, A. T.; Cavell, K. J., Donor-Functionalised N-Heterocyclic Carbene Complexes of Group 9 and 10 Metals in Catalysis: Trends and Directions. *European Journal of Inorganic Chemistry* **2008,** *2008* (18), 2781-2800.

52.   Garrison, J. C.; Youngs, W. J., Ag (I) N-heterocyclic carbene complexes: synthesis, structure, and application. *Chemical Reviews* **2005,** *105* (11), 3978-4008.

53.   A. J. Arduengo, H. V. R. D., J. C. Calabrese and F. Davidson, Homoleptic carbene-silver(I) and carbene-copper(I) complexes. *Organometallics* **1993,** *12*, 3405-3409.

54.   Lin, H. M. J. W. a. I. J. B., Facile synthesis of silver (I)− carbene complexes. Useful carbene transfer agents. *Organometallics* **1998,** *17*, 972-975.

55.   Shul'pin, G. B.; Gradinaru, J.; Kozlov, Y. N., Alkane hydroperoxidation with peroxides catalysed by copper complexes. *Organic & biomolecular chemistry* **2003,** *1* (20), 3611-3617.

56.   Knor, E. T. a. G., Synthesis and characterisation of cobalt, nickel, and copper complexes with tripodal 4H ligands as novel catalysts for the homogeneous partial oxidation of alkanes. *Inorganica Chimica Acta* **2013,** *402*, 90-96.

57.   Martins, L. M. D.; Martins, A.; Alegria, E. C.; Carvalho, A.; Pombeiro, A. J., Efficient cyclohexane oxidation with hydrogen peroxide catalysed by a C-scorpionate iron (II) complex immobilized on desilicated MOR zeolite. *Applied Catalysis A: General* **2013,** *464*, 43-50.

58.   Cuervo, L. G.; Kozlov, Y. N.; Süss-Fink, G.; Shul'pin, G. B., Oxidation of saturated hydrocarbons with peroxyacetic acid catalyzed by vanadium complexes. *Journal of Molecular Catalysis A: Chemical* **2004,** *218* (2), 171-177.

59.   Schroder D., S., H., C-H and C-C bond activation by bare transition metal oxide cations in the gas phase. *Angewandte Chemie* **1995,** *34* (18), 1973-1995.

60.   Elwell, C. E.; Gagnon, N. L.; Neisen, B. D.; Dhar, D.; Spaeth, A. D.; Yee, G. M.; Tolman, W. B., Copper–oxygen complexes revisited: structures, spectroscopy, and reactivity. *Chemical reviews* **2017,** *117* (3), 2059-2107.

61.   Weissermel, K.; Arpe, H.-J.; Lindley, C. R.; Hawkins, S., *Industrial organic chemistry*. Wiley Online Library: 1997; Vol. 2.

62.   JA, G. S. A. M. L., Faller JW. Crabtree RH. *Organometallics* **2001,** *20*, 5485.

63.   Grasa, G. A., Moore, Z., Martin, K. L., Stevens, E.D., Nolan, E.D., Paquet, V. and Lebel H. , Structural characterization and catalytic activity of the rhodium-carbene complex. *Organometallic chemistry* **2002,** *1-2* (658), 126-131.

64.   Meyer, F. J., A.; Nuber, B.; Rutsch, P.; Zsolnac, L.; , Pyrazole. *Inorganic Chemistry* **1998,** *37*, 1213.

65.   Juanita L. van Wyk, B. O., Divambal Appavoo, Ilia A. Guzei, and James Darkwa, Solvent free sysnthesis of 3,5-di-tert-butylpyrazole and 3,5-di-substituted-butylpyrazol-1-ylethanol. *Chemical Research* **2012,** 474-477.

66.   Ibrahim, H.; Bala, M. D., Improved methods for the synthesis and isolation of imidazolium based ionic salts. *Tetrahedron Letters* **2014,** *55* (46), 6351-6353.

67.   https://chem.libretexts.org/, Leaving Groups. 2020.

68.   Gottlieb, H. E.; Kotlyar, V.; Nudelman, A., NMR chemical shifts of common laboratory solvents as trace impurities. *Journal of Organic Chemistry* **1997,** *62* (21), 7512-7515.

69.   Ibrahim, H.; Bala, M. D., Earth abundant metal complexes of donor functionalised N-heterocyclic carbene ligands: synthesis, characterisation and application as amination catalysts. *New Journal of Chemistry* **2016,** *40* (8), 6986-6997.

70.   Chem synthesis.

71.   Voss, M. E.; Beer, C. M.; Mitchell, S. A.; Blomgren, P. A.; Zhichkin, P. E., A simple and convenient one-pot method for the preparation of heteroaryl-2-imidazoles from nitriles. *Tetrahedron* **2008,** *64* (4), 645-651.

72.   Alberico, D.; Scott, M. E.; Lautens, M., Aryl− aryl bond formation by transition-metal-catalyzed direct arylation. *Chemical reviews* **2007,** *107* (1), 174-238.

73.   Barton, D. H.; Bévière, S. D.; Chavasiri, W.; Csuhai, É.; Doller, D., The functionalisation of saturated hydrocarbons. Part XXI. The Fe (III)-catalyzed and the Cu (II)-catalyzed oxidation of saturated hydrocarbons by hydrogen peroxide: a comparative study. *Tetrahedron* **1992,** *48* (14), 2895-2910.

74.   M. S. Seo, J. Y. K., J. Annaraj, Y. Kim, Y. Lee, S. Kim, J. Kim, W. Nam, [Mn(tmc)(O$_2$)]$^+$: one side-on peroxido manganese(III) cpmplex bearing a non-heme ligand. *Angewandte Chemie* **2007,** *46* (3), 377.

75.   S.M. Yui, W. L. M., T. C. Lau, Efficient Catalytic oxidation of Alkanes by Lewis Acid/[Os^{VI}(N)Cl$_4$]$^-$ Using Peroxides as Terminal Oxidants. Evidensce for Metal Based Active Intermediate *American Chemical Society* **2008,** *130* (32), 10821-10827.

76.   J. A. Mata, M. P., E. Peris, Structral and catalytic properties of chelating bis- and tris-*N*-heterocyclic carbenes *Coordination chemistry reviews* **2007,** *251*.

77.   Przyojski, J. A.; Arman, H. D.; Tonzetich, Z. J., NHC complexes of cobalt (II) relevant to catalytic C–C coupling reactions. *Organometallics* **2013,** *32* (3), 723-732.

78.   Zhang, D.; Zhou, S.; Li, Z.; Wang, Q.; Weng, L., Direct synthesis of cis-dihalido-bis (NHC) complex of nickel (II) and catalytic application in olefin addition polymerization: Effect of halogen co-ligands and density functional theory study. *Dalton Transactions* **2013,** *42* (33), 12020-12030.

79.   Zhou, Y.; Chen, W., Synthesis and Characterization of Square-Planar Tetranuclear Silver and Gold Clusters Supported by a Pyrazole-Linked Bis(N-heterocyclic carbene) Ligand. *Organometallics* **2007,** *26* (10), 2742-2746.

80.   Pototschnig, G.; Maulide, N.; Schnürch, M., Direct functionalization of C− H bonds by iron, nickel, and cobalt catalysis. *Chemistry–A European Journal* **2017,** *23* (39), 9206-9232.

81.   S. Enthaler, K. J., M. Beller, Sustainable metal catalysis with iron from rust to a ring star? *Angewandte Chemie International Edition* **2008,** *47* (18), 3317-3321.

82.   Lawal, N. S.; Ibrahim, H.; Bala, M. D., Cu(I) mediated hydrogen borrowing strategy for the α-alkylation of aryl ketones with aryl alcohols. *Monatshefte für Chemie - Chemical Monthly* **2021,** *152* (2), 275-285.

83.   Tordin, E.; List, M.; Monkowius, U.; Schindler, S.; Knör, G., Synthesis and characterisation of cobalt, nickel and copper complexes with tripodal 4N ligands as novel catalysts for the homogeneous partial oxidation of alkanes. *Inorganica chimica acta* **2013,** *402*, 90-96.

84.   Lin, I. J. B.; Vasam, C. S., Preparation and application of N-heterocyclic carbene complexes of Ag(I). *Coordination Chemistry Reviews* **2007,** *251* (5), 642-670.

85.   Abubakar, S.; Bala, M. D., Transfer Hydrogenation of Ketones Catalyzed by Symmetric Imino-N-heterocyclic Carbene Co (III) Complexes. *ACS omega* **2020,** *5* (6), 2670-2679.

86.   Abubakar, S.; Ibrahim, H.; Bala, M. D., Transfer hydrogenation of ketones catalyzed by a trinuclear Ni(II) complex of a Schiff base functionalized N-heterocyclic carbene ligand. *Inorganica Chimica Acta* **2019,** *484*, 276-282.

87.   Bala, M. D.; Ikhile, M. I., Application of three-legged piano-stool cyclopentadienyl-N-heterocyclic carbene iron (II) complexes as in situ catalysts for the transfer hydrogenation of ketones. *Journal of Molecular Catalysis A: Chemical* **2014,** *385*, 98-105.

88.   π-Bonding between Metals and Ligands. 2021.

89.   Carabineiro, S. A.; Silva, L. C.; Gomes, P. T.; Pereira, L. C.; Veiros, L. F.; Pascu, S. I.; Duarte, M. T.; Namorado, S.; Henriques, R. T., Synthesis and characterization of tetrahedral

and square planar bis (iminopyrrolyl) complexes of cobalt (II). *Inorganic chemistry* **2007,** *46* (17), 6880-6890.

90.	Kowalkowska-Zedler, D.; Dołęga, A.; Nedelko, N.; Łyszczek, R.; Aleshkevych, P.; Demchenko, I.; Łuczak, J.; Ślawska-Waniewska, A.; Pladzyk, A., Structural, magnetic and spectral properties of tetrahedral cobalt(ii) silanethiolates: a variety of structures and manifestation of field-induced slow magnetic relaxation. *Dalton Transactions* **2020,** *49* (3), 697-710.

91.	Ragavendran, P.; Sophia, D.; Arul Raj, C.; Gopalakrishnan, V., Functional group analysis of various extracts of Aerva lanata (L.,) by FTIR spectrum. *Pharmacologyonline* **2011,** *1*, 358-364.

92.	Jan Novotny, J. V., Pankaj L Bora, Michal Repisky, Michal Straka, Stanislav, Komorovsky, Radek Marek, Linking the Character of the Metal-Ligand Bond to the Ligand NMR Shielding in Transition-Metal Complexes: NMR Contributions from Orbit Coupling *Journal of Chemical Theory and Computation* **2017,** *13* (83586-3601).

93.	Morris, P. C. a. R., Getting Down to Earth: The Renaissance of Catalysis with Abundant Metals. *Accounts of Chemical Research* **2015,** *48* (9), 2495-2495.

94.	Albrecht, M.; Bedford, R.; Plietker, B., Catalytic and Organometallic Chemistry of Earth-Abundant Metals. *Organometallics* **2014,** *33* (20), 5619-5621.

95.	Su, B.; Cao, Z.-C.; Shi, Z.-J., Exploration of Earth-Abundant Transition Metals (Fe, Co, and Ni) as Catalysts in Unreactive Chemical Bond Activations. *Accounts of Chemical Research* **2015,** *48* (3), 886-896.

96.	Lazreg, F.; Nahra, F.; Cazin, C. S. J., Copper–NHC complexes in catalysis. *Coordination Chemistry Reviews* **2015,** *293-294*, 48-79.

97.	Crispini, A.; Cretu, C.; Aparaschivei, D.; Andelescu, A. A.; Sasca, V.; Badea, V.; Aiello, I.; Szerb, E. I.; Costisor, O., Influence of the counterion on the geometry of Cu(I) and Cu(II) complexes with 1,10-phenanthroline. *Inorganica Chimica Acta* **2018,** *470*, 342-351.

98.	Conry, R. R., Copper: Inorganic and Organic Chemistry. *Encylopedia of Inorganic Chemistry* **2006**.

99.	Andreas A. Danopoulos, T. S., and Pierre Braunstein, N-Heterocyclic Carbene Complexes of Copper, Nickel, and Cobalt. *Chem. Soc. Rev* **2018**.

100.	Constable, E. C.; Housecroft, C. E., Coordination chemistry: the scientific legacy of Alfred Werner. *Chemical Society Reviews* **2013,** *42* (4), 1429-1439.

101.	Qun Zhao, G. M., Michal Szostak*, Steven P. Nolan*, N-Heterocyclic Carbene Complexesin C-H activation reactions. *Chemical Reviews* **2020**.

102.	https://chem.libretexts.org, A Coordination Chemistry and Crystal Field Theory: Tetrahedral Complexes. **2021**.

103.	D. H. R. Barton, S. D. B. v. r., W. Chavasiri, E. Csuhai, D.; Doller, *Tetrahedron* **1992,** *48*, 2895-2910.

104.	A. Conde, L. V., D. Balcells, M. M. D az-Requejo, A.; Lleds, P. J. P. r., *American Chemical Society* **2013,** *135*, 3887-3896.

105.	Insights, F. M., Cyclohexanone Market: Global industry analysis 2012-2016. *Chemicals and Materials* **2012**.

106.	Mnube, S. G., Application of triazolium-based metal complexes for catalytic oxidation of octane. **2014**.

107.	Tordin, E.; List, M.; Monkowius, U.; Schindler, S.; Knör, G., Synthesis and characterisation of cobalt, nickel and copper complexes with tripodal 4N ligands as novel catalysts for the homogeneous partial oxidation of alkanes. *Inorganica chimica acta* **2013,** *402* (100), 90-96.

108.	Ribeiro, A. P.; Martins, L. M.; Hazra, S.; Pombeiro, A. J., Catalytic oxidation of cyclohexane with hydrogen peroxide and a tetracopper (II) complex in an ionic liquid. *Comptes Rendus Chimie* **2015,** *18* (7), 758-765.

109.	T. C. O. M. Leod, M. V. K., A. J. L. Pombeiro, M. A. Schiavon and M. D. Assis, A Comparative Approach for the CH Bond Oxidation of Arylalkanes in Water Using ASS-M (acac) n. *Applied Catalysis A: General* **2017,** *372*, 191-198.

110.	van Asselt, W. J.; van Krevelen, D. W., Preparation of adipic acid by oxidation of cyclohexanol and cyclohexanone with nitric acid: Part I. Reaction mechanism. *Recueil des Travaux Chimiques des Pays-Bas* **1963,** *82* (1), 51-67.

111.   Pan, D.; Li, G.; Su, Y.; Wei, H.; Luo, Z., Kinetic study for the oxidation of cyclohexanol and cyclohexanone with nitric acid to adipic acid. *Chinese Journal of Chemical Engineering* **2021,** *29*, 183-189.

112.   Vang, Z., Ring Opening Polymerization. *CSB* **2018**.

113.   Brydson, J. A., Polyamides and polyimides. *Plastics and Materials* **1999**.

114.   A. M. Kirillov, M. V. K., A.J.L. Pombeiro, Advances in Organometallic Chemistry and Catalysis. *John Wiley and Sons* **2014**.

115.   M.V. Kirillov, M. L. K., Y.N. Kozlov, L.S. Shul'pina, A.Kitaygorodskiy, AJL. Pombeiro, G.B. Shul'pin, Remarkably fast oxidation of alkanes by hydrogen peroxide catalyzed by a tetracopper (II) triethanolaminate complex: Promoting effects of acid co-catalysts and water, kinetic and mechanistic features. *Catalysis* **2009,** *268* (1), 26-38.

116.   Williams, D. B. G. L., M., , Drying of organic solvents: quantitative evaluation of the efficiency of several desiccants. *The Journal of organic chemistry* **2010,** *75* (24), 8351-8354.